ELSEVIER

Macroporous copolymer networks

O. Okay[a,b,*]

[a]*Department of Chemistry, Istanbul Technical University, 80626 Maslak, Istanbul, Turkey*
[b]*TUBITAK Marmara Research Center, P.O. Box 21, Gebze, Kocaeli, Turkey*

Abstract

Macroporous copolymer networks form as a result of the phase separation during the free-radical crosslinking copolymerization of vinyl and divinyl monomers in the presence of an inert diluent. In this article, the developments achieved in the field of macroporous networks over the last few years are presented. Special attention is paid to the preparation techniques of macroporous networks in an effort to highlight the new synthesis strategies developed in the recent years. It has been demonstrated that a variety of porous structures can be obtained during or after the cross linking process by changing the independent variable of the network synthesis, i.e. the extent of the polymer–(diluent + monomer) interactions, the amount of the crosslinker and the diluent as well as the initiator concentration or the polymerization temperature. The reaction system leading to macroporous networks is a (quasi)ternary system composed of a polymer network, soluble polymers, and low molecular compound (monomers and diluent). All concentrations and properties of the components of the system change continuously during the crosslinking process. It will be shown that the theoretical models developed recently correctly predict the phase separation condition during the crosslinking process as well as the total porosity of the resulting macroporous networks. © 2000 Elsevier Science Ltd. All rights reserved.

Keywords: Macroporous networks; Heterogeneous networks; Free-radical crosslinking copolymerization; Gel formation; Porosity; Phase separation; Swelling; Kinetic modeling

Contents

 * Tel.: +212-2853156; fax: +212-2856386.
  E-mail address: okayo@itu.edu.tr (O. Okay).

Nomenclature

α	Fractional volume conversion of the monomers
χ_{12}^{mon}	Monomer–polymer interaction parameter
χ_{12}^{sol}	Solvent–polymer interaction parameter
χ_{ij}	Interaction parameter between the species I and J
δ_1	Solubility parameters of the diluent
δ_2	Solubility parameters of the polymer
$\Delta\delta^2$	$(\delta_1 - \delta_2)^2$
ΔG_{el}	Change in the free energy of elastic deformation
ΔG_{m}	Change in the free-energy of mixing
ϵ	Contraction factor
Φ_{s}	Volume fraction of the (non)solvent in the diluent mixture
$[\eta]$	Intrinsic viscosity
μ_i	Chemical potential of the component i
v_2^{00}	Initial volume fraction of the monomers in the reaction mixture
v_2^{0}	Volume fraction of polymer network after preparation
v_2	Volume fraction of polymer in the equilibrium swollen hydrogel
v_{g}	Volume fraction of the network phase in the reaction system at volume conversion α
v_i	Volume fraction of the species i
$\bar{v}_{\text{p}}$ Volume fraction of sol + gel polymer in the whole reaction system	
AAm	Acrylamide
AIBN	2,2$'$-Azobis(isobutyronitrile)
AN	Acrylonitrile
BAAm	N,N'-Methylene(bisacrylamide
BD	Blue Dextran
c	A constant for fixed crosslinker content in FCC system

CH–OH   Cyclohexanol
d_0 Apparent density
d_1 Density of the swelling agent
d_2 True density
d_M Density of the monomer
d_p Density of the polymer.
DOP   Di-2-ethylhexyl phthalate
DVB   Divinylbenzene
DVM   Divinyl monomer
EGDM   Ethylene glycol dimethacrylate
ES   Ethyl styrene
f Initiator efficiency
f_2 Mole fraction of DVM at conversion x
f_{20} Mole fractions of DVM at zero conversion
FCC   Free-radical crosslinking copolymerisation
GMA   Glycidyl methacrylate
HEMA   2-Hydroxyethylmethacrylate
I Initiator
k_{cyc} Fraction of divinyl monomer units consumed by cyclization reactions
k_d Decomposition rate constant of the initiator
k_{mc} Average number of multiple crosslinks formed per intermolecular link
k_{pl} Instantaneous rate constants for propagation with vinyl group M_1
k_{p2} Instantaneous rate constants for propagation with vinyl group M_2
k_{p2}' Propagation rate constant between radicals and m-DVB
k_{p2}'' Propagation rate constant between radicals and p-DVB
k_{p3} Instantaneous crosslinking rate constant
k_{pji} Propagation rate constant between radicals M_j^* and vinyls M_i
k_t^0 Termination rate constant
k_{tcij} Termination rate constant between radicals of types M_i^* and M_j^* by coupling
k_{tdij} Termination rate constant between radicals of types M_i^* and M_j^* by disproportionation
LA   Lauryl alcohol
m *meta*
M_0 Initial monomer concentration
M_1 Vinyl group on monovinyl monomer
M_2 Vinyl group on divinyl monomer
M_3 Vinyl group on polymer chains (pendant vinyls)
M_1^* Macroradicals with monovinyl monomer unit at the end
M_2^* Macroradicals with divinyl monomer unit with one unreacted vinyl at the end
M_3^* Macroradicals with divinylmonomer unit with both reacted vinyls at the end
MA   Methacrylic acid
MAn   Maleic anhydride
MCDME   Monochlorodimethyl ether
MMA   Methyl methacrylate

$\bar{M}_{\mathrm{w}}$	Weight-average molecular weight
MWD	Molecular weight distribution
n_{t}	Moles of the species i
N	Number of segments between two successive crosslinks of the network
NIPA	*N*-isopropylacrylamide
NONSOL	Nonsolvating diluent
p	*para*
P	Total porosity
POLY	Polymeric diluent
P_r	A polymer molecule composed of r structural units
q_{v}	Equilibrium volume swelling ratio of the network
$q_{\mathrm{v},0}$	Equilibrium volume swelling ratio of the network prepared in the absence of a diluent
q_{w}	Equilibrium weight swelling ratio of the network
$q_{\mathrm{w},0}$	Equilibrium weight swelling ratio of the network prepared without using a diluent
Q_n	nth moment of the polymer distribution ($n = 0, 1, 2, ...$)
r	Volume of the diluent added per ml of the monomers
r_{12}	Reactivity ratio of S with the first double bond of *m*-DVB
r_{12^*}	Reactivity ratio of S with the first double bond of *p*-DVB
$\bar{r}_{32}$	Average reactivity ratio of pendant vinyls to Monomeric vinyls on DVB isomers
R	Gas constant
R^*	Radical
S	Styrene
SAXS	Small angle X-ray scattering
S_{d}	Volume of the diluent added per gram of the monomers
SOL	Solvating diluent
t_{c}	Time required for the onset of gelation
T	Temperature
$T_{\mathrm{g}12}$	Glass transition temperature of the gel
TRIM	Trimethyloplpropane trimethacrylate
U	Solvent regain of the network prepared in the presence of a diluent
U_0	Solvent regain of the network prepared without using a diluent
V_0	Initial reaction volume
V	Reaction volume
$\bar{V}_i$	Molar volume of the monomer of type I
V_{p}	Total pore volume
V_{s}	Molar volume of solvent
W_{g}	Gel fraction
x	Monomer conversion
X_{c}	Gel point conversion
x_j	Instantaneous mole fraction of the radical M_j^*
$\bar{X}_i$	ith average chain length of polymer molecules ($i = 1, 2, 3, ...$)
y	Number of segments in the soluble polymer
Z_1, Z_2	Adjustable parameters describing the variation of the termination rate constant with the monomer conversion

1. Introduction

The formation conditions of heterogeneous (macroporous) structures in crosslinked polymers has been the subject of both applied and fundamental research for many years. Macroporous, crosslinked polymers, are effective efficient materials for many separation processes, and therefore, they are widely used as starting material, for ion exchange resins and as specific sorbents.

Initially ion exchange materials were produced by the sulfonation of natural materials such as coal, lignite, and peat. Later, the crosslinked materials based mainly on phenol–formaldehyde condensation products were used in ion exchange processes [1]. While some control of the crosslinked polymer structure was possible with this type of resin, a better design of the polymer structure has been achieved with the use of crosslinked polystyrenes. These resins, now known as the conventional or gel-type resins, or as homogeneous gels, were obtained by free-radical crosslinking copolymerization of styrene (S) and divinylbenzene (DVB) monomers using suspension polymerization [2,3] As first reported in 1935 by Staudinger and Huseman, the copolymerization of S in the presence of a small amount of DVB yielded a product that swells in good solvents but does not dissolve in them [4]. The degree of swelling can readily be adjusted by the amount of DVB used in the gel synthesis. Thus, the flexibility of the network chains in S–DVB copolymers has been useful for many ion-exchange applications.

However, there were still several limitations of S–DVB networks because a number of their properties is inversely coupled. For example, decreasing the degree of crosslinking of the networks in order to increase their 'molecular porosity' resulted in a considerable volume change of the copolymers as well as in their accelerated chemical degradation. Moreover, since the molecular porosity was a result of the swelling of the beads, they exhibited negligible 'pore structure' in nonsolvents, which restricted the use of such materials.

Towards the end of the 1950s, a new polymerization technique was discovered that yielded cross-linked polystyrenes having a porous structure in the dried state [5–22]. This technique involved the suspension polymerization of a S–DVB monomer mixture in the presence of an inert substance (the diluent), which is soluble in the monomer mixture but a poor solvent for the copolymer. After polymerization, the diluent was removed from the network, leaving a porous structure within the highly crosslinked polymer particles, which provided sufficient mechanical stability. Thus, the inert diluent acts as a pore-forming agent, and plays an important role in the design of the pore structure of crosslinked materials. Electron micrographs showed that the networks prepared without using a diluent consist of a continuous polymer phase whereas those prepared by using a diluent consist of agglomerates of particles of various sizes. These new materials were called 'macroporous' or 'macroreticular' polymer networks. Subsequently, several diluents were used in the polymerization such as solvents or nonsolvents for the polymer chains (solvating or nonsolvating diluents, respectively), or inert linear polymers [23].

It is now well understood that a phase separation during the formation of the network is mainly responsible for the formation of porous structures in a dried state. In order to obtain macroporous structures, a phase separation must occur during the course of the crosslinking process so that the two-phase structure is fixed by the formation of additional crosslinks [23]. Depending on the synthesis parameters, phase separation takes place on a macroscale (macrosyneresis, deswelling) or on a microscale (microsyneresis) [23].

During the past 40 years, the synthesis of macroporous copolymer networks based on the various chemical compositions has been the subject of many studies. The history of macroporous gels reflects

the progress of our understanding on polymer gels formed by free-radical crosslinking copolymerization. The existence of elastically ineffective crosslinks (cycles and multiple crosslinks), trapped radicals and pendant vinyl groups, inhomogeneities and heterogeneities in polymeric gels as well as the possibility of a first-order volume phase transitions in gels depending on the external conditions were the topics investigated during the past 40 years in parallel with the studies on phase separation during the network formation process leading to macroporous networks.

Three reviews were published on macroporous networks formed by free-radical crosslinking copolymerization, covering the developments in this field until 1982 [23–25]. One of these reviews [23], published in 1967 in the German language covers all the fundamental aspects of macroporous networks. This work contributed to the rapid development in the field of macroporous networks by consolidating the individual publications and patents. One of the co-authors of this review, Karel Dusek, also made significant advances in the theoretical and experimental aspects of macroporous networks. Therefore, he can be considered as the founder of macroporous networks formed by free-radical crosslinking copolymerization.

The objective of this review is to present new developments achieved in macroporous networks. This manuscript is organized as follows: in Section 2, the preparation and characterization techniques of porous networks are reviewed with a focus on the new synthetic strategies developed in recent years. Section 3 is devoted to the development of a mechanistic picture on the formation of porous structures during the crosslinking polymerization. In Section 4, a review is given concerning experimental findings regarding the relationships between the synthesis condition and the pore structure of polymers. In Section 5, the semi-emprical equations describing the equilibrium swelling ratio–porosity relations of macroporous networks are discussed and are compared with experimental data. One of the most striking feature of the macroporous copolymer networks is that their porous structures are not fixed. The structure can be modified by treating the networks with solvents. Experimental studies that relate the pore structure variation during the post-treatment of polymer networks are reviewed in Section 6. Finally Section 7 deals with a detailed kinetic and thermodynamic analysis of free-radical crosslinking copolymerization leading to macroporous networks.

1.1. Definitions

In the early work on ion-exchange resins, the space between the network chains in a swollen gel available for the transfer of solutes was defined as 'porosity' or 'molecular porosity'. However, this term is clearly misleading because the distance between the chains cannot be measured independently and it varies between zero and several nanometers depending on the external conditions [26]. On the other hand, a gel is a two-phase system consisting of the network chains and solvent molecules. Removing the solvent from a homogeneous gel results in a polymer network which is nonporous.

After the development of porous networks towards the end of 1950s, it became necessary to distinguish these new materials from the conventional materials and the terms 'macroporous' and 'macroreticular' were introduced. The conventional resins were called as 'microporous' or 'microreticular'. However, these definitions are also incorrect due to the fact that macropores refer, according to IUPAC, [27] pores of larger than 500 Å, whereas macroporous networks usually have a broad pore size distribution ranging from 10^1 to 10^4 Å. Today, the terms porous, macroporous, microporous, macroreticular, permanently porous, sponges, heterogeneous were used synonymously to describe such materials [28].

The definition of 'macroporous' or 'macroporosity' has been extensively debated. Millar defined

monovinyl monomer

divinyl monomer

initiator

inert diluent

(solvent, non-solvent, or polymer)

reaction mixture

continuous phase

filtration and extraction

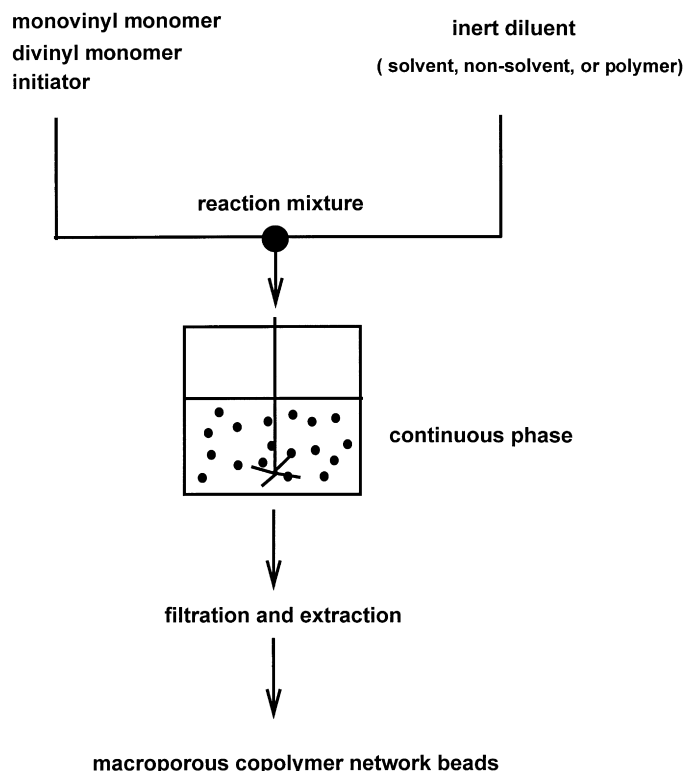**macroporous copolymer network beads**

Fig. 1. Schematic representation of the suspension polymerization technique to produce macroporous copolymer network beads.

macroporosity as being the property of S–DVB networks which are able to regain more than 0.1 ml cyclohexane (nonsolvent) per gram of the dry copolymer [19]. Haupke and Pientka defined macroporous copolymers as opaque and white materials with a measurable surface area; such materials start to form in S–DVB copolymerization at moderate or high crosslinker contents and at intermediate concentrations of diluent [29,30]. In order to define the macroporous domain, these authors used a diagram with the amount of DVB as abscissa and the amount of the diluent as ordinate. Jacobelli et al. defined the macroporous copolymers as materials in which all sizes of intraparticular clusters (nuclei, microspheres and agglomerates) are visible in the electron microscope, i.e. materials having pores from a few angstroms up to several thousands of angstroms [31]. They noted that the copolymers formed at low DVB and diluent contents are gel type whereas at a high diluent content, a material with a fused morphology forms in which only the shapes of the microspheres can be detected in electron micrograph. According to these authors, a macroporous structure is characterized by a three-level morphology [32–34]. Sederel and De Jong defined micro and macroporosity with respect to the size of the pores inside the dry network [35]. Thus, they distinguish the microporosity as the interstices between the nuclei whereas macroporosity includes the pores between the microspheres and larger agglomerates [35]. Rabelo and Coutinho defined macroporous S–DVB copolymers according to the kinetic data of their heptane uptake; those able to absorb more than 0.1 ml heptane per gram of copolymer within a short time (<5 min) are called macroporous [36]. In general, macroporous copolymers refer to materials

Table 1

Comonomer systems other than S–DVB for the synthesis of macroporous networks (BAAm = N,N'-methylene(bis)acrylamide; DVB = divinylbenzene; EGDM = Ethyleneglycol dimethacrylate; HEMA = 2-Hydroxyethylmethacrylate; GMA = Glycidyl methacrylate; MMA = Methyl methacrylate; NIPA = N-isopropylacrylamide; TRIM = Trimethylolpropane trimethacrylate)

Comonomer system	Reference
Acrylamide/BAAm	[38]
Acrylic acid/EGDM	[39]
Acrylonitrile/DVB	[40–44]
Acrylonitrile/ethyl or butyl acrylate/DVB	[45–47]
Acrylonitrile/vinyl acetate/DVB	[48]
Dimethacrylates with various chain lengths	[49–51]
DVB/1,4-di(methacryloyloxymethyl) naphthalene	[52,53]
2,3-Epithiopropyl methacrylate/EGDM	[54]
GMA/EGDM	[55–60]
GMA/2-hydroxypropylene dimethacrylate	[61]
HEMA/EGDM	[62–67]
NIPA/dihydroxyethylenebisacrylamide	[68]
Maleic anhydride/styrene/DVB	[69,70]
Methacrylic acid/DVB	[71–74]
Methacrylic acid/triethyleneglycol dimethacrylate	[75]
Methacrylonitril/DVB	[76,77]
N-methylacrylamide/alkylene(bis)acrylamides	[78]
MMA/DVB	[79,80]
MMA/1,4-di(methacryloyloxymethyl) naphthalene	[81,82]
Phenyl methacrylate/DVB	[83]
TRIM	[84–87]
TRIM/GMA	[88]
TRIM/BAAm	[89]
TRIM/MMA	[90]
N-vinylcarbazole/DVB	[91]
2- or 4-Vinylpyridine/DVB	[92–94]
Vinyl toluene/DVB	[95]

prepared in the presence of a pore-forming agent (diluent) and having a dry porosity, characterized by a lower density of the network due to the voids than that of the matrix polymer [24]. All these definitions are unsatisfactory because, macroporous polymer defines a material having pores larger than 500 Å. Since the term macroporous is most commonly used in polymer science and technology it is reasonable to accept it as the generic name of crosslinked polymers having dry state porosity, irrespective of the size of the pores. Another problem with the definition of macroporosity arises from the variation of the pore structure of the networks depending on their post-treatment process [37]. For example, a macroporous copolymer may become nonporous if it is first swollen in a good solvent and then dried at an elevated temperature. Subsequently the loss of porosity can be recovered by a solvent exchange procedure and the original swollen state porosity called maximum porosity can be preserved in the dried state. Because only the maximum porosity is a characteristic property for a given material, it is appropriate to define the macroporosity with respect to the maximum porosity.

2. General aspects of macroporous copolymer synthesis

2.1. Preparation of macroporous copolymer networks

The suspension polymerization technique has generally been used for the preparation of macroporous copolymer networks in the form of beads of diameter ranging between 0.1 and 1.5 mm. To illustrate the synthetic procedure, this technique is shown schematically in Fig. 1. First, a monovinyl–divinyl monomer mixture containing a free-radical initiator is mixed with an inert diluent. The inert diluent must usually be soluble in the monomer mixture but insoluble in the continuous phase of the suspension polymerization. The reaction mixture is then added into the continuous phase under agitation, so that it distributes in the form of droplets inside the continuous phase. The copolymerization and crosslinking reactions taking place in the monomer–diluent droplets result in the formation of beads having a glassy, opaque, or milky appearance. The beads are then extracted with a good solvent to remove the soluble polymers and the diluent from the network.

Mainly, water-insoluble monomers have been used in the synthesis of macroporous copolymers. In addition to the widely used S–DVB comonomers, various comonomer systems used in the synthesis of macroporous networks are tabulated in Table 1. The classical suspension polymerization technique is the method of choice in which an aqueous phase containing additives is utilized as the continuous phase of the reaction. For the preparation of macroporous maleic anhydride–S–DVB copolymer beads, it was shown that glycerol can be successfully used as the dispersing medium instead of water to protect the anhydride groups [69,70]. A precipitation polymerization method can also be used to make porous particles 4–7 μm in size [96]. Several diluents or diluent mixtures have been used for the preparation of hydrophobic porous particles including aliphatic and aromatic hydrocarbons, alcohols, esters, etc. Some diluents used in the synthesis of macroporous S–DVB networks are shown in Table 2.

Although the inert diluent must be soluble in the monomer mixture (organic phase) and insoluble in the continuous water phase, organized surfactant assemblies such as inverse micelles can be used to capture monomer-insoluble diluents such as water inside the organic phase. Thus, the crosslinking copolymerization in the continuous phase of a water-in-oil microemulsion also yields macroporous networks [122–124]. The nature of the porous structure is largely dependent on the microstructure of the microemulsion [125,126]. Short chain alcohols have been used as cosurfactants together with conventional surfactants for the formation of microemulsions [127–129]. For example, it was shown that water solubilized in reverse micelles can be used as a diluent in the production of porous S–DVB copolymer beads by suspension polymerization. [130] By this technique, sodium bis(2-ethylhexyl) sulfosuccinate (a surfactant commonly known as Aerosol OT or AOT) is used as the surfactant for the formation of reverse micelles. Depending on the amount of water solubilized in the micelles, the size of the water droplets inside the S–DVB monomer mixture is different. Thus, the size of the pores is controlled by adjusting the water content in the reverse micelles prior to polymerization [122,131–133].

If water is added slowly to a stirred solution of a surfactant of low hydrophilic–lipophilic balance dissolved in the oil phase, an internal phase volume of water up to 99% is achievable, and, in this state, the water droplets in the oil phase strongly interact [134]. When the continuous oil phase is composed of a monovinyl–divinyl monomer mixture, the crosslinking polymerization in the continuous phase results in a solid crosslinked polymer which contains the water droplets [135]. Removal of the water droplets by washing with ethanol, and vacuum drying, yields a highly porous monolith of extremely low density

Table 2
Diluents used in the preparation of macroporous S–DVB copolymer networks

Diluent	Reference
Benzyl alcohol	[31,97]
Benzyl alcohol/various solvents	[98]
Cyclohexane	[99,100]
Cyclohexanol	[99–101]
Cyclohexanol/toluene mixtures	[102,103]
Cyclohexanone	[99,100]
Decane	[104]
Decane/toluene mixtures	[105]
Di-2-ethylhexylphosphoric acid	[100,106]
Di-2-ethylhexyl phthalate (DOP)	[107]
2-Ethyl-1-hexanoic acid	[108]
2-Ethyl-1-hexanol	[109]
2-Ethyl-1-hexanol/*n*-heptane mixtures	[110]
2-Ethyl-1-hexanol/toluene mixtures	[111]
Gasoline/toluene mixtures	[112]
Isoamyl alcohol/various solvents	[98]
n-Heptane	[31]
n-Heptane/ethylacetate	[113]
n-Heptane/isoamyl acetate	[113]
n-Heptane/tetraline mixtures	[105]
n-Heptane/toluene mixtures	[105,114,115]
n-Heptane/various solvents	[116]
n-Hexane/toluene mixtures	[82,112]
Pentanol	[31]
Poly(styrene-*co*-methyl methacrylate)/dibutyl phthalate	[117]
Polystyrene/2-ethyl-1-hexanol mixtures	[111]
Polystyrene/dibutyl phthalate	
Polystyrene/gasoline mixtures	[111,118]
Polystyrene/*n*-hexane mixtures	[35,119]
Polystyrene/toluene mixtures	[35,119]
Toluene	[104,112]
Tri-*n*-butylphosphate	[100,106]
1,2,3-Trichloropropane/2-ethyl-1-hexanol mixtures	[120]
2,2,4-Trimethyl pentane (isooctane)	[121]

(about 0.2 g/ml compared to 1.1 g/ml polymer) [135,136]. This porous material has an open pore structure indicating that there are holes in the walls separating the water droplets. Such porous materials are called Polyhipe® (HIPE = water-in-oil High Internal Phase Emulsion). The average diameter of water droplets within a HIPE used to prepare a S–DVB Polyhipe is about 10 μm, and therefore, the surface area of the resulting materials is rather low (about 5 m^2/g) [136]. In order to increase their surface area, diluents such as toluene are added to the oil phase [137]. In this way, porous materials with a specific surface area of about 350 m^2/g were obtained having large pores (water droplets), and a second generation of small pores due to the phase separation in the oil phase.

Macroporous crosslinked polystyrenes can also be prepared starting from linear polystyrene. For example, materials called 'isoporous' or 'hypercrosslinked' resins are obtained by crosslinking linear polystyrene chains in a homogeneous solution using chloromethylated compounds and a Friedel–Crafts catalyst [138,139]. Such materials exhibit a specific surface area as high as 1200 m^2/g and they swell both in solvents and nonsolvents [140–143]. Synthesis of isoporous networks has been described starting from S–vinylbenzyl chloride copolymers of various compositions [144]. It has reported that by decreasing the initial concentration of the linear polymer in the solution to favor cyclization reactions, macroporous intramolecularly crosslinked macromolecules, i.e. macroporous microgels of 10^2 Å in diameter can be prepared [145].

The suspension polymerization technique yields macroporous polymer particles with a relatively broad particle size distribution, that cannot be used directly for fine chromatographic separations. Alternate procedures that afford monodisperse macroporous beads have been reported. For example, the seeded emulsion polymerization, which has been developed for the production of monodisperse polymer particles, may be used in the initial stage of the suspension polymerization process in order to prepare the shape template particles. These modified suspension processes include Vanderhoff's multistep seeded polymerization [146] and Ugelstad's activated swelling and polymerization techniques [147,148]. These procedures can be used for the preparation of macroporous monodisperse polymer beads [117,119,149–157]. The monodisperse, porous polymer particles in the size range of 10 μm in diameter [151,152] can be prepared by the seeded emulsion polymerization method. By this technique, 8.7 μm diameter monodisperse polystyrene latexes are used as seed particles and as a polymeric diluent for S–DVB copolymerization. By introducing an additional inert diluent (a solvent or a nonsolvent) together with monomers into the swellable monodisperse polystyrene latex, porous structures within the particles may be obtained upon the removal of the diluent after polymerization [151,152].

Hydrophilic crosslinked macroporous particles have also received much interest in recent years. They can be prepared by the classical suspension polymerization technique, in which water-insoluble derivatives of the monomers are used for the polymerization and the beads formed are subsequently hydrolyzed or aminolyzed [158–162]. Attention has recently been devoted to the direct synthesis of hydrophilic particles by use of this technique starting from water soluble comonomer systems such as acrylamide-*N*, *N*-methylene(bis)acrylamide (AAm–BAAm), or 2-hydroxyethylmethacrylate–ethylene glycol dimethacrylate (HEMA–EGDM) systems. For this purpose, various salts were added into the water phase in order to diminish the water solubility of the monomers (salting out effect). For example, Galina and Kolarz reported the synthesis of porous crosslinked polymethacrylic acid beads in an aqueous phase containing calcium chloride [71–73]. Horak et al. used an aqueous solution of polyvinylpyrrolidone as the water phase and a mixture of higher boiling alcohols as the diluent of the monomer phase for obtaining crosslinked poly(HEMA) beads [163]. They pointed out that the diluent in the monomer phase reduces the water solubility of the HEMA monomer. Mueller et al. [164], Peppas et al. [165–167], Jayakrishnan et al. [168], Okay et al. [64], and Horak et al. [65] described the various techniques for the synthesis of poly(HEMA) beads in an aqueous phase containing sodium chloride and other additives. The presence of sodium chloride in the aqueous phase reduces the monomer solubility and thus allows formation of spherical, hydrophilic beads.

Another approach to prepare hydrophilic beads is the inverse suspension polymerization technique by which the water-soluble monomers or their aqueous solutions are suspended in an organic phase and

polymerized therein to give copolymer beads having a controlled size [169–177]. For example, the crosslinking polymerization of an aqueous solution of N-isopropylacrylamide (NIPA) and BAAm in paraffin oil as the continuous phase results in crosslinked poly(NIPA) beads of sizes 0.25 to 2.8 mm in diameter [178,179]. Several diluents soluble in the monomer mixture were reported as inert diluents in the production of hydrophilic macroporous copolymer networks [38,66,78]. Also, various surfactants forming ordered structures in the aqueous monomer solution were reported to be as efficient diluents for the synthesis of hydrophilic macroporous materials based on acrylamides [180]. Crosslinked poly (HEMA) is an important class of hydrophilic crosslinked polymers, which is widely used as a hydrogel for contact lenses [181–184]. Coupek et al. first described synthesis of macroporous polymers from HEMA and EGDM [63]. The maximum equilibrium swelling of poly(HEMA) gels in water is thermodynamically limited to 39 wt%. Thus, although there has been some diversity in reporting this value [66,182,185–191] if HEMA is polymerized in the presence of greater than 39 wt% water, a phase separation occurs and an opaque heterogeneous gel forms [192]. Huglin and Yip estimated the size and the concentration of phase separated domains in poly(HEMA) gels using the turbidity ratio method as 0.1 ± 0.05 μm and 0.25–2.2% of the swollen gel, respectively [192].

By varying the amount of water as a diluent in the crosslinking polymerization of HEMA, a large range of porosities can be attained in the final networks [66,193]. In addition to water, several diluents such as cyclohexanol/lauryl alcohol mixture, [63] benzyl alcohol, [168] cyclohexanol/1-dodecanol mixture, [65,163] were used in the synthesis of macroporous poly(HEMA) beads. It was also shown that porous poly(HEMA) networks can be obtained by producing a microemulsion of which the monomer HEMA forms the continuous phase and the added diluent methylcyclohexane forms the discontinuous phase using anionic or nonionic surfactants [62]. The crosslinking polymerization of the microemulsion using UV radiation results in a porous material which absorbs larger amount of water than the nonporous poly(HEMA). The size of the pores varies between 100 and 2000 nm and increases as the amount of the diluent increases [62]. Another technique to create pores inside a hydrophilic network is the freeze-thaw technique [67,194]. This technique consists of freezing the initial polymerization mixture (monomer + crosslinker + diluent) to a solid monomer matrix containing diluent crystals. Polymerization of the monomer matrix using UV radiation and removing of the diluent by thawing result in a macroporous film or bead [67,194].

The crosslinking copolymerization of N-methylacrylamide with alkylene(bis)acrylamides in the presence of methanol, acetic acid, water, dimethylsulfoxide (DMSO), or dimethylformamide as diluents has been used for the preparation of macroporous polyamides [78]. It was shown that more polar solvents (water, methanol) produce materials with higher specific surface area and internal pore volume than those prepared with less polar solvents such as DMSO [78]. Also, decreased cross-linker flexibility increased the porosity of the resulting networks [78]. Xie et al. described the preparation conditions of macroporous networks from AAm and BAAm with pore sizes up to 1000 nm using DMSO/alcohol mixtures as a diluent [38]. It was shown that, as the chain length of the alcohols used in combination with DMSO increases from C_1 to C_8, larger microspheres and thus larger pores form in the final material. Further increase in the chain length of alcohol decreased the size of the pores [38]. Poly(N-isopropylacrylamide) (poly(NIPA)) gels exhibit a lower critical solution temperature (LCST) of about 34°C in water [195,196]. Thus, poly(NIPA) gel swells in water when $T <$ LCST but it deswells or collapses when $T >$ LCST. This feature of

poly(NIPA) gels has been used to construct porosity inside the poly (NIPA) matrix [68,197–199]. Wu et al. prepared macroporous poly(NIPA) gels above their LCST in the absence and presence of hydroxypropyl cellulose as a diluent [68].

Svec et al. [55,200] prepared a series of macroporous glycidyl methacrylate (GMA)/EGDM copolymer beads by classical suspension polymerization technique using lauryl alcohol (LA)/cyclohexanol diluent mixture. The copolymers exhibited a high specific surface area, which increased markedly with increasing content of the crosslinker EGDM. An increasing portion of LA in the diluent mixture leads to the formation of large pores and small surface areas [55]. Synthesis of uniformly sized porous GMA/EGDM beads was described by Smigol et al. [56,57]. Here, monodisperse polystyrene shape templates prepared by emulsifier-free emulsion polymerization were swollen with GMA/EGDM monomer mixture. The crosslinking polymerization resulted in the formation of 10 μm sized monodisperse porous GMA/EGDM beads [56,57].

The experimental data indicate that the following reaction parameters are the main factors determining the porous structure of the copolymer beads: the crosslinker concentration, the monomer concentration in the reaction mixture, and the type of the diluent. The following variables are convenient for defining the composition of the reaction mixture.

1. *Crosslinker concentration.*

$$\% \text{ Crosslinker} = \frac{\text{mol or mass of crosslinker (divinyl monomer)}}{\text{total mol or mass of monomers}} 10^2 \tag{1}$$

2. *Monomer dilution.* Volume fraction of the monomer in the reaction mixture, v_2^{00}, i.e.

$$\nu_2^{00} = \frac{\text{volume of the monomers}}{\text{total volume of the reaction mixture (monomers + diluent)}} \tag{2}$$

or the volume ratio of the diluent to the monomers, r, i.e.

$$r = \frac{\text{volume of the diluent}}{\text{volume of the monomers}} \tag{3}$$

3. *The solvating power of the diluent.* The difference between the solubility parameters of the diluent (δ_1) and the copolymer (δ_2), i.e. $\delta_1 - \delta_2$, or its square $(\delta_1 - \delta_2)^2$ are generally used to represent the solvating power of a diluent in a network formation system. According to the Hildebrand theory, [201] the solubility of a polymer in a solvent is favored when $(\delta_1 - \delta_2)^2$ is minimized. For instance, since the solubility parameter of S–DVB copolymers δ_2 is 18.6 $(\text{MPa})^{1/2}$, a given solvent is a solvating diluent if δ_1 is close to this value (e.g. toluene with $\delta_1 = 18.2$ $(\text{MPa})^{1/2}$), whereas it is a nonsolvating diluent if $(\delta_1 - \delta_2)^2 \gg 0$ (e.g. benzyl alcohol with $\delta_1 = 24.7$ $(\text{MPa})^{1/2}$)

It was also shown that instead of the Hildebrand solubility parameter, the three-dimensional solubility parameter of Hansen is a better predictor for the diluent-polymer affinity in S–DVB copolymerization [202].

2.2. Characterization of macroporous copolymer networks

The macroporous network beads were mainly characterized in a dried state. The following quantities have been measured for the pore structure determinations:

1. The apparent density d_0:

$$d_0 = \frac{\text{mass of the bead}}{\text{volume of the bead}} \tag{4}$$

2. The true density d_2:

$$d_2 = \frac{\text{mass of the bead}}{\text{volume of the polymer}} \tag{5}$$

According to Eqs. (4) and (5), a material is homogeneous if its apparent density is equal to its true density. The lower the apparent density, the higher is the porosity of the material. The density measurements of the beads are carried out by the mercury pycnometry which measures the volume of the beads including the pores of radius above 7000 nm [203]. Other liquids such as aliphatic hydrocarbons can also be used for the apparent density measurements.

3. The total porosity P:

$$P = \frac{\text{volume of the pores}}{\text{volume of the beads}} \tag{6a}$$

or

$$P\% = \frac{\text{volume of the pores}}{\text{volume of the beads}} 10^2 \tag{6b}$$

4. The total pore volume V_p:

$$V_p = \frac{\text{volume of the pores}}{\text{mass of the beads}} \tag{7}$$

The total porosity and the total pore volume can be calculated from the densities using the following equations:

$$P = 1 - \frac{d_0}{d_2} \tag{8}$$

$$V_p = \frac{1}{d_0} - \frac{1}{d_2} \tag{9}$$

or can be measured from the water uptake capacity of S–DVB copolymer beads after surface treatment with methanol in order to reduce their water repellence [19,204].

The distribution of pore sizes in a macroporous polymer can be measured by electron microscopy,

[205,206] nitrogen desorption isotherms, [207] size exclusion chromatography, [117,208–210] and mercury intrusion porosimetry [211]. Application of the Kelvin equation to the desorption isotherm with nitrogen as the sorbate allows the measurement of pore diameters up to sizes of about 200 nm [207]. The mercury intrusion porosimetry is the most widely used technique for the measurement of the pore diameters in the range 15,000 nm up to 20 nm. This technique involves the penetration of mercury, at known pressures, into the pores of the dry polymer and is based upon Washburn' relationship [212] that the pressure required to force mercury into a capillary of diameter d is $-4\sigma \cos \theta/d$ where σ is the surface tension of mercury and θ is the contact angle of mercury with the polymer. For a given polymer, the surface tension and the contact angle are constants and therefore, application of a known pressure yields the corresponding pore diameter while changes in the penetration volume at increasing pressures indicate the volume of pores of a given diameter. However, the applicability of the mercury porosimetry for the measurement of pores smaller than about 500 nm is questionable. This is due to the high pressure necessary to force mercury into a pore smaller than 500 nm, which may cause deformation of the polymer rather than mercury intrusion [213]. For the measurement of the pores of sizes 200–500 nm, size exclusion chromatography technique can also be used [117,208–210].

On the other hand, visual appearance of porous beads also gives an indication about the size of the agglomerates inside the particles [213]. For polymers having internal agglomerates of 200 nm in diameter or larger, the beads appear white or opaque. If the size of the agglomerates is smaller than 200 nm, they appear translucent. The particles with no internal pore structure appear transparent.

The specific surface area of the beads is measured by nitrogen adsorption isotherms. The BET equation is used to analyze the nitrogen adsorption isotherms in order to calculate the surface area of particles [214].

The equilibrium weight swelling ratio of macroporous copolymers q_w (mass of equilibrium swollen beads/mass of dry beads) is measured by the centrifugation technique in which the excess of the swelling agent is centrifuged from the beads. For the determination of the equilibrium volume swelling ratio q_v (volume of a equilibrium swollen bead/volume of the dry bead), the individual beads are examined under an optical microscope. The swelling rate of the beads is measured either by measuring the diameter of the beads at various time intervals using an optical microscope, or by the graduated cylinder method [107]. An alternative method of determining the swelling ratio of hydrophilic gels was developed by Huglin and Yip [215]. By this technique, the hydrogel is swollen in an aqueous solution of Blue Dextran (BD) of known concentration. Owing to the high molecular weight of BD, it cannot enter the gel phase as the gel swells. Thus, the increase in the BD concentration in the external solution phase, measured by a spectroscopic technique, reflects the volume-swelling ratio of the hydrogel in the aqueous solution of BD. The extrapolation of the swelling ratios to zero BD concentration leads to the swelling ratio of the hydrogel in water [215].

3. Formation of porous structures during crosslinking

The free-radical crosslinking copolymerization (FCC) system for the production of macroporous copolymers includes a monovinyl monomer, a divinyl monomer (crosslinker), an initiator, and the inert diluent. The decomposition of the initiator produces free-radicals which initiate the polymerization and crosslinking reactions. After a certain reaction time, a three-dimensional network of infinitely large size may start to form. The term 'infinitely large size', according to Flory, [216] refers to a molecule
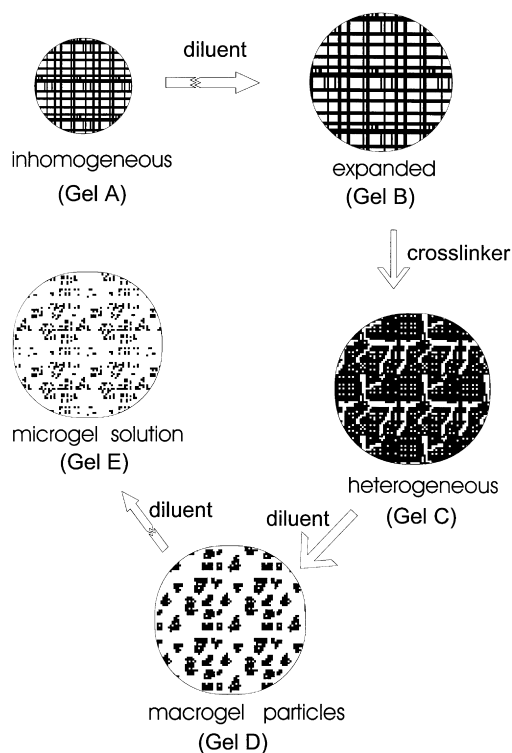
Fig. 2. Formation of various structures in free-radical crosslinking copolymerization (FCC) of vinyl/divinyl monomers with or without using a diluent.

having dimensions of an order of magnitude approaching that of the containing vessel. At this point (the gel point) the system (monomer–diluent mixture) changes from liquid to solid-like state. Continuing polymerization and crosslinking reactions decreases the amount of soluble reaction components by increasing both the amount and the crosslinking density of the network. After complete conversion of monomers to polymer, only the network and the diluent remain in the reaction system.

Crosslinked copolymers prepared by FCC exhibit different structures and properties depending on the amounts of the crosslinker and the diluent present during the reactions as well as on the solvating power of the diluent. Fig. 2 shows schematically, how the polymer structure changes depending on these parameters.

In the absence of a diluent, if a small amount of a crosslinker is used in the network synthesis, an inhomogeneous gel structure is obtained as illustrated by Gel A in Fig. 2. The gels formed by FCC are always inhomogeneous due to the fact that the crosslinker has at least two vinyl groups and therefore, if one assumes equal vinyl group reactivity, the reactivity of the crosslinker is twice that of the monovinyl monomer. As a consequence, the crosslinker molecules are incorporated into the growing copolymer chains much more rapidly than the monomer molecules so that the final network exhibits a crosslink density distribution [217]. The network regions formed earlier are higher crosslinked that those formed later.

If a good solvent is included in the FCC system as an inert diluent, the gel thus obtained will have a

KEY:

white area = liquid phase
hached area = gel phase
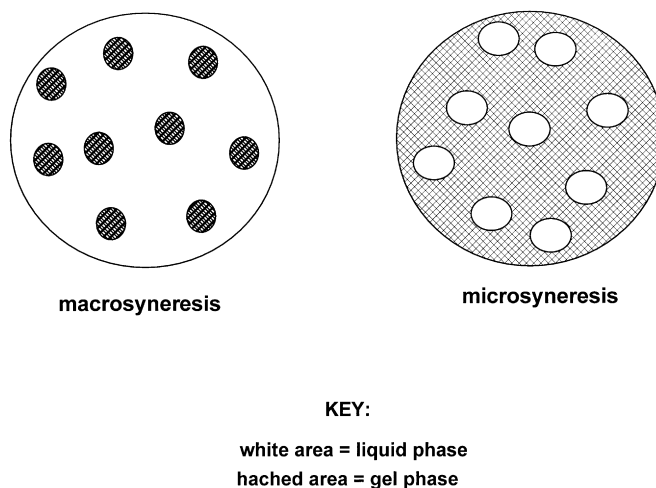
Fig. 3. Schematic representation of macrosyneresis and microsyneresis during crosslinking polymerization.

supercoiled (expanded) structure (Gel B). The expanded Gel B thus formed collapses during the removal of the diluent after its synthesis and therefore, it is nonporous in the glassy state. Gel B swells in good solvents much more than Gel A which is synthesized in bulk.

If the amount of the crosslinker in the reaction mixture is increased while the amount of the diluent (good solvent) remains constant (Gel B → Gel C in Fig. 2), the highly crosslinked network formed cannot absorb all the diluent molecules present in the reaction mixture. As a result, a phase separation occurs during the gel formation process. The process of phase separation may proceed either in the form of macrosyneresis or microsyneresis, as proposed by Dusek (Fig. 3) [218]. According to the model of macrosyneresis, the growing gel deswells (or collapses) at the critical point for phase separation and becomes a microgel (nucleus), whereas the separated liquid remains as a continuous phase in the reaction mixture (Fig. 3). As the polymerization and crosslinking proceed, new nuclei are continuously generated due to the successive separation of the growing polymers, which react with each other through their pendant vinyl groups and radical centers locating at their surfaces. These agglomeration processes result in the formation of a heterogeneous gel (Gel C in Fig. 2) which consists of two continuous phases, a gel and a diluent phase. Removal of the diluent from the gel after synthesis creates voids (pores) of various sizes. This material is a macroporous copolymer network. It is seen that, in the presence of a good solvent as a diluent, the porous structures form due to the effect of monomer dilution which is higher than the swelling capacity of the network This type of porosity formation in polymeric materials is called by Dusek as ν-induced syneresis, [23,218] where ν refers to the crosslink density of the network.

According to the model of microsyneresis, phase separation results in the formation of a dispersion in the reaction system instead of deswelling (Fig. 3) [218]. Thus, the liquid phase during the gel formation process separates in the form of small droplets inside the gel and it becomes discontinuous. Compared to the macrosyneresis process, the volume of the gel phase does not change much after microsyneresis but the gel becomes turbid due to the scattering of light from the separated liquid droplets. Further polymerization and crosslinking reactions fix the two-phase structure in the final material. The relative importance of micro and macrosyneresis depends mainly on the crosslinker content. It has been

shown that at low crosslinker contents, phase separation occurs in the form of microsyneresis [192,218]. This is due to the fact that, at low crosslinker contents, the long network chains slowly relax from swollen to the collapsed state, so that their swollen state may become fixed by additional crosslinks, and the solvent molecules remain inside the gel in the form of droplets. It is seen that the nonequilibrium state formed by microsyneresis is stabilized in the final material due to the chemical reactions. In this connection, decreasing the rate of the crosslinking reactions during the gel formation process should favor macrosyneresis. On the other hand, at high crosslinker contents, the phase separated liquid droplets combine with each other to give a bulky liquid phase, whereas the network chains rapidly attract each other to form spherical nuclei. Recently, it was shown that the process of microsyneresis also occurs if a highly swollen hydrogel is immersed in a poor solvent [219]. In this case, the swollen gel sample on contact with the poor solvent first segregates into a solvent-rich and a polymer-rich phase; if the polymer-rich regions of the sample are in the glassy state, they block solvent diffusion and the deswelling of the whole sample. Thus, the gel cannot reach its equilibrium state in the poor solvent and the heterogeneous structure is stabilized [219].

If the amount of the diluent is further increased (Gel C → Gel D in Fig. 2), a critical point is passed, at which the system becomes discontinuous, because the amount of the monomer is not sufficient and the growing chains cannot occupy the entire available volume. Consequently, a dispersion of macrogel particles in the solvent results (Gel D in Fig. 2). Increasing the amount of solvent decreases the size of the gel particles, and finally they are as small as ordinary macromolecules. These gel particles are microgels [217] which are dissolved as a colloidal solution (Gel E).

If a nonsolvent or a linear polymer is used in FCC as the diluent, a phase separation may occur in the reaction system before the gel point. This results in the formation of a dispersion of separated (discontinuous) polymer phase in the continuous monomer + diluent phase (Gel D). Continuing the polymerization increases the amount of the polymer. As a result, the first phase separated and intramolecularly crosslinked particles (nuclei) agglomerate into larger clusters called microspheres. Continuing the reactions increase the number of clusters in the reaction system so that the polymer phase becomes continuous. Thus, a system consisting of two continuous phases results (Gel C in Fig. 2). Again removing the diluent from the gel produces a macroporous copolymer as illustrated in Fig. 2. It is seen that, in the presence of nonsolvents or linear polymers as a diluent, the incompatibility between the network segments and the diluent molecules is responsible for the porosity formation. This mechanism is called χ-induced syneresis, [23,218] where χ is the polymer–solvent interaction parameter, which relates to $(\delta_1 - \delta_2)^2$. Comparison of the mechanisms of ν- and χ-induced syneresis suggests that the pore structure formed by the first mechanism should result in more ordered and smaller agglomerates than formed in the latter mechanism. Note that if the amount of the diluent is above a certain value, the separated polymer phase remains discontinuous after the complete conversion of the monomers, i.e. the Gel D becomes the final product.

According to this picture of the gel formation, three main transitions can be distinguished: (1) the transition from expanded to heterogeneous (porous) gels (macrophase separation, Gel B → Gel C; (2) The "solid-liquid" transition Gel C → Gel D; and (3) the macrogel–microgel transition Gel D → Gel E. The preparation of macroporous gels thus requires a careful choice of the experimental parameters. Currently, the formation of porous networks by FCC is qualitatively quite well understood by using the knowledge about the properties of porous gels. Also, theories have been developed which predict the total volume of the pores in the networks from their synthesis conditions (see Section 7). However, a
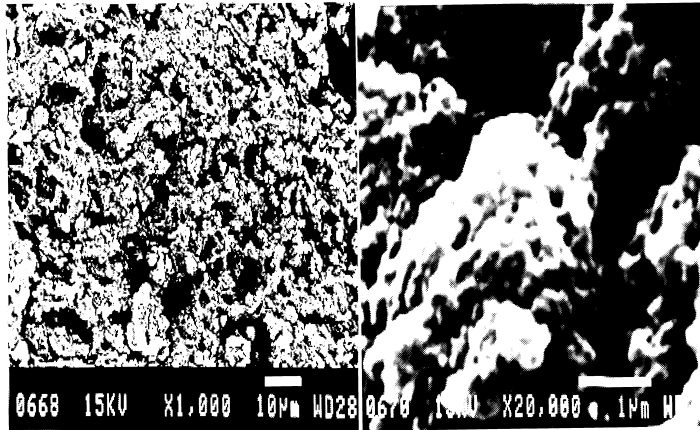
Fig. 4. SEM micrographs of crosslinked macroporous poly(methyl methacrylate) copolymers obtained with toluene (left) and cyclohexanol (right) as the diluent. [80] Crosslinker (EGDM) = 40 wt%. Diluent/monomer volume ratio = 1/1. The scaling bar corresponds to 100 nm (left) and 10,000 nm (right).

quantitative treatment about the size and size distribution of the pores depending on the synthesis parameters is desirable.

The above mechanism of porosity formation during FCC also suggests that the final copolymer consists of agglomerates of particles of various sizes. Indeed, the electron micrographs of macroporous copolymers reveal the existence of particles of various sizes which look like cauliflowers (Fig. 4) [213]. As a consequence, almost all macroporous networks formed by FCC are characterized by a relatively
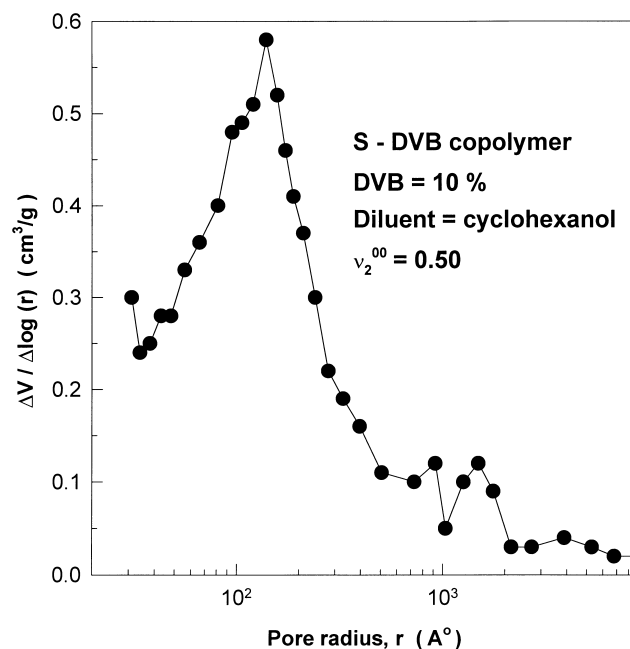
Fig. 5. A typical pore size distribution curve of S–DVB copolymer beads.
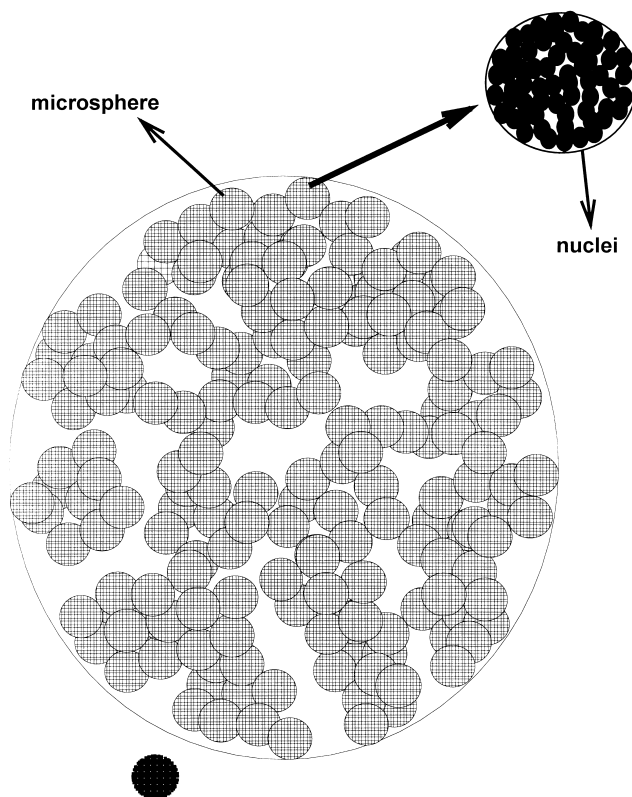
Fig. 6. Schematic representation of various agglomerates in macroporous copolymer networks formed by FCC.

broad pore size distribution ranging from micropores to macropores. The definition of micro or macropores comes from the IUPAC classification of pores based on the pore width as follows [27]:

1. Micropores have widths of up to 20 Å.
2. Mesopores have widths in the range 20–500 Å.
3. Macropores have widths greater than 500 Å.

A typical pore size distribution of a styrene–divinylbenzene copolymer network prepared in the presence of a nonsolvating diluent is shown in Fig. 5. Pores from a few tens of angstroms up to several thousands of angstroms in radius exist inside the macroporous material. Agglomerates of particles of various sizes inside the porous copolymer are responsible for this broad size distribution of pores. The pores are, in fact, irregular voids between agglomerates which are typically interconnected [220]. In S–DVB copolymers, the types of agglomerates and thus, the formation process of the porous structure can be divided into three stages [26,35,108,221]. These agglomerates are shown schematically in Fig. 6:

1. The smaller particles called nuclei are about 10^2 Å in diameter. The nuclei are nonporous and
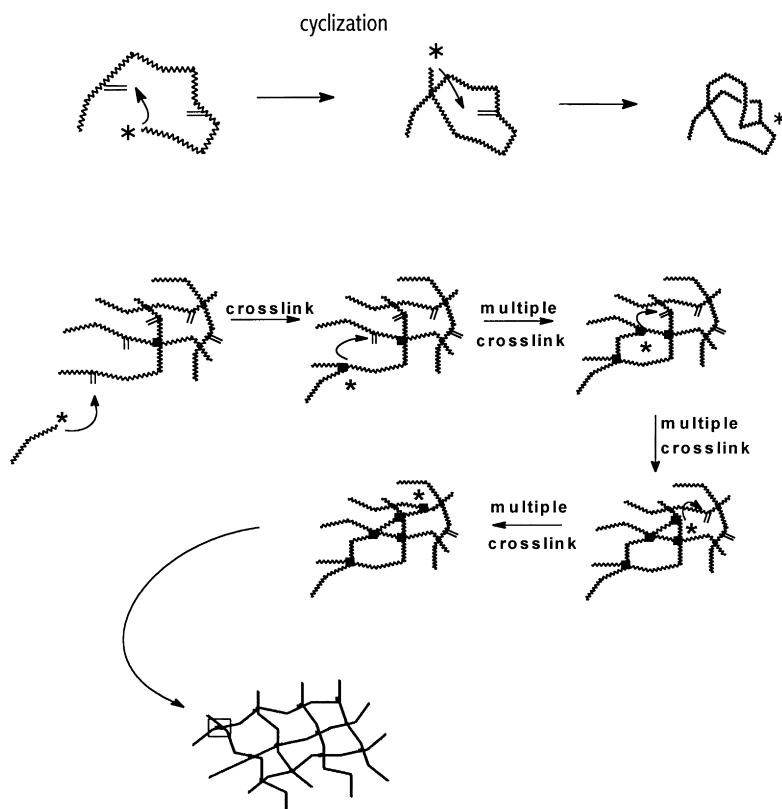
Fig. 7. Schematic representation of cyclization and multiple crosslinking reactions during FCC of vinyl/divinyl monomers leading to the formation of highly crosslinked regions in the final polymer network. ● = crosslink, ⊥ = pendant vinyl, ∗ = radical center.

constitute the highly crosslinked regions of the network. Micropores defined with widths of up to 20 Å appear between the nuclei.

2. The agglomerations of nuclei are called microspheres and they are about 10^3 Å in diameter. Mesopores constitute the interstices between the microspheres.
3. Microspheres are agglomerated again into larger irregular moieties of 2500–10,000 Å inside the polymer material. Meso and macropores appear between the agglomerates of the microspheres [119].

The nuclei are formed by cyclization reactions during the early stages of the polymerization at which the growing polymer chains are richer in DVB units [221]. In crosslinking polymerization of DVB or S–DVB in dilute toluene solutions, it was found that 30–60% of pendant vinyl groups are used by cyclization reactions and, on average, 100–800 multiple crosslinkages occur per one intermolecular crosslink formed [222]. Cyclization and multiple crosslinking reactions, as shown schematically in Fig. 7, are mainly responsible for the formation of compact nuclei in FCC of S–DVB copolymerization. The densely packed structure of nuclei due to the extensive cyclization and multiple crosslinking was manifested in the intrinsic viscosity $[\eta]$–weight-average molecular weight $\bar{M}_w$ plots of pre-gel polymers [222]. Fig. 8 shows such plots for polymers obtained at different reaction conditions. The slope of the
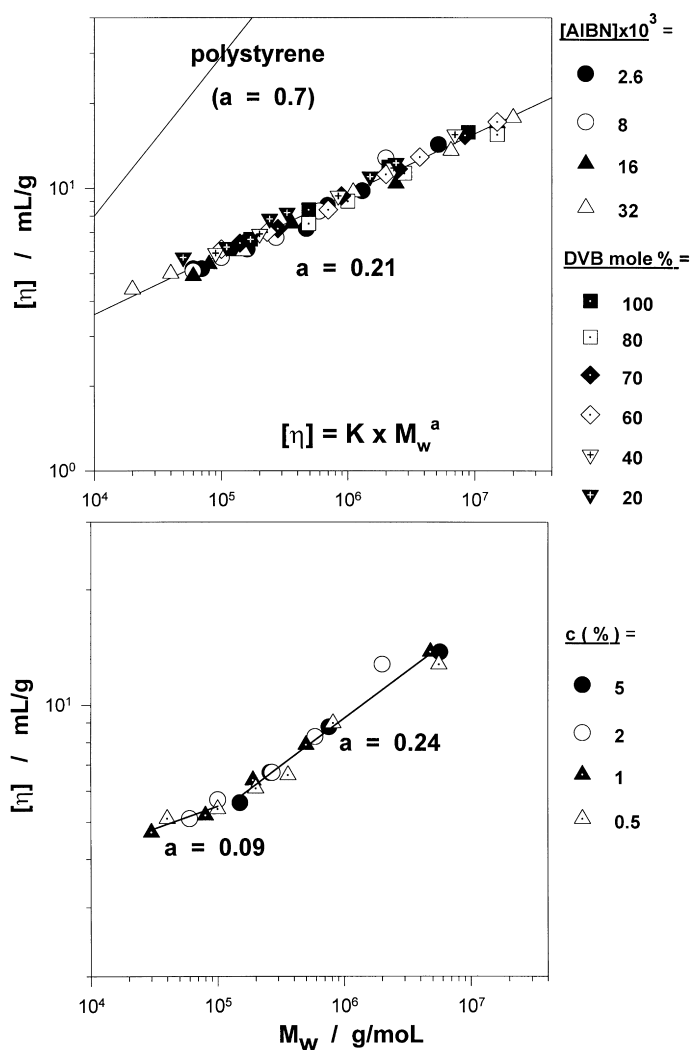
Fig. 8. Intrinsic viscosity $[\eta]$ versus $\bar{M}_w$ plots for pre-gel S–DVB copolymers formed in toluene as a diluent and at various reaction conditions. [222] The synthesis parameters varied were the initiator (AIBN) concentration, comonomer composition (DVB, mol%), and the initial monomer concentration (c, %). The slope of $[\eta]$ versus $\bar{M}_w$ curve approaches to 0 at low molecular weights ($\bar{M}_w < 10^5$ g/mol) due to the predominant cyclization and multiple crosslinking, and becomes 0.2 above this molecular weight, compared to the value of 0.7 for linear polystyrene in benzene.

double-logarithmic $[\eta]$–$\bar{M}_w$ plot is 0.2, which is between the value of massive spheres (0) and the unperturbed Gaussian chain (0.5).

After the formation of the compact nuclei, their agglomerations lead to microspheres with a relatively broad size distribution. Agglomerations of the microspheres result in the formation of the final network structure.

Depending on the synthesis parameters, these structural elements are more or less separated by holes. For example, the size and the swellability of the nuclei depend on the DVB concentration as well as on
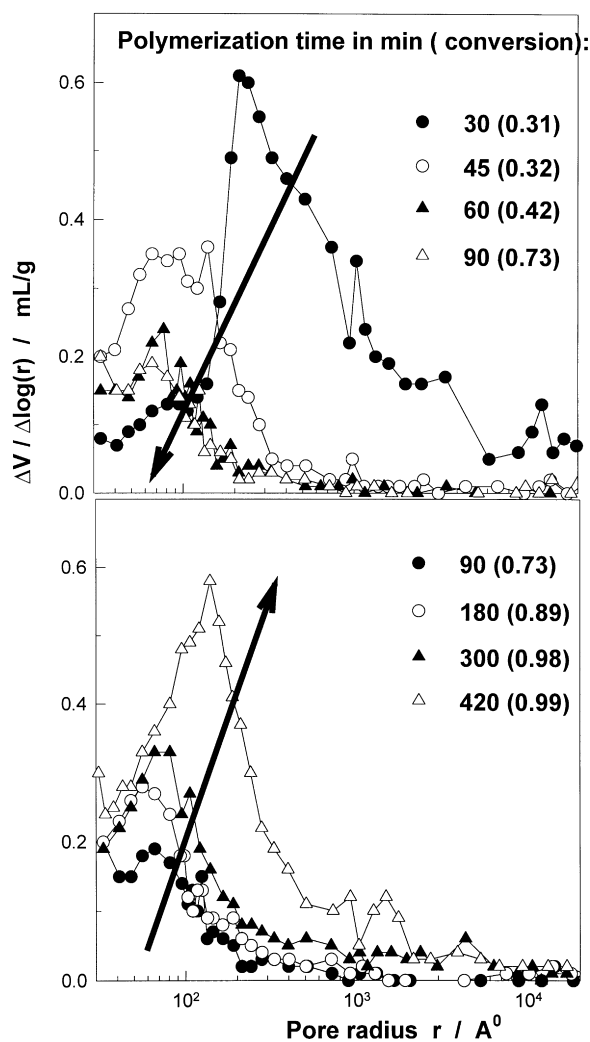
Fig. 9. Differential pore size distribution of S–DVB copolymer beads isolated at different reaction times. DVB = 10 mol%. $\nu_2^{00} = 0.50$. Diluent = cyclohexanol. The reaction times and the fractional monomer conversions (in parenthesis) are indicated in the figure.

the type and the amount of the diluent. At high DVB contents, the nuclei are highly intramolecularly crosslinked and largely unswollen [222]. Thus, increasing the crosslinker content in the copolymer synthesis creates rigid nuclei so that the number of micropores increases and their size decreases [108]. Since the main part of the specific surface area of a polymer bead comes from the surface of the nuclei, the factors decreasing the size of the nuclei or increasing their stiffness such as the crosslinker content increase the specific surface area of the beads. Moreover, in the presence of a large amount of a solvating diluent, polymerization is kinetically preferred within the nuclei because the local concentration of the monomers is higher than in the surrounding solution. As a consequence, loose and large nuclei form at high diluent concentrations that tend to be fused after synthesis. On the other hand, poor solvents
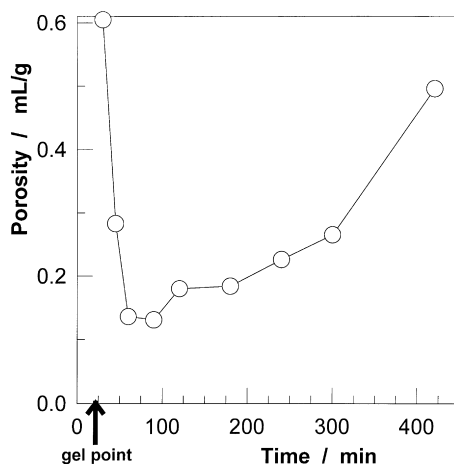
Fig. 10. Total porosity of S–DVB copolymers shown as a function of the reaction time. See caption of Fig. 9 for the reaction conditions.

or linear polymers as a diluent promote phase separation during the polymerization and facilitate formation of bigger clusters and thus, meso and macropores.

The development of the porous structures during FCC of S and DVB was recently studied using the mercury porosimetry [223]. Fig. 9 illustrates how the pore size distribution spectra of S–DVB copolymer networks vary depending on the polymerization time. The crosslinking reactions were carried out using 10 mol% DVB in the feed and cyclohexanol as a nonsolvating diluent. The initial volume fraction of the monomers in the organic phase (ν_2^{00}) was 0.5. Before drying of the copolymer samples for the porosity measurements, they were first swollen in toluene and then dried from methanol; thus, Fig. 9 represents the actual (swollen state) porosities of the samples [223].

At the very early stage of the copolymerization, the polymer was completely soluble in toluene. The first insoluble material appeared between a polymerization time of 20 and 25 min. The first sample for the porosity measurements was taken from the reactor after 30 min of polymerization. As seen from Fig. 9, this sample exhibits large number of meso and macropores of sizes 10^2–10^4 Å in radius. As the polymerization time increases from 30 to 90 min, (i.e. as the monomer conversion x increases from 0.3 to 0.7), the number of these pores decreases and finally disappears. This indicates that the pores of larger than 10^2 Å in radius appearing just beyond the gel point mainly form due to the unreacted monomers and the sol polymers acting as an intrinsic diluent of the reaction system. Since the extended continuing polymerization converts monomer and sol polymer to the gel, their sites (interparticle spaces) inside the network gradually fill up with the gel material, resulting in a decrease in porosity when the polymerization time is increased from 30 to 90 min.

Allowing polymerization to proceed from 90 to 420 min creates new pores of 40–100 Å in radius (Fig. 9). The number of these pores increases and the pore size distribution slightly shifts toward the larger pore sizes on increasing the polymerization time. The increase in the porosity is initially slight up to a polymerization time of 300 min but because ($x > 0.98$) is rapid after that. These results can be explained with the increasing crosslink density of the gel due to the reaction of pendant vinyl groups with macroradicals to form crosslinks and multiple crosslinks. Thus, the phase separated particles shrink and the voids between the particles increase as the reactions proceed.
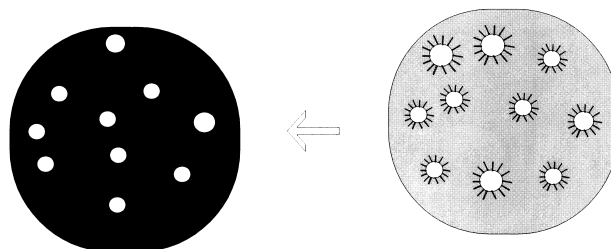
Fig. 11. Schematic representation of porosity formation in the presence of insoluble diluents such as water solubilized using surfactants in S–DVB monomer mixture.

In Fig. 10, the total porosities of these copolymers are shown as a function of the polymerization time. It is seen that the swollen state porosity first decreases on rising the post-gelation time due to decreasing degree of dilution of the gel phase. Thereafter, it increases continuously on rising the reaction time due to the increasing crosslink density of the gel. Kun and Kunin also observed that during the S–DVB copolymerization in the presence of *tert*-amyl alcohol as a diluent, the total porosity first decreases but then increases with increasing polymerization time while the specific surface area of the beads continuously increases [221]. It must be noted that the scheme given above for the porosity formation can only be applied if the diluent is soluble in the monomer mixture. Otherwise, for monomer-insoluble diluents such as water solubilized using surfactants in S–DVB monomer mixture, the pore structure of the final material depends only on the size and the size distribution of the water droplets in the starting monomer phase (Fig. 11).

4. Porous structure versus synthesis parameters

The total volume of pores inside a crosslinked polymer as well as their size distribution can be varied by changing the independent variables of synthesis. The sensitive dependence of the properties of the porous structure on the synthesis parameters allows one to design a tailor-made macroporous material for a specific application. The main experimental parameters are the type and the amount of the diluent, the crosslinker concentration, the polymerization tempera-ture and the type of the initiator.

4.1. Effect of the diluent

Porous structures start to form when the amount of the diluent and and the amount of the crosslinker pass a critical value. The solvating power of the diluent has a critical effect on the porous structure of macroporous copolymers. Note that the net solvating power of the medium (unreacted monomer mixture + diluent) changes during the course of the reaction as the monomers become consumed and this change is particularly severe where the diluent is a nonsolvent for the copolymer. There are three methods to prepare macroporous S–DVB copolymer networks: [23]

1. Addition of a solvating diluent (SOL) such as toluene or dichloroethane produces small average pore diameter and therefore a considerable specific surface area (50–500 m^2/g) and a relatively low pore
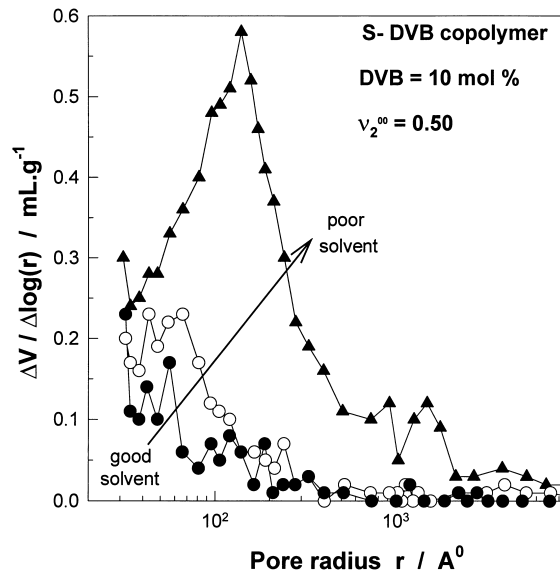
Fig. 12. Effect of the solvating power of the diluent on the pore size distribution of macroporous S–DVB copolymers. $\nu_2^{00} =$ 0.50. DVB = 10%. Diluent = toluene (●), cyclohexanol/toluene (75/25 v/v) (○), and cyclohexanol (▲).

volume (up to about 0.8 ml/g). The pore size distribution of the network is characterized by a large proportion of micro and mesopores.

2. Addition of a nonsolvating diluent (NONSOL) such as *n*-heptane or alcohols results in a large pore volume (0.6–2.0 ml/g), a relatively large average pore diameter and a specific surface area varying from 10 to 100 m^2/g. The pore size distribution of the networks is characterized by a large proportion of meso and macropores.

3. Addition of a polymeric diluent (POLY) such as linear polystyrene produces a pore volume up to about 0.5 ml/g, a specific surface area of 0.1 to 10 m^2/g and very large pores reaching the micrometer range.

These experimental findings are expected from the mechanism of the pore structure formation given in the previous section. Note that the values given above only show the general tendencies and, depending on the DVB concentration, they change considerable. For instance, in the presence of NONSOL diluents, macroporous S–DVB copolymers with a specific surface area up to 900 m^2/g can be synthesized at very high crosslinker concentrations [224]. A very large number of experimental data have been reported in the literature. These data demonstrate the effect of various diluents on the pore structure of crosslinked polymers formed by free-radical crosslinking copolymerization. Some of the diluents used in S–DVB copolymerization are collected in Table 2. From the diluents used, cyclohexanol is one of the most efficient diluents for building up the highest porosity even at low amounts of DVB [99,101]. The effect of the type of the diluent is also reflected in the appearance of the surface of S–DVB copolymer beads. Decreasing the solvating power of the diluent changes smooth surfaces to rough surfaces having large and irregularly distributed channels [114].

Fig. 12 illustrates how the pore size distribution of S–DVB copolymer beads with 10% DVB varies with the solvating power of the diluent [225]. Toluene, cyclohexanol/toluene (3/1; v/v) and
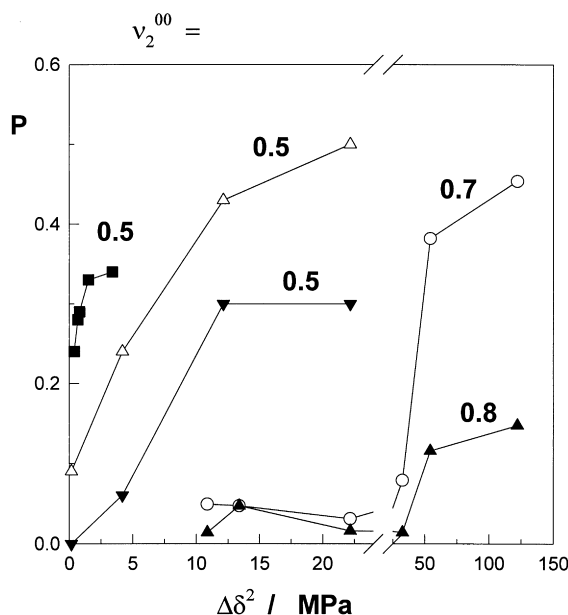
Fig. 13. The total porosity P of S–DVB copolymer networks shown as a function of the diluent quality $\Delta \delta^2 = (\delta_1 - \delta_2)^2$, where δ_1 and δ_2 are the solubility parameters of the diluent and the polymer, respectively. The initial volume fraction of the monomer ν_2^{00} is shown in the figure. Experimental data points are from Seidl et al, [23] Wieczorek et al. [226], and Okay. [101,102] The curves only show the trend of the data. Diluent = aliphatic alcohols of various chain length [23], DVB = 20%, $\nu_2^{00} = 0.70$ (○), and 0.80 (▲). Diluent = toluene/cyclohexanol mixtures [101,102], $\nu_2^{00} = 0.50$, DVB = 10 (▼) and 25% (△); Diluent = n-heptane/toluene mixtures [226], $\nu_2^{00} = 0.50$, DVB = 50% (■).

cyclohexanol were used as a diluent at a fixed concentration ($\nu_2^{00} = 0.50$). Toluene is known to be a good solvent for polystyrene and its thermodynamic properties are roughly the same as the monomers. Cyclohexanol has a solubility parameter value of 23.3 $(MPa)^{1/2}$ in contrast to the value of 18.6 $(MPa)^{1/2}$ for polystyrene which indicates that cyclohexanol is a nonsolvating diluent for S–DVB copolymerization. By passing from toluene to cyclohexanol as a diluent, i.e. by decreasing the solvating power of the diluent, the number of meso and macropores (>20 Å) significantly increases. Also, the average pore size becomes larger and larger and the pore size distribution shifts toward the larger pores on worsening of polymer–diluent interactions. This is a consequence of a change in the mechanism of pores formation from ν- to χ-induced syneresis.

In Figs. 13 and 14, some of the reported total porosity P data of S–DVB copolymer networks are collected. This data is presented as a function of the quality and the amount of the diluent, respectively. The diluent quality is represented by the square of the differences in the solubility parameters of the diluent and the copolymer, i.e. $\Delta \delta^2 = (\delta_1 - \delta_2)^2$. Experimental data are for different diluents, i.e. aliphatic alcohols of various chain length, [23] toluene/cyclohexanol, [101,102] and toluene/n-heptane mixtures [226,227] of various compositions. For a fixed monomer dilution ν_2^{00}, the total porosity P increases on decreasing the polymer–solvent interactions during the gel process of formation (Fig. 13). The increase in P is initially rapid and then it increases slightly on increasing the $\Delta \delta^2$ parameter value of the diluent. For a given type of diluent, the porosity increases with increasing degree of monomer dilution up to $\nu_2^{00} = 0.3$ (Fig. 14). In the
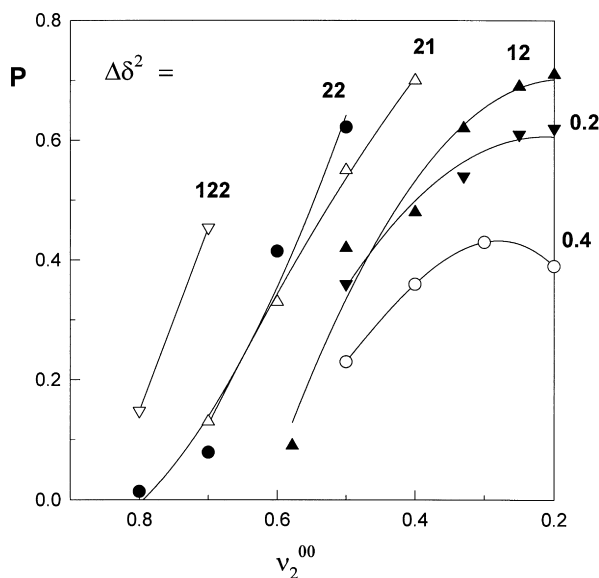
Fig. 14. The total porosity P of S–DVB copolymer networks shown as a function of the monomer dilution ν_2^{00}. The difference between the solubility parameters of the diluent and the polymer (in MPa) is shown in the figure Experimental data points are from Seidl et al. [23], Wieczorek et al. [226], Okay [102], and Jun et al. [227]. The curves only show the trend of the data. DVB = 20%, diluent = methanol [23] (▽), *n*-butanol [23](●), isooctane [23] (△), and toluene/cyclohexanol (1/3) mixture [102] (▲). DVB = 50%, diluent = *n*-heptane/ toluene (1/9) mixture [226] (○). DVB = 98.4%, diluent = toluene [227] (▼).

region of $\nu_2^{00} < 0.3$, experimental data indicate that the rate of increase in the porosity slows further with an additional dilution the monomer. This is attributable to the fact that the polymer networks formed at a low monomer concentration cannot hold the isochoric condition due to the loose network structure. Consequently, the pores in such networks collapse upon drying or upon removal of the diluent. Both the swelling measurements and inverse gas chromatography also suggest that the S–DVB copolymers prepared in the presence of a large amount of diluent have a looser structure than those obtained with less diluent [228].

The extent of solvation of the macroporous S–DVB copolymers dependence on the type of the diluent was studied by Shea et al. using fluorescence technique [229,230] using macroporous networks with a dansyl probe covalently attached to the gel structure. Their data indicate that the gel phase of highly crosslinked macroporous networks prepared using a solvating diluent is much more accessible to solvents and nonsolvents than those prepared using a nonsolvating diluent. These results can be rationalized on the basis of formation of smaller internal agglomerates in the presence of solvating diluents resulting in increases of the gel phase surface area.

The crosslinking polymerization of trimethylolpropane trimethacrylate (TRIM) in the presence of toluene as a solvating diluent produces macroporous networks having two pore size distributions; [84] one consisting of small pores (radius <50 Å) and one of large pores (radius >50 Å). The size distribution of the small pores shows a very sharp peak at 20 Å indicating that the polymer has a very regular structure on the microlevel, probably attributable to the structure of the TRIM monomer [84].

Different diluent types in various combinations can be used to regulate the pore size distribution of the copolymers [35,98,105,111,113,116,117]. For instance, by varying the composition
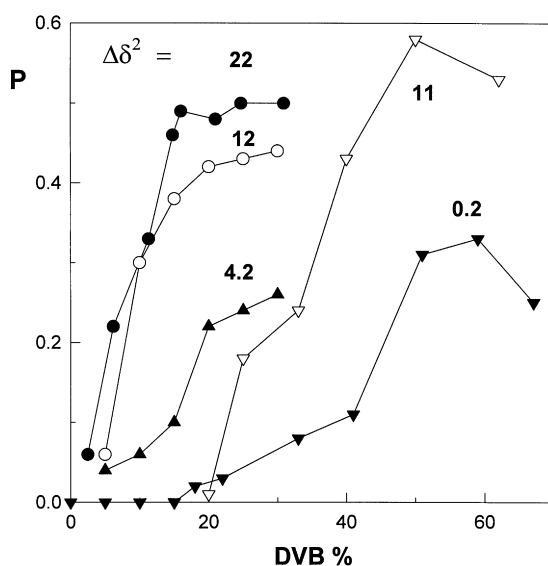
Fig. 15. The total porosity P of S–DVB copolymer networks shown as a function of the DVB concentration. The difference between the solubility parameters of the diluent and the polymer (in MPa) is shown in the figure. Experimental data points are from Poinescu et al. [112], and Okay [101,102]. The curves only show the trend of the data. $\nu_2^{00} = 0.50$, diluent = cyclohexanol [101] (●), toluene/cyclohexanol (1/3) [102] (○), toluene/cyclohexanol (1/1) [102] (▲), toluene [101] (▼). $\nu_2^{00} = 0.40$, diluent = toluene/gasoline (1/100) [112] (V).

of a 2-ethyl-1-hexanol/toluene diluent mixture at a given degree of monomer dilution and DVB content, the average diameter of the pores in S–DVB copolymers can be varied between 54 and 237 Å [111]. In general, increasing the SOL content of a SOL/NONSOL diluent mixture, produces smaller pores and thereby increases the internal surface area although the total volume of the pores decreases. In the presence of 2-ethyl-1-hexanol/n-heptane diluent mixture, porosity versus diluent composition plot shows a minimum at a 1:1 volume ratio of the diluent composition, at which the solubility parameter of the diluent mixture approaches that of the S–DVB network [110]. In HEMA–EGDM copolymerization using cyclohexanol/dodecanol as a SOL/NONSOL diluent mixture, it was found that the porosity of macroporous poly (HEMA) beads can be readily adjusted by changing the diluent composition [65].

Several combinations of a polymeric diluent with solvating or nonsolvating diluents (SOL/POLY or NONSOL/POLY) have been used for the synthesis of macroporous S–DVB networks. At a constant DVB content, the specific surface area and the pore volume of polymer particles prepared using only linear polymer (POLY) as a diluent are much lower than the particles prepared with a mixture of linear polymer and solvent (SOL/POLY) or nonsolvent (NONSOL/POLY) as diluents [119]. Similar results were observed in macroporous GMA/EGDM networks [60]. In GMA–EGDM copolymerization, at a high EGDM content, addition of POLY to SOL decreases the specific surface area and shifts the pore size distribution to larger pores [60]. The role of high molecular weight linear polymers as an inert diluent is to create macropores, whereas addition of SOL or NONSOL diluents enhances the phase separation and structural heterogeneity. In turn this leads to higher specific surface area and pore volume of the porous particles [119]. It was also shown that, in S–DVB copolymerization, increasing the amount of SOL in SOL/POLY diluent mixture increases the pore volume without changing the pore size
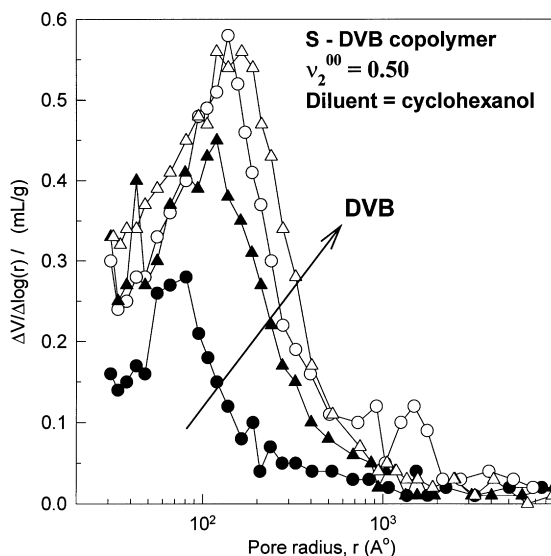
Fig. 16. Effect of the DVB concentration on the pore size distribution of macroporous S–DVB copolymers. $\nu_2^{00} = 0.50$. Diluent = cyclohexanol. DVB = 5 (●), 10 (○), 17.5 (▲), and 24% (△).

distribution [35]. Smaller average pore sizes were obtained using NONSOL/POLY diluents than POLY or SOL/POLY diluents [119].

The molecular weight and the molecular weight distribution (MWD) of polymeric diluents significantly effect the structure of macroporous particles. For example, decreasing molecular weight of POLY in SOL/POLY or NONSOL/POLY diluent mixtures shifts the pore size distribution toward smaller pores increases the specific surface area, whereas the total volume of the pores remains constant [60,117,119]. It was also shown that the shape of the pore size distribution depends on the MWD of POLY diluent. [119] The pore size distribution is narrowest for the linear polymer with the narrowest MWD, whereas broad pore size distributions can be obtained using linear polymers with a broader MWD [119]. This demonstrates the extreme sensitivity of the pore size distribution on the molecular weight of the polymeric diluent.

4.2. Effect of the crosslinker

In Fig. 15, some experimental total porosity data of S–DVB networks published in the literature [101,102,112] are collected and are shown as a function of the DVB concentration. It is seen that, at a given degree of monomer dilution and the diluent quality, the porosity increases on raising the DVB concentration and then remains constant. The maximum value of the total porosity that can be achieved at a given monomer dilution can be predicted from the reaction conditions, as will be explained in the following section. The slight decrease in the porosity above 60% DVB is due to the destruction of the rigid pore structure during the polymerization or during the measurements.

Fig. 16 illustrates how the pore size distribution of S–DVB copolymers varies with the DVB concentration at a fixed monomer concentration [225]. Increasing the DVB content increases the number of meso and macropores. The specific surface area of porous networks, which is an indicator for the
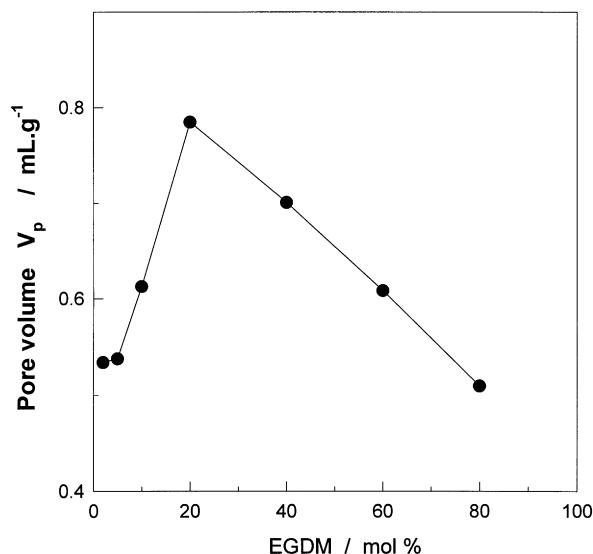
Fig. 17. Pore volume of HEMA–EGDM copolymer networks shown as a function of the crosslinker (EGDM) concentration. Diluent = toluene. $\nu_2^{00} = 0.5$.

number of micropores increases with increasing DVB content. [106] A high concentration of DVB is necessary to get a high surface area. [108] For example in the presence toluene as a diluent, copolymers with a specific surface area as high as $1100 \text{ m}^2/\text{g}$ can be synthesized using 70 mol% DVB in the feed. [224] The meso and macropores account for most of the surface area if the DVB content is less than 20%, but their contribution diminishes as the DVB concentration increases [108]. When the amount of the DVB decreases, the size of the microspheres and the nuclei decreases and the microspheres tend to be slightly fused [108].

It must be pointed out that there are some comonomer systems such as acrylonitrile (AN)/DVB [40–42] or methacrylic acid (MA)/DVB [71–73] that do not follow the above relationship. In these systems, increasing the amount of DVB decreases the porosity of the polymer beads, which is exactly opposite to the relationship between the porosity and the crosslinker content observed in S–DVB system. For example, the crosslinking copolymerization of AN and DVB yields macroporous networks regardless of the crosslinker content [43]. This behavior is due to the different reactivities and thermodynamic properties of the monomers. Both AN and MA are less reactive than the monomer DVB for the copolymerization so that the polymer formed at the initial stages of polymerization contains more DVB units than in the monomer mixture. Since both AN and MA monomers are poor solvents for the DVB microgels, as the fraction of AN or MA in the system increased, the earlier the phase separation or precipitation of microgels occurs. Thus, in such systems, the monovinyl monomers AN or MA act as an intrinsic nonsolvating diluent so that decreasing crosslinker content increases the porosity of the final material [72]. Therefore, addition of AN in S–DVB comonomer system increases the porosity of copolymer networks. [231]

Another interesting pore-forming system is the crosslinking copolymerization of HEMA and EGDM in the presence of toluene as a diluent; [64] here, the total volume of the pores first increases with increasing crosslinker (EGDM) content up to 20 mol% but then it decreases continuously (Fig. 17). This

Table 3
Solubility Parameter, δ, of the monomers, polymers, and the diluent toluene in HEMA-EGDM copolymerization

Component	δ (MPa)$^{1/2}$
HEMA	23.3
EGDM	18.2
Poly(HEMA)	29.7
Poly(EGDM)	19.2
Toluene	18.2

behavior was explained based on the thermodynamic properties of the monomers, toluene and the copolymer [64]. Table 3 shows the solubility parameter δ of the monomers, polymers and the diluent. Fig. 18 provides a plot of the variation $(\delta_1 - \delta_2)^2$ during the course of HEMA–EGDM copolymerization depending on the initial EGDM concentration and on the monomer conversion. Note that δ_1 represents the solubility parameter of the unreacted monomers–diluent mixture in the reaction system. It is seen that at low EGDM contents, the residual monomer–toluene mixture is a nonsolvent for the growing copolymer chains, whereas it becomes a good one as the EGDM concentration increases. At higher EGDM content, $(\delta_1 - \delta_2)^2$ is closely matched so that a phase separation during the copolymerization may only occur as a consequence of the increasing crosslink density of the copolymer chains. Accordingly, the porous structures formed at low EGDM contents are due to the polymer–(diluent + monomers) incompatibility in the polymerization system (χ-induced syneresis), whereas at higher EGDM contents, due to the increasing degree of crosslinking (ν-induced syneresis). This is a result of the different solubility parameters of the monomer HEMA and the crosslinker EGDM [64].
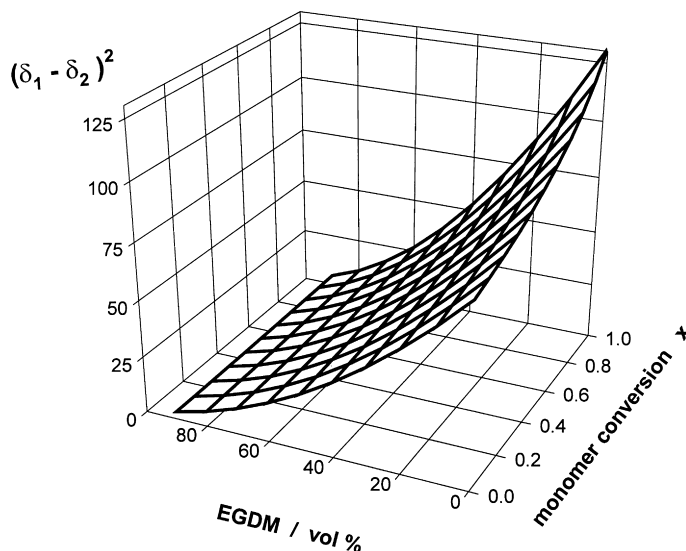

Fig. 18. Variation of $(\delta_1 - \delta_2)^2$ during the course of HEMA–EGDM copolymerization in the presence of toluene as a diluent depending on the initial EGDM concentration and on the monomer conversion.
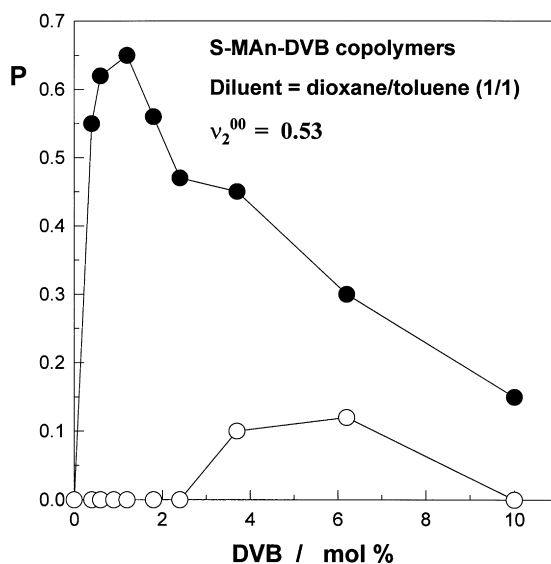
Fig. 19. Variation of the porosity P in S–MAn–DVB copolymerization depending on the crosslinker (DVB) concentration.

In the crosslinking copolymerization of maleic anhydride (MAn)–S–DVB and using a dioxane–toluene mixture as a diluent, it was found that the porous structures start to form at a very low degree of the crosslinker content [69]. The filled symbols in Fig. 19 illustrate the total porosity of the MAn–S copolymers plotted as a function of the DVB concentration in the feed. The MAn content in the starting monomer mixture is 40 mol%. The porosity increases abruptly and approaches 65% at 1.2% DVB. A further increase in the DVB concentration results in a decrease in the porosity. The results was explained based on the formation of rigid copolymer chains due to the MAn repeat units, which accelerates the phase separation during the crosslinking process. The decrease in the porosity above 1.2% DVB is due to the destruction of the rigid pore structure during the polymerization or during the measurements. Interestingly, the porous structures formed below 3% DVB are absent if the copolymers are dried in a swollen state (open symbols in Fig. 19). This unstable pore structure results from to the low crosslink density of the networks; since the connections between the phase separated nuclei are loose, the pores between the nuclei disappear during drying in the swollen state [69].

4.3. Effect of the temperature and the initiator

The effect of the polymerization temperature on the porous structure of glycidyl methacrylate (GMA)–EGDM networks was studied by Svec and Frechet using cyclohexanol/dodecanol mixture as a diluent [232]. It was shown that although the total volume of the pores does not change much in the temperature range 60–90°C, the size distribution of pores varies significantly with temperature. Increasing the temperature shifts the pore size distribution towards smaller pores [232]. The higher the temperature, the smaller the pores. Since the specific surface area is mainly determined by the number of small pores, increasing the polymerization temperature also increases the specific surface area. A similar effect of the polymerization temperature on the pore size has been observed in AAm/BAAm copolymerization
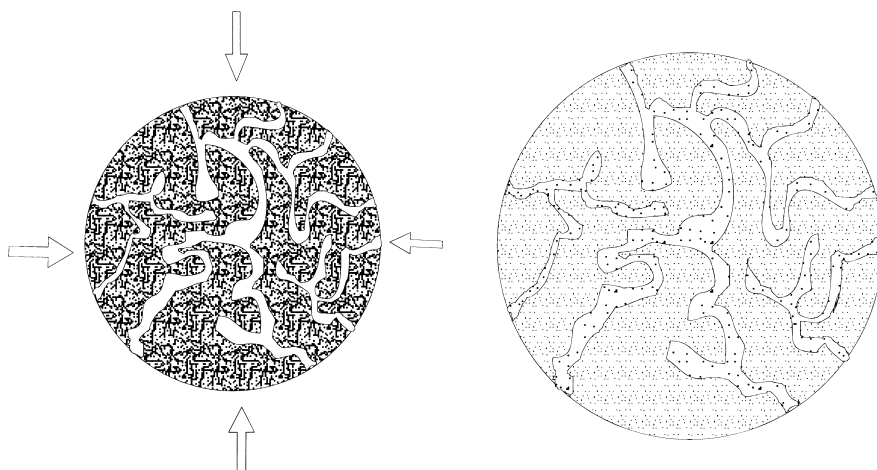
Fig. 20. Schematic representation of a macroporous bead before and after swelling.

using DMSO/alcohol mixtures as a diluent [38]. The polymerization temperature-porous structure rela-
tion is a consequence of the increasing decomposition rate of the initiator on increasing the temperature
[232]. The higher the reaction temperature, the greater the number of free-radicals generated per unit
time and the greater the number of nuclei and microspheres formed. Increasing the number of nuclei and
microspheres necessarily decreases their size so that smaller voids between them appear in the final
copolymer. In contrast, if the polymerization temperature is low, the rate of polymerization is slow and
the transfer of a substantial part of the monomers from solution in the nuclei can occur, which results in
the growth of the nuclei in larger sizes [232]. Note that increasing the solvating power of the diluent by
increasing the temperature may also contribute to the shift of the pore size distribution towards smaller
pores. In the polymerization of trimethylolpropane trimethacrylate (TRIM) in toluene, it was also found
that increasing the polymerization temperature increases the total volume of the pores smaller than 30 Å,
i.e. the specific surface area of the polymers is increased [87].

Owing to the same reason, increasing the decomposition rate of the initiator (e.g. using AIBN as an
initiator instead of benzoyl peroxide) decreases the size of the pores at a given polymerization tempera-
ture due to the increasing rate of polymerization [232].

It was also shown that the isothermal polymerization condition provides a much narrower distribution
of pore sizes than in the nonisothermal polymerization [213]. Similar results were reported by Takeda et
al. [120]. They conducted the S–DVB copolymerization by rising the polymerization temperature from
20 up to 90°C. As the time for raising the temperature from 20 to 90°C becomes shorter (i.e. as the
polymerization rate becomes faster), products with a broader size distribution of pores and with smaller
mean diameters are obtained [120].

5. Relation between the swelling degree and the porosity

Fig. 20 represents schematically a crosslinked porous bead before and after immersion in a solvent.
During the swelling process, the channels (pores) inside the bead are rapidly filled with the solvent; at the

same time, the network region takes up solvent from the environment whose extent depends on the attractive force between the solvent molecules and the network segments. The two separate processes thus govern the swelling of a heterogeneous network.

5.1. Solvation of network chains

The main driving force of the solvation process is the changes in the free energies of mixing and elastic deformation during the expansion of the network. The extent of network solvation is determined by the crosslinking density of the network, by the degree of dilution after the gel preparation, and by the extent of the interactions between solvent molecules and the network chains. The Flory–Rehner theory gives the following well known relation between the equilibrium swelling ratio of the gels and their structural parameters [233]:

$$\ln(1 - v_2) + v_2 + \chi v_2^2 + N^{-1}(v_2^{1/3} v_2^{0^{2/3}} - v_2/2) = 0 \tag{10}$$

where v_2 is the volume fraction of polymer in the equilibrium swollen hydrogel, i.e. the inverse of the volume swelling ratio q_v (volume of swollen gel/volume of dry gel), χ is the polymer–solvent interaction parameter, N is the number of segments between two successive crosslinks of the network, and v_2^0 is the volume fraction of polymer network after preparation. According to Eq. (10), the equilibrium swelling degree of a network in a given solvent increases as the crosslink density N^- [1] or the monomer concentration at the gel preparation v_2^0 decreases.

5.2. Filling of voids (pores) by the solvent

The extent of swelling due to the filling of the pores by the solvent depends on the total volume of (open) pores, i.e. on the volume of the diluent separated out of the network phase during the crosslinking copolymerization.

Note that the equilibrium weight swelling ratio q_w (mass of swollen gel/mass of dry gel) includes the amount of solvent taken by both of these processes, i.e. q_w includes the solvent in the gel as well as in the pore regions of the network. Thus, both the solvation and filling processes are responsible for the q_w values of macroporous networks. On the contrary, if we assume isotropic swelling, that is the volume of the pores remains constant upon swelling, volume swelling ratio q_v of heterogeneous networks is caused by the solvation of the network chains, i.e. by the first process. Thus, q_v only includes the amount of solvent taken by the gel portion of the network. Accordingly, relative values of q_w and q_v of heterogeneous networks together with the degree of monomer dilution used in the gel preparation provides information about the distribution of the diluent between the gel and diluent phases at the end of the network formation process, and can be used in the calculation of the pore volume of the networks.

The distribution of the diluent in the network structure after its formation, the networks can be classified into three groups: [234]

1. *Expanded (preswollen) networks.* Expanded network structures are obtained if the diluent present during the network formation remains in the gel throughout the polymerization (Gel B in Fig. 2). Expanded networks are thus nonporous. During the removal of the diluent or during drying, the expanded network collapses, but reversibly. Addition of a good solvent allows it to reexpand to its

earlier state. Both the weight and volume degrees of swelling of expanded networks increase with increasing dilution due to the increasing solvation of the network chains.

2. *Heterogeneous dry networks.* The diluent separates totally out of the network phase during the polymerization and acts only as a pore-forming agent. The increase in the weight-swelling ratio with increasing dilution is due to the increasing volume of the pores, which are filled by the solvent. Since the diluent exists as a separate phase during the polymerization, the effects of cyclization and change in the contents of trapped entanglements on the network structure can be neglected. Thus, the volume degree of swelling does not change with the degree of dilution.

3. *Heterogeneous swollen networks.* The diluent separates partially out of the network phase during the polymerization. Thus, it distributes between network and diluent phases after synthesis. A part of the diluent acts as a pore-forming agent, whereas the other part remains in the network structure and increases its volume degree of swelling.

The experimental data on macroporous networks indicate that the weight swelling ratio q_w of the networks in solvents is a linear function of the monomer dilution concentration used in the gel preparation [104,107]. The linear relation between the equilibrium weight swelling ratio of the networks and the monomer concentration was first observed by Millar in S–DVB copolymer networks prepared using toluene as a diluent and is given by [19]:

$$U = U_0 + S_d \tag{11}$$

where U and U_0 are the solvent regains for the networks prepared with and without using a diluent (both in ml/g), and S_d is the volume of the diluent added per gram of the monomers. In terms of the weight swelling ratio q_w Eq. (11) can also be written as:

$$q_w = q_{w,0} + rd_1/d_M \tag{12}$$

where $q_{w,0}$ is the equilibrium weight-swelling ratio of the network prepared without using a diluent, r is the volume of the diluent added per ml of the monomers, d_1 and d_M are the densities of the swelling agent and the monomers, respectively.

On the other hand, assuming isotropic swelling, the volume swelling ratio of the networks, q_v, can be calculated from their weight swelling ratio, q_w, and apparent density, d_0, as follows: [235,236]

$$q_v = d_0\left(\frac{1}{d_2} + \frac{q_w - 1}{d_1}\right) \tag{13}$$

where d_2 is the density of the homogeneous polymer. Substitution of Eq. (12) into Eq. (13) leads to:

$$q_v = \frac{d_0}{d_2}(q_{v,0} + rd_2/d_M) \tag{14}$$

where $q_{v,0}$ is the value q_v of the network prepared in the absence of a diluent (volume swelling ratio of homogeneous networks). Since the porosity P relates to the apparent density through Eq. (8), using Eqs. (8) and (14) the porosity of the networks can be calculated as [234,237]:

$$P = 1 - \frac{q_v}{q_{v,0} + rd_2/d_M} \tag{15}$$

Eq. (15) predicts the porosity of the networks from the volume swelling ratio of heterogeneous (q_v) and
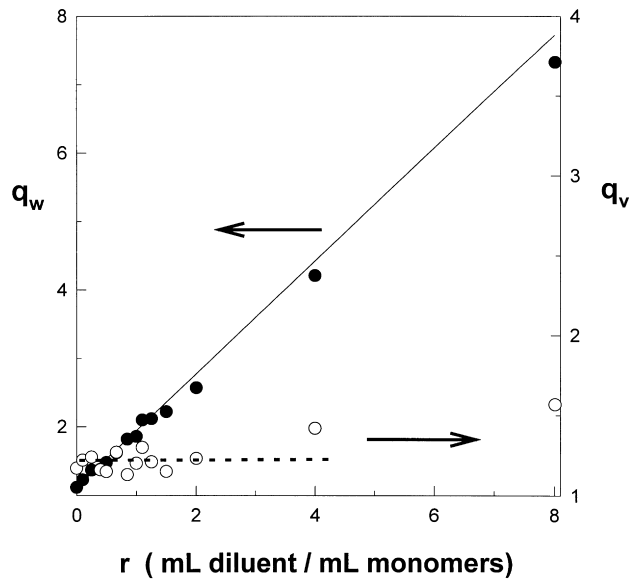
Fig. 21. Dependencies of the weight (●) and the volume (○) swelling ratios (q_w and q_v, respectively) on the degree of monomer dilution r for EGDM networks formed in toluene. The solid line was calculated using Eq. (12).

corresponding homogeneous networks ($q_{v,0}$) and from the degree of monomer dilution (r). The only assumption inherent in the derivation of Eq. (15) is the isotropic swelling condition of the networks.

Eqs. (14) and (15) predicting the volume swelling ratio and the porosity of the networks can be simplified for two limiting cases given below:

- In the case of heterogeneous dry networks, since the diluent separates totally out of the gel phase, the volume swelling ratio of heterogeneous network is equal to that of the corresponding homogeneous network, i.e.

$$q_v = q_{v,0} \tag{16a}$$

and Eq. (15) reduces to

$$P = \frac{1}{1 + c/r} \tag{16b}$$

where $c = q_{v,0} d_M / d_2$ and is fixed for a given crosslinker content.
- The other limit of interest is the expanded gel in which the diluent remains in the gel phase. In this case

$$P = 0 \tag{17a}$$

and Eq. (14) gives the volume swelling ratio of expanded gels as
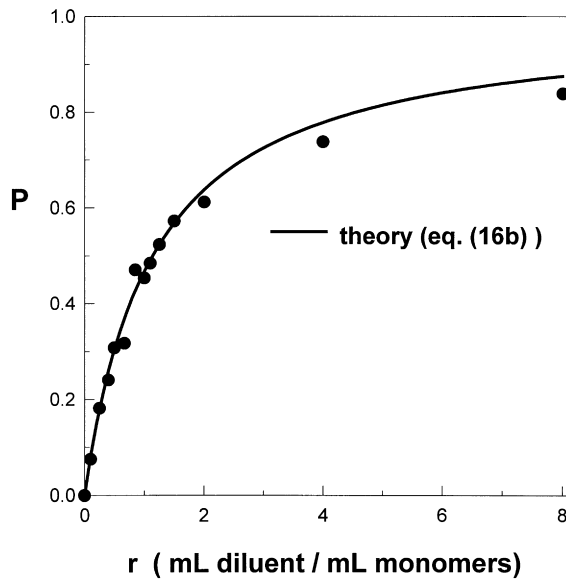
$$q_v = q_{v,0} + r(d_2/d_M) \tag{17b}$$

Fig. 22. Variation of the porosity of EGDM networks formed in toluene with the degree of monomer dilution. The solid curve was calculated using Eq. (16b).

Experimental verification of the equations given above has been reported for S–DVB copolymer networks as well as for ethylene glycol dimethacrylate (EGDM) networks [101–103,234]. The filled symbols in Fig. 21 shows q_w values of macroporous EGDM networks plotted as a function of the monomer dilution r [234]. The solid line was calculated using Eq. (12) and for $q_{w,0} = 1.12$, $d_1 = 0.867$ g/ml, and $d_M = 1.05$ g/ml. It is seen that Eq. (12) correctly predicts the weight swelling ratio of macroporous networks up to a dilution degree of $r = 2$ ml diluent/ml monomer. The slight deviation at high dilutions may be a result of experimental error or of a loss of a small fraction of the diluent during the network formation process.

Measurements of the total porosity P of the EGDM network samples reported in Ref. [234] are shown in Fig. 22 as experimental points plotted as a function of the monomer dilution r according to Eq. (16b). It is seen that the change in the values of P is at first abrupt and then slowly increases as the monomer dilution increases. Satisfactory agreement between the calculated $P - r$ dependence and the results from measurements is observable at diluent concentrations between $r = 0$ and 2, indicating that all the diluent (toluene) separates out of the network phase during the course of the polymerization. Indeed, the equilibrium volume swelling ratio q_v for these networks are almost constant and is equal to 1.20 ± 0.06 with respect to the value $q_{v,0} = 1.17$ (open symbols in Fig. 21). At high dilutions, it is reasonable to expect that a part of the diluent remains in the gel phase after synthesis due to the good solvating character of the diluent toluene for EGDM polymers. This causes an increase in the volume swelling ratio (Fig. 21) and, according to Eq. (15), a decrease in the slope of $P - r$ dependence, as observed for diluent concentrations above $r = 2$ (Fig. 22).
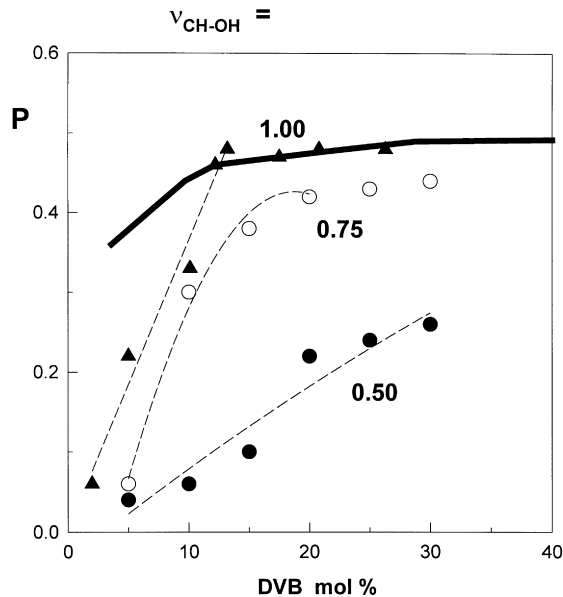
Fig. 23. Variation of the total porosity P with the DVB concentration in S–DVB copolymerization. Diluent = toluene/cyclo-hexanol mixture of various compositions represented by ν_{CH-OH} (volume fraction of cyclohexanol in the diluent mixture). The solid curve was calculated using Eq. (16b). The dashed curves show the trend of the data points.

In Fig. 23, the total porosities P, of S–DVB copolymer networks prepared at a fixed monomer dilution ($r = 1.00$) are shown as a function of the DVB concentration. Cyclohexanol (CH–OH)–toluene mixtures of various compositions were used as the diluent in the network synthesis [101–103]. Increasing the volume fraction of CH–OH, ν_{CH-OH}, in the diluent mixture increases the total porosity of the networks at a given DVB concentration (Fig. 23). The solid curve in Fig. 23 was calculated using Eq. (16b); thus, it assumes that all the diluent separates out of the gel phase during the network formation and it predicts the maximum porosities. It is seen that with the exception of the networks prepared at $\nu_{CH-OH} = 1.00$ and equal to more than 12.5 mol% DVB, the experimental measured porosities remain below those predicted by Eq. (16b) indicating that the separated copolymers during the network formation process are more or less swollen with the diluent mixture. From Figs. 21–23, it is seen that heterogeneous dry networks can be obtained at high crosslinker contents or, at medium crosslinker contents and using nonsolvating diluents.

These plots show that Eq. (15) correctly predicts the total porosity of macroporous networks from their volume swelling ratio and synthesis parameters (crosslinker and diluent concentrations) and also confirm the validity of isotropic swelling condition in macroporous networks. The 3D plots shown in Fig. 24 illustrate the dependence of the total porosity P of the networks on the monomer dilution r and on the reduced volume swelling ratio $q_v/q_{v,0}$, as predicted by Eq. (15). Calculations were for two different $q_{v,0}$ values, i.e. for two different crosslinker contents. It is seen that the heterogeneity in the networks appears after passing a critical degree of monomer dilution r; this critical value strongly depends on the $q_{v,0}$ values, i.e. on the volume swelling ratio of the corresponding homogeneous networks. Since $q_{v,0}$ depends inversely on the crosslinker content used in the network synthesis, increasing crosslinker concentration increases the porosity of the networks formed at a given monomer dilution. Another
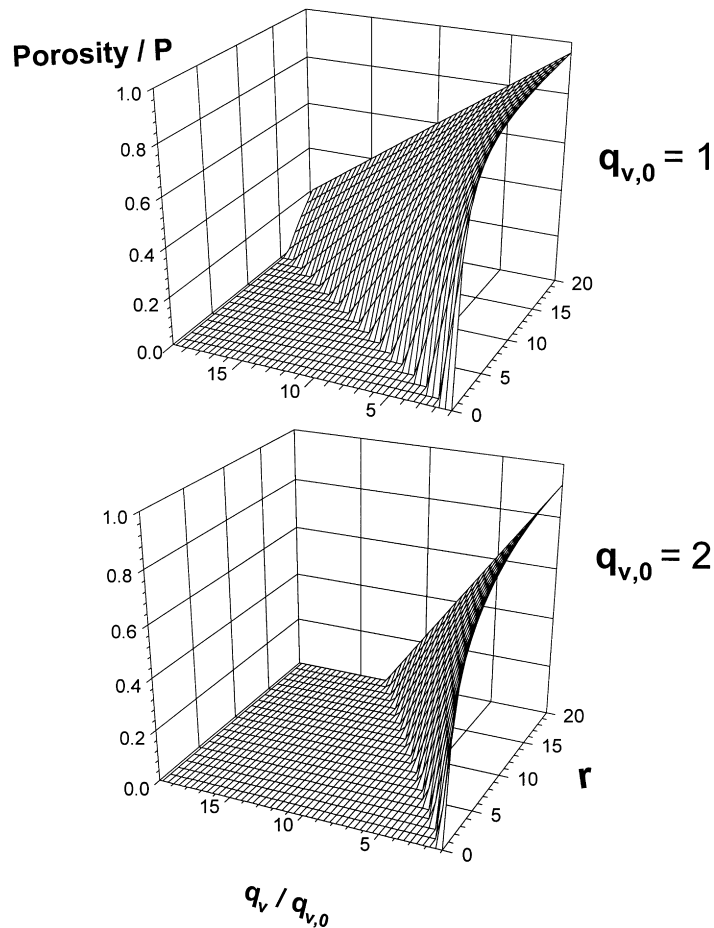
Fig. 24. The total porosity P shown as a function of the degree of monomer dilution r and the $q_v/q_{v,0}$ ratio. Calculations were using Eq. (15) and for two different $q_{v,0}$ values.

point shown in Fig. 24 is that higher porosities can be obtained at low relative volume swelling ratios $q_v/q_{v,0}$.

6. Variation of the porous structure after the gel preparation

Although the final pore structure of polymer networks is fixed during the gel formation process when the network is in a rubbery state, its structural characterization is performed with the polymer sample in the glassy state. Kun and Kunin observed a partial collapse of the pore structure in S–DVB copolymers during the removal of the diluent by steam distillation [221]. Krska et al. [238] used HEMA as a swelling agent for macroporous cation-exchange resins based on S and DVB and then, the swollen state of these resins was fixed by the polymerization of HEMA. Electron microscopic investigation of HEMA swollen low crosslinked polymers showed a porous structure whereas the pore structure was not visible in the
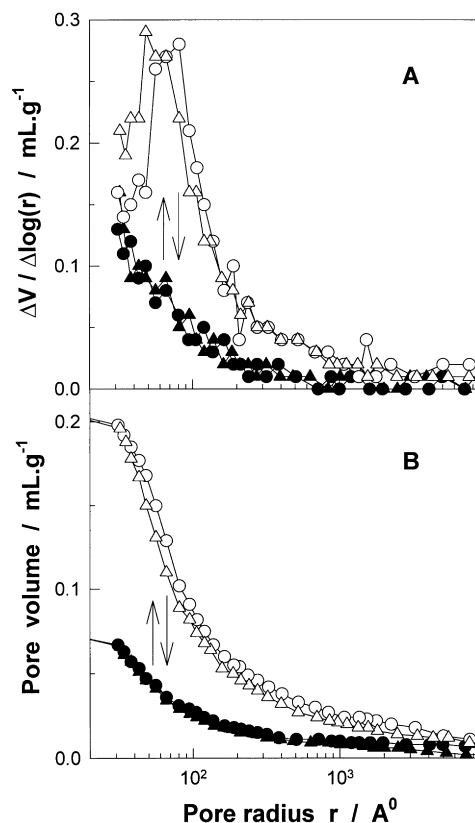
Fig. 25. Pore size distribution of a macroporous S–DVB copolymer dried from toluene (filled symbols) and methanol (open symbols) in differential (A) and integral modes (B). The copolymer samples dried from toluene (●) and from methanol (○). The sample dried from toluene swollen again in toluene and thereafter dried from methanol (△) and vice versa (▲). $\nu_2^{00} = 0.5$. DVB = 10%. Diluent = cyclohexanol.

dried state. These investigators were the first to directly show the difference between the pore structure of S–DVB copolymers in the swollen and the dried states.

Haupke and Pientka [30] as well as Hilgen et al. [239] observed a porosity loss in S–DVB copolymer beads if they are first swollen in toluene and then dried at a high temperature. This porosity loss was due to the collapse of pores during drying of the copolymers in a swollen state. Many investigators also reported that the drying process of S–DVB networks swollen in good solvents leads to a partial or total collapse of the pores [30,112,236]. Even at 98% DVB content, a variation in the pore structure was reported at high dilution degrees [227]. The collapse of the porous structure was ascribed to cohesional forces when the solvated polymer chains are approaching each other due to the loss of solvent [239]. The degree of monomer dilution has a stronger effect on the extent of the collapse of the pores than the solvating power of the diluent used in the polymerization [226].

It was also found that the collapsed pores re-expand again if S–DVB copolymer beads are first swollen in a good solvent such as toluene and then the good solvent in the gel is replaced with a poor one, such as methanol or water, before the drying process [30,236,240]. This process for the re-expansion of the collapsed pores is called 'solvent exchange' or 'pore-opening' process. It was shown
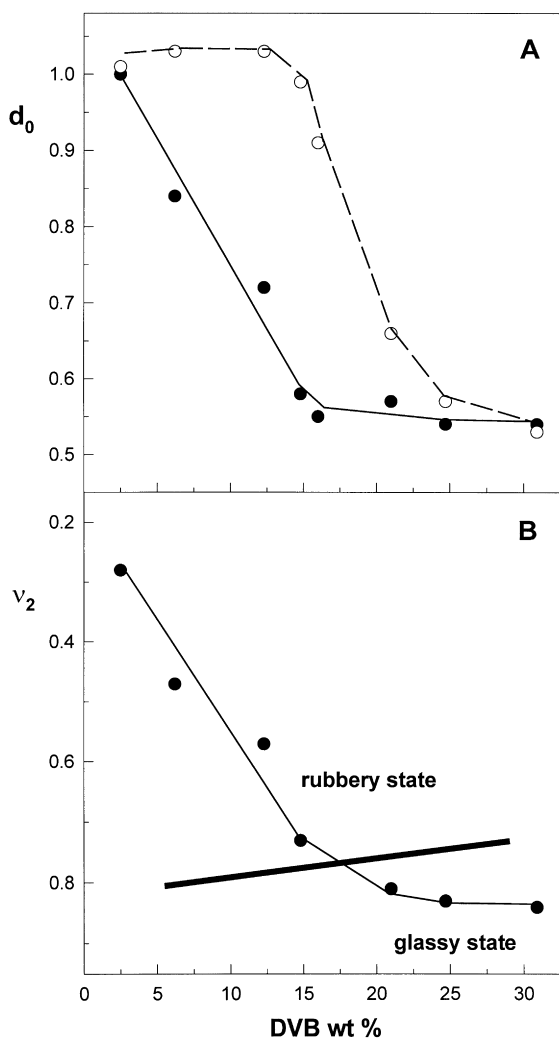
Fig. 26. (A) The apparent densities of S–DVB networks d_0 dried from toluene (open symbols) and from water (filled symbols) plotted as a function of the DVB concentration. [101] The copolymers were prepared in the presence of cyclohexanol as a diluent at $\nu_2^{00} = 0.50$. (B) The swelling ratio of the networks in toluene, in terms of the volume fraction of the network in the equilibrium swollen gel ν_2, shown as a function of their DVB content. The solid line represents the glassy transition line, i.e. the networks swollen in toluene are in a glassy state below this line.

that by treating S–DVB copolymers with a series of solvents of decreasing solvating power, increase in the pore volume as well as in the specific surface area can be achieved [240]. Later on, the difference between the dry and swollen state porosities was demonstrated by small angle X-ray scattering (SAXS) measurements on S–DVB copolymers [241]. Using this technique, it was shown that the swollen state porosity is constant and it is close to the porosity of the copolymer networks dried after the solvent exchange process [236,241]. The swollen state porosity of the networks or the porosity of the networks dried after the pore opening procedure is called 'the maximum porosity'. It seems that the swollen state
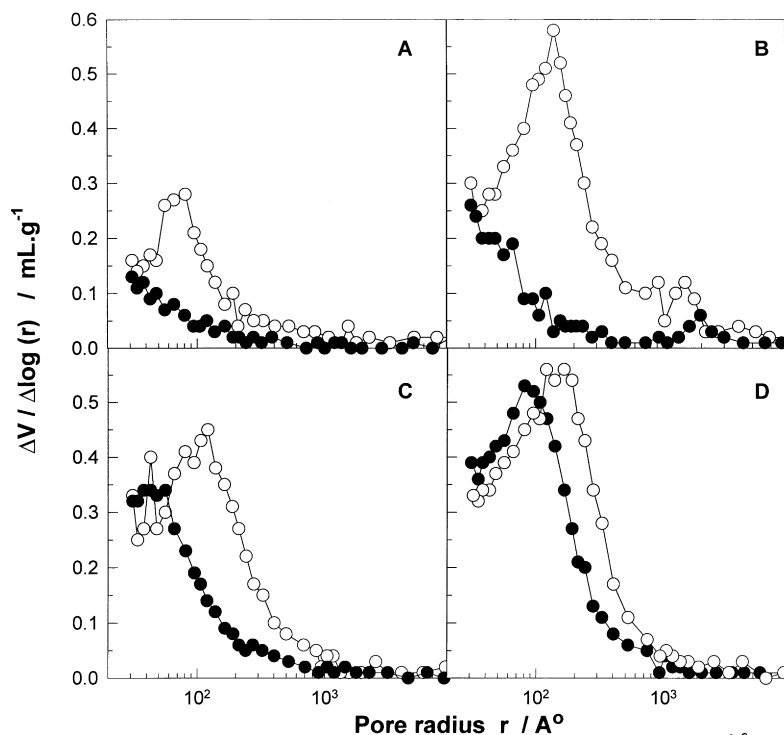
Fig. 27. Effect of the DVB concentration on the pore size distribution of macroporous S–DVB copolymers dried from toluene (●) and methanol (○). $\nu_2^{00} = 0.5$. Diluent = cyclohexanol. DVB = 5 (A), 10 (B), 17.5 (C), and 24% (D).

porosity (maximum porosity) can be preserved in the dried state if the interactions between the polymer and the solvent are decreased before the drying process.

The porosity loss has also been observed in sulfonic acid group containing S–DVB copolymers during drying from water [242,246] or in crosslinked poly(2,3-dihydroxypropyl methacrylate-*co*-sodium methacrylate) beads depending on the solvent treatment [243]. In contrast to this, however, chloromethylation of S–DVB copolymers with monochlorodimethyl ether (MCDME) increased both the pore volume and the specific surface area of the copolymers at medium crosslinker contents [109,244,246,248]. This is explained by the fact that MCDME is a good solvent for S–DVB copolymers; since after chloromethylation the samples are rinsed with nonsolvents, the chloromethylation process is similar to the solvent exchange process by toluene–methanol treatment [109,244,248]. It has also been reported that the change in the total porosity is dependent on the solvent treatment and is a reversible process [109,239]. Fig. 25 illustrates the reversibility of the pore structure variation in S–DVB copolymers [225]. The pores of sizes 10^2 Å radius disappear during drying from toluene; if the same polymer is re-swollen in toluene and then, after the solvent exchange procedure, dried from methanol, the same pores can be detected by mercury porosimetry. This indicates that the actual pore structure formed during the crosslinking process is memorized by the copolymer network [225].

Fig. 26A shows the apparent densities of S–DVB networks dried from toluene (open symbols) and from water (filled symbols) plotted as a function of the DVB concentration [101]. The copolymers were prepared in the presence of cyclohexanol as a diluent at $\nu_2^{00} = 0.50$. Note that the density of nonporous
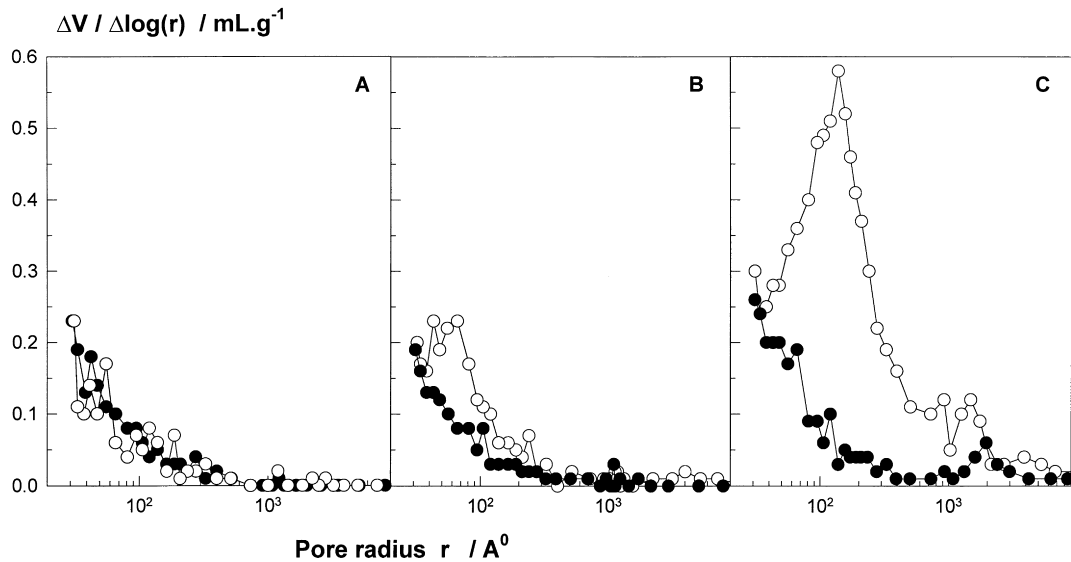
Fig. 28. Effect of the solvating power of the diluent on the porosity variation of macroporous S–DVB copolymers dried from toluene (●) and methanol (○). $\nu_2^{00} = 0.5$. DVB = 10%. Diluent = toluene (A), cyclohexanol/toluene (75/25 v/v) (B), and cyclohexanol (C).

S–DVB networks is $1.05–1.08$ g/cm^3; thus, the smaller the apparent density of the networks from this value, the higher is their porosities. It is seen that cyclohexanol as a nonsolvating diluent induces a heterogeneous structure even at a very low degree of crosslinking. The density of the networks dried from water decreases linearly with increasing DVB content up to 15%, and then remains constant at about 0.55 g/cm^3 which corresponds to a total porosity of 50%. However, the pores formed at low crosslinker contents are unstable; the structure of the networks with <20% DVB shrinks on drying and all the pores disappear in the dried state. The stability of the porous structure starts to increase as the DVB content increases from 15 to 30%. The pore size spectra of the copolymer networks shown in Fig. 27 also show that increasing DVB content up to 18% increases the number of meso and macropores [225]. However, these pores are unstable and collapse upon drying from toluene. Further increase in the DVB concentration does not change the total porosity but increases the stability of the pores.

The plot in Fig. 26B illustrates the swelling ratio of these networks in toluene. The volume fraction of the network in the equilibrium swollen gel ν_2, is plotted as a function of their DVB content. As expected, increasing the DVB content of the networks at a given degree of monomer dilution decreases their swelling ratio in toluene, i.e. increases the polymer concentration in the equilibrium swollen gel. Using the modified Couchman–Karasz equation, [245,246] the glass transition temperature of the gels T_{g12} was calculated. The solid line in Fig. 26B is the glassy transition line of S–DVB networks equilibrium swollen in toluene. It is seen that the networks with <20% DVB swollen in toluene are in the rubbery state at room temperature. The networks with a higher DVB content, at which a stable porous structure starts to appear, are in the glassy state. This result demonstrates that the pores in the network structure collapse if the network is in the rubbery state before the drying process, whereas they do not collapse in the glassy state [101,246]. Thus, increasing rigidity of the structure due to the increasing DVB content
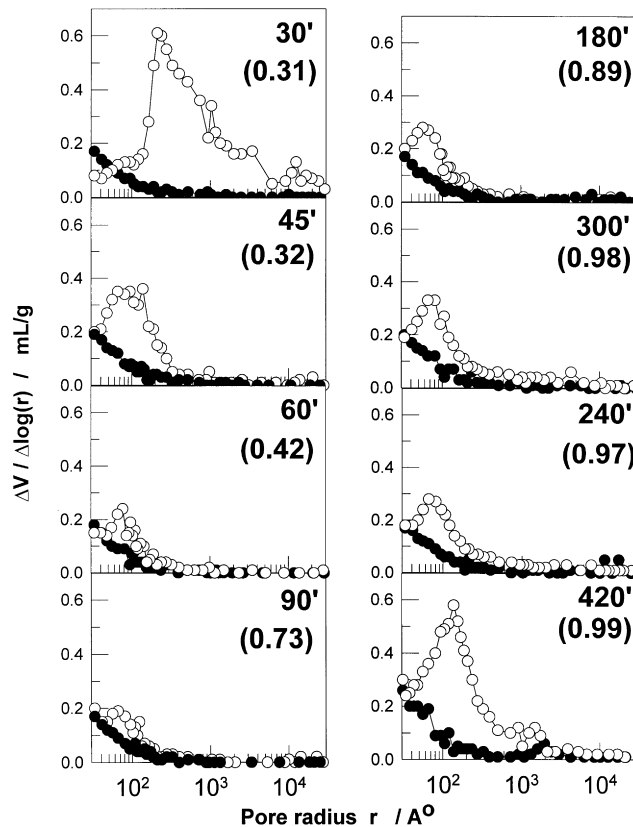
Fig. 29. Differential pore size distribution of S–DVB copolymer beads dried from toluene (●) and methanol (○). DVB = 10 mol%. $\nu_2^{00} = 0.50$. Diluent = cyclohexanol. The reaction times and the fractional monomer conversions (in parenthesis) are indicated in the figure.

favors the conservation of the porosity in the dry state due to the transition of the toluene swollen network to the glassy state.

The extent of the pore structure variation depends on the relative magnitude of the glass transition temperature T_{g12} of the network–solvent (gel) system and the drying temperature T [236]. If $T_{g12} > T$, most of the pores remain stable. Since T_{g12} of a gel increases with the increasing crosslink density of the network or with the decreasing volume fraction of the solvent inside the gel, highly crosslinked networks have a stable pore structure (Fig. 27) [115].

Even when the pore stability condition given by the relation $T_{g12} > T$ is achieved, a portion of the number of pores collapses and the extent of the pore collapse is increased in networks prepared with poor solvents as a diluent. Or conversely, if $T_{g12} < T$, some of the pores remain stable after the drying process. This behavior can be seen in Fig. 28, which represents the pore-size spectra of S–DVB copolymers with 10% DVB content prepared in the presence of a fixed amount of a diluent [225]. The diluents used were a good, medium, and nonsolvent in Fig. 28A–C, respectively. It is seen that the network prepared in nonsolvent has mostly unstable pores whereas the network structure formed in a good solvent is stable. This behavior is a consequence of the crosslink density distribution within the

network structure [226,247]. Due to the higher reactivity of the DVB monomer relative styrene, the final S–DVB network consists of regions of high and low crosslink densities, i.e. regions that swell either less or more than the average degree of swelling of the network. The pores in loosely crosslinked (rubbery) regions collapse on drying whereas those in the highly crosslinked (glassy) regions do not collapse. Decreasing solvating power of the diluent used in the polymerization increases the extent of the inhomogeneities in the gel so that the pore structure variation becomes significant.

Fig. 29 illustrates how the variation in stability of the porous structure of S–DVB copolymer networks varies as a function of time [223]. The crosslinking reactions were carried out using 10 mol% DVB in the feed and using cyclohexanol as a nonsolvating diluent. The initial volume fraction of the monomers in the organic phase was 0.5. Open symbols in the figures represent the porosities of the copolymer samples dried from methanol; they correspond to the actual (swollen state) porosities. The filled symbols belong to the network samples dried from toluene, i.e. they represent the stable part of the pores that cannot collapse upon drying. Gelation occurs in the reaction system after a reaction time of 25–30 min [223]. It is seen that the pore sizes 10^2–10^4 Å in radius formed during the polymerization are unstable and they collapse during the drying process. However, the pores of sizes less than 100 Å in radius that appear at the gel point, exist during the whole course of the polymerization reaction (filled symbols in Fig. 29). These experimental results demonstrate that the stable pores in S–DVB copolymers form just beyond the macrogelation.

This is probably due to the higher reactivity of the DVB monomers compared to styrene; at the beginning of the copolymerization, much more DVB is incorporated into the copolymer than is expected based on the initial composition of the monomer mixture. Accordingly, the earlier formed and phase separated nuclei and their agglomerates (microspheres) are highly crosslinked than those formed in a later stage of the copolymerization when the major part of the DVB monomers have been used up [226,247]. The early formed gel regions will constitute the interior of the microspheres whereas the later formed and loosely crosslinked regions will locate at the surface of the microspheres. Thus, the pores inside the first formed regions of the network remain stable during the drying process because these regions will have higher crosslink density. Since the meso and macropores form the interstices of the microspheres and agglomerates that form at later stages of the reactions, these network regions are loosely crosslinked and so the pores in these regions collapse upon drying in the rubbery state.

This feature of macroporous S–DVB networks was used to estimate their crosslink density distribution [237]. In Fig. 30, the change in the apparent density is plotted against the solubility parameter δ of the solvents used to treat the network. The apparent density d_0 decreases, i.e. the porosity increases with increasing solubility parameter or polarity of the solvent. At a critical value of the polarity, d_0 reaches its minimum value and then remains constant. This critical value corresponds to the transition of the whole network from the rubbery to the glassy state. If one assumes a homogeneous crosslink density for the globules inside the polymer network, the glassy transition of the network, and thus the opening of the pores should occur abruptly in a critical solvent. However, Fig. 30 shows that the porosity increases gradually by increasing the solvent polarity, indicating that the network regions pass into the glassy state in different solvents. On exchanging a swelling solvent for a less solvating one, the highly crosslinked regions cross the glass transition line first. With increasing concentration of DVB, the porosity changes occur over a wider range of the solubility parameter values. This indicates that the inhomogeneity in the networks increases with increasing DVB concentration. Note that the networks with lower crosslink densities pass into the glassy state earlier, i.e. in less polar solvents than those with higher DVB concentration. The results indicate that the crosslink density of the less crosslinked regions of the
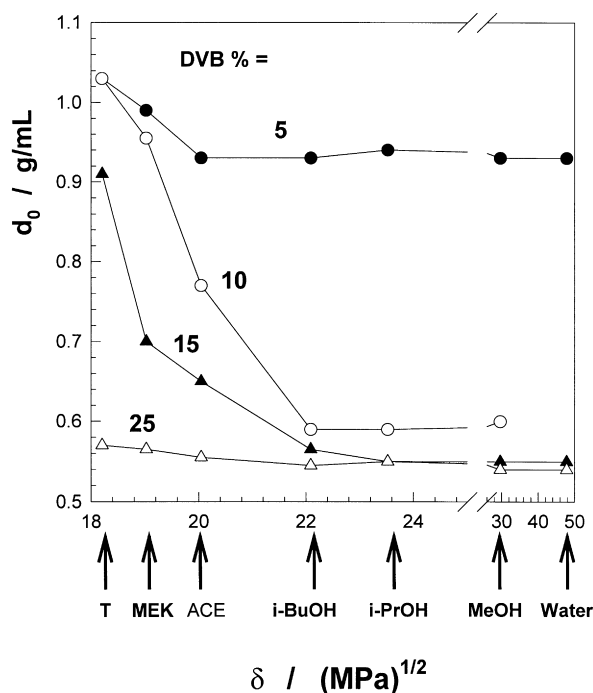
Fig. 30. The apparent densities of S–DVB networks shown as a function of the solubility parameter of the solvent used to treat the network. Diluent used in the network synthesis = cyclohexanol. $\nu_2^{00} = 0.50$. T = toluene, MEK = methyl ethylketone, ACE = acetone, i-BuOH = iso-butanol, i-PrOH = iso-propanol, MeOH = methanol.

network decreases with increasing DVB concentration. By using SAXS it was shown that the degree of inhomogeneity increases as the crosslinker content increases [249].

7. Theoretical considerations

Although many experimental studies have dealt with the porosity formation in FCC in the presence of several diluents, only a few were concerned with the theory of formation of heterogeneities in such systems. The feature of FCC is that a network forms at relatively low conversions and is therefore highly swollen with the diluent–monomer mixture, so that phase separation occurs not far from the gel point. Dusek [250–252] was the first who treated the phase separation during the network formation process under the assumption of thermodynamic phase equilibrium between the network and separated phases in every step of the polymerization reaction. By using Flory's theory of swelling equilibrium and the theory of rubber elasticity, he derived relations between the volume of the network phase and the monomer conversion [251].

Similar thermodynamic relations were also reported by Boots et al. [253] to predict the onset of phase separation in crosslinking copolymerization of divinyl monomers. An important assumption involved in the derivation of Dusek's and Boots equations is that all polymer molecules beyond the gel point belong to the gel. Thus, in these models, the existence of sol molecules in the reaction system is simply ignored.

However, the gel fraction W_g, i.e. the weight fraction of polymer chains that belong to the gel, is known to be zero at the gel point and it increases as the polymerization proceeds, but never attains unity at a monomer conversion less than 100%. Therefore, a realistic thermodynamic model that describes the phase equilibria in an FCC system should take into account the distribution of soluble polymers between the gel and the separated diluent phases. Moreover, in Dusek's and Boots models, the kinetics of FCC was not taken into account. For example, different vinyl group reactivities in the FCC system as well as the variation of the gel crosslink density, depending on the reaction conditions are neglected.

The prediction of the porosity of the copolymers formed by FCC of vinyl/divinyl monomers requires both a kinetic and thermodynamic treatment of the reaction system. A kinetic-thermodynamic model developed recently takes into account all the features of a heterogeneous crosslinking copolymerization system [254,255]. Comparison of the model predictions with the experimental data provided good agreement [255]. In the following section, a review of this model and comparison with experiments will be presented.

7.1. Condition of phase separation during crosslinking polymerization

The reaction mixture of FCC beyond the gel point remains homogeneous as long as the growing polymer network is able to absorb all the available monomers and the diluent [250]. In other words, the reaction mixture is homogeneous if ν_2 of the partially formed network is smaller than its degree of dilution ν_2^0. As the copolymerization and crosslinking reactions proceed, that is, as the crosslink density of the network increases, a critical point is passed at which ν_2 becomes equal to ν_2^0, i.e. the equilibrium degree of swelling of the network in the monomer–diluent mixture becomes equal to its degree of dilution. At this point, since the dilution of a network cannot be greater than its equilibrium degree of swelling, the reaction system will separate into two phases; network and separated phases. Note that the separated phase, which consists of soluble components, will constitute the porous structure of the final material.

Thus, the condition for incipient phase separation during FCC is given by [250]

$$\nu_2 \geq \nu_2^0 \tag{18}$$

After phase separation, both ν_2 and ν_2^0 will change with further polymerization but the equality given by Eq. (18) still holds for the network phase. Let α and ν_2^{00} be the fractional volume conversion of the monomers and the initial volume fraction of the monomers in the monomer–diluent mixture, neglecting the volume contraction, ν_2^0 increases with the monomer conversion α as follows:

$$\nu_2^0 = \alpha \nu_2^{00} \tag{19}$$

At complete monomer conversion ($\alpha = 1$), the phase separation condition given by Eq. (18) reduces to:

$$\frac{\nu_2^{00}}{\nu_2} \leq 1 \tag{20}$$

In order to test the validity of Eqs. (20) or (18) for the formation of a macroporous structure, experiments were carried out using S–DVB comonomer system and using cyclohexanol [101,102] and di-2-ethylhexyl phthalate (DOP) [107,246] as the diluent. Fig. 31A shows how the ν_2^{00}/ν_2 ratio varies with the DVB concentration used in the network synthesis. It is seen that the ν_2^{00}/ν_2 ratio decreases
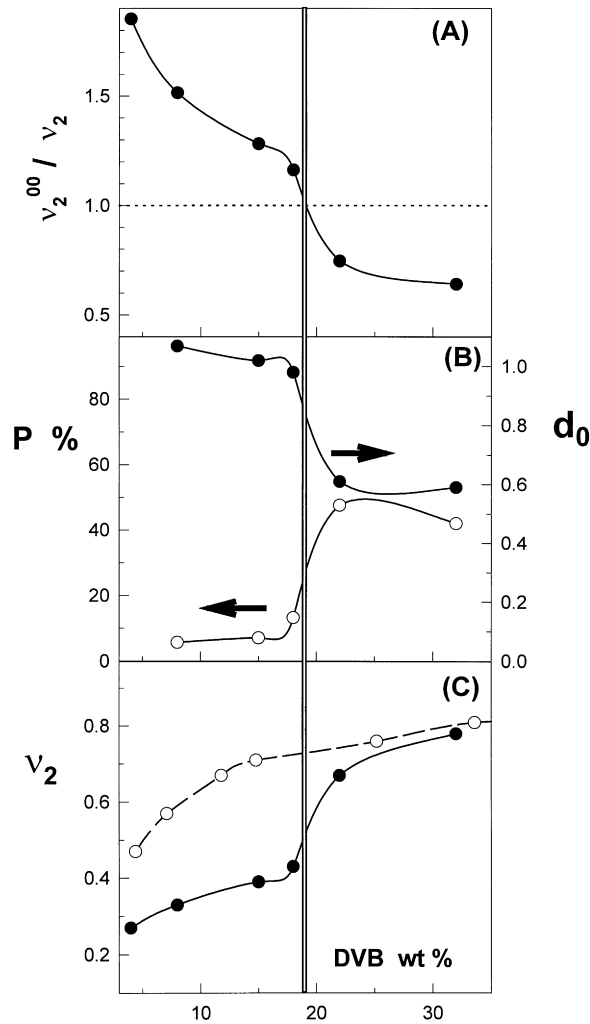
Fig. 31. ν_2^{00}/ν_2 ratio (A), the total porosity P% and the apparent density d_0 (B), and the swelling ratio in toluene ν_2(C) of S–DVB networks plotted as a function of their DVB contents. Diluent = DOP, $\nu_2^{00} = 0.52$. The open symbols in (C) represent the swelling ratio of the networks prepared without using a diluent.

below unity between 18 and 22% DVB, which is the phase separation condition of Eq. (20). Indeed, an abrupt increase in the porosity P (or decrease in the apparent density d_0) of the networks appears between the same DVB concentrations (Fig. 31B). In Fig. 31C, the volume swelling ratio of the networks in toluene in terms of ν_2 is shown as a function of the DVB concentration. The filled and open symbols represent ν_2 values of the networks prepared with and without using a diluent, respectively. It is seen that that the networks formed below 18% DVB are in a swollen state, i.e. they swell much more than the corresponding networks prepared without using a diluent. This indicates that the diluent used in the synthesis remains in the gel phase during the reactions. However, above 18% DVB, ν_2 rapidly increases and approaches that of homogeneous networks, indicating separation of the diluent out of the network
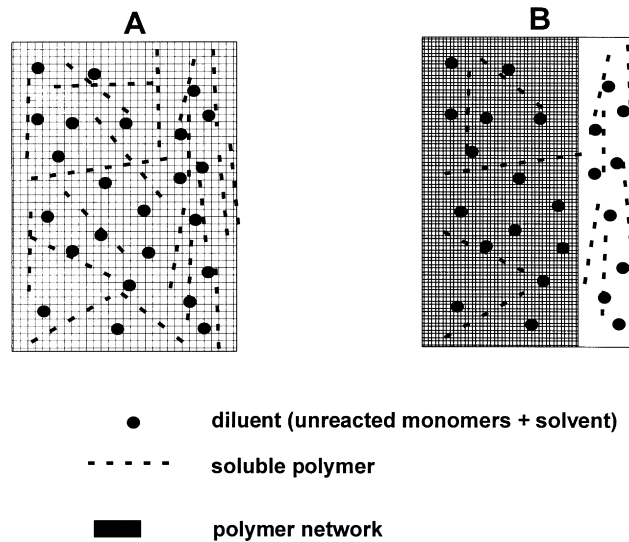
Fig. 32. Schematic representation of FCC system (A) before and (B) after phase separation.

phase. Fig. 31 thus shows that Eq. (18) correctly predicts the formation condition of porosity during FCC.

7.2. Conversion-dependent phase equilibria

In free-radical crosslinking copolymerization (FCC) of vinyl/divinyl monomers, the reaction system beyond the gel point involves the unreacted monomers, (non)solvent, soluble polymers and a polymer network. Usually, the network starts to form at relatively low monomer conversion and is therefore highly swollen with the diluent–monomer mixture, so that phase separation occurs not far from the gel point. In the following, we will call the mixture of the unreacted monomers and the (non)solvent as the diluent. The FCC system at a given degree of monomer conversion can be considered as a ternary system consisting of the diluent, network, and the soluble polymer (Fig. 32A). For this ternary system consisting of three components, the diluent, network, and soluble polymer, respectively, all concentrations and properties of the components are functions of the monomer conversion. Consider the reaction system at a volume conversion of the monomers α, which is above the critical conversion for the onset of a phase separation. At this conversion, the diluent and soluble polymers will distribute between the network and separated phases, whereas the network will only exist in the network phase (Fig. 32B). We can thus analyze the system as a network immersed in a polymer solution. Swelling of a nonionic polymer network in such a system is governed by at least two free energy terms [256,257], i.e. the changes in the free-energy of mixing ΔG_m and in the free energy of elastic deformation ΔG_{el} :

$$\Delta G = \Delta G_m + \Delta G_{el} \tag{21}$$

According to the Flory–Huggins theory [233], ΔG_m is given by

$$\Delta G_m = RT\left(\sum_i n_i \ln \nu_i + \sum_{i<j} n_i \nu_j \chi_{ij}\right) \tag{22a}$$

where n_i is the moles of the species i ($i = 1, 2,$ and 3), ν_i its volume fraction, χ_{ij} the interaction parameter between the species i and j, R the gas constant, and T is temperature. According to the affine network model, the free energy of elastic deformation ΔG_{el}, is given by [233]

$$\Delta G_{el} = (3/2)(RT/NV_s)((\nu_2^0/\nu_2)^{2/3} - 1 - \ln(\nu_2^0/\nu_2)^{1/3}) \tag{22b}$$

where N is the average number of segments in the network chains and V_s is the molar volume of solvent. Substitution of Eqs. (22a) and (22b) into Eq. (21) and differentiating with respect to the number of moles of the diluent n_1 and the soluble polymer n_3 yield the following equations for the excess chemical potentials μ of the components 1 and 3 in both network and separated phases [254]

$$\frac{\Delta\mu_1}{RT} = N^{-1}(\nu_2^{1/3}\nu_2^{0^{2/3}} - \nu_2/2) + \ln\nu_1 + (1 - \nu_1) - \nu_3/y + (\chi_{12}\nu_2 + \chi_{13}\nu_3)(1 - \nu_1) - \chi_{23}\nu_2\nu_3 \tag{23a}$$

$$\frac{\Delta\mu_1'}{RT} = \ln\nu_1' + \nu_3'(1 - 1/y) + \chi_{13}\nu_3'^2 \tag{23b}$$

$$\frac{\Delta\mu_3}{yRT} = N^{-1}(\nu_2^{1/3}\nu_2^{0^{2/3}} - \nu_2/2) + (1/y)\ln\nu_3$$

$$+ (1/y)(1 - \nu_3) - \nu_1 + (\chi_{13}\nu_1 + \chi_{23}\nu_2)(1 - \nu_3) - \chi_{12}\nu_1\nu_2 \tag{24a}$$

$$\frac{\Delta\mu_3'}{yRT} = (1/y)\ln\nu_3' - \nu_1'(1 - y^{-1}) + \chi_{13}\nu_1'^2 \tag{24b}$$

where y is the number of segments in the soluble polymer. Note that the symbols with a prime (′) relate to the separated phase, whereas those without this superscript relate to the network phase. The state of equilibrium between the network and separated phases in FCC is obtained when the diluent and the soluble polymers inside the network phase are in thermodynamic equilibrium with those in the separated phase. This equilibrium state is described by the equality of the chemical potential of these components in both phases. Thus, at swelling equilibrium, we have:

$$\Delta\mu_1 - \Delta\mu_3' = 0 \tag{25}$$

$$\Delta\mu_3 - \Delta\mu_3' = 0 \tag{26}$$

Substitution of Eqs. (23a)–(24b) into Eqs. (25) and (26) and using the phase separation condition given by Eq. (18), one obtains the following system of equations describing the equilibrium condition

between the network and separated phases during FCC [254,255]

$$0.5N^{-1}\nu_2^0 + \ln\left(\frac{\nu_1}{\nu_1'}\right) + (1 - \nu_1 - \nu_3')$$

$$-(\nu_3 - \nu_3'/y) + \chi_{12}\nu_2^{0^2} + \chi_{13}(\nu_3^2 - \nu_3'^2) + (\chi_{12} + \chi_{13} - \chi_{23})\nu_2^0\nu_3 = 0 \tag{27}$$

$$-\ln\left(\frac{\nu_1}{\nu_1'}\right) + (1/y)\ln(\nu_3/\nu_3') + 2\chi_{13}(\nu_3' - \nu_3) + (\chi_{23} - \chi_{12} - \chi_{13})\nu_2^0 = 0 \tag{28}$$

Application of material balance to each phase gives the two additional equations:

$$\nu_1 + \nu_2^0 + \nu_3 = 1 \tag{29}$$

$$\nu_1' + \nu_3' = 1 \tag{30}$$

At the start of the polymerization, the reaction mixture only contains the monomers and the solvent with volume fractions ν_2^{00} and $1 - \nu_2^{00}$, respectively. Let W_g be the weight fraction of polymer chains that belong to the gel and v_g be the volume fraction of the network phase in the reaction system at volume conversion α, from the material balance, we have the following equalities:

$$\nu_2^0 = \bar{\nu}_p W_g / v_g \tag{31}$$

$$\bar{\nu}_p(1 - W_g) = \nu_3 v_g + \nu_3'(1 - v_g) \tag{32}$$

where $\bar{\nu}_p$ is the volume fraction of sol + gel polymer in the whole reaction system (network + separated phases), i.e.

$$\bar{\nu}_p = \frac{\alpha\nu_2^{00}(1 - \epsilon)}{(1 - \alpha\nu_2^{00}\epsilon)} \tag{33}$$

ϵ is the contraction factor defined by $\epsilon = 1 - d_M/d_P$, d_M and d_P being the densities of the monomers and the polymer respectively (we assume equal densities for the monomers used).

The system of the six equations (Eqs. (27)–(32)) contains 15 parameters. Five of these parameters (ν_2^{00}, χ_{12}, χ_{13}, χ_{23}, and ϵ) are system specific and therefore, they are fixed by the experimental conditions (type and concentration of the monomers and the diluent). However, three parameters (W_g, N, and y) change continuously with the monomer conversion. These three conversion-dependent parameters are the output of the kinetic model of FCC given in the following section. Thus, knowing these 8 parameters and taking α as the independent variable, Eqs. (27)–(32) can be solved numerically for the six remaining unknowns: v_g, ν_1, ν_2^0, ν_3, ν_1' and ν_3'. Note that the porosity P of the networks relates to v_g through the equation $P = 1 - v_g$, and the ν_3/ν_3' ratio represents the distribution of soluble polymers between the network and the separated phases.

7.3. Kinetics of gel formation and growth during free-radical crosslinking copolymerization

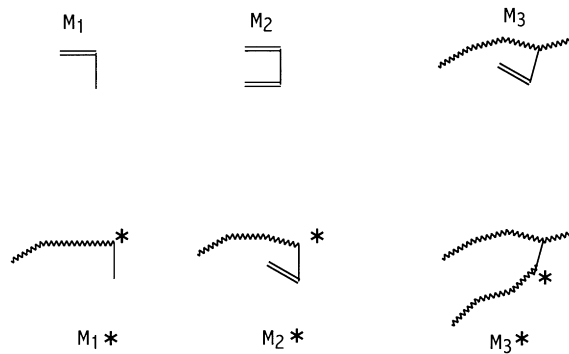Although several theories of gel formation and gel growth have been developed in the past half

Fig. 33. Types of the vinyl groups and the radical centers present during FCC of vinyl/divinyl monomers.

century, kinetic approaches are widely used to describe the gel formation process in free-radical cross-linking copolymerization (FCC) [24,258–266]. This is mainly due to the fact that kinetic models take into account all the kinetic features of FCC and so offer a more realistic approach to the microscopic phenomena occurring during the free-radical polymerization reactions.

The kinetic treatment of FCC usually makes the following assumptions:

1. Steady-state approximation for the concentration of each radical species.
2. Cyclization and multiple crosslinking reactions occur at constant rates.
3. Equal reactivity for the vinyl groups on the divinyl monomer (crosslinker).
4. All the functional groups distribute homogeneously in the reaction system. This assumption is a consequence of the mean-field nature of the kinetic theories.

Vinyl–divinyl monomer copolymerization reactions involve at least three types of vinyl groups: (i) those on monovinyl monomer (M_1); (ii) on divinyl monomer (M_2); and (iii) on polymer chains, i.e. pendant vinyls (M_3). Copolymerization of the three types of vinyl groups results in the formation of three types of growing radicals, depending on the location of the radical center, namely, those with monovinyl monomer unit at the end (M_1*), divinyl monomer unit with one unreacted vinyl (pendant vinyl) at the end (M_2*), and divinylmonomer unit with both reacted vinyls at the end (M_3*) (Fig. 33). In order to simplify the kinetic treatment of the reaction system, the instantaneous rate constants for propagation (k_{p1}, k_{p2}), crosslinking (k_{p3}), and termination reactions (k_t^0) are defined as follows:

$$k_{pi} = \sum_j k_{pji} x_j \tag{34a}$$

$$k_{tc}^0 = \sum_i \sum_j k_{tcij} x_i x_j \tag{34b}$$

$$k_{td}^0 = \sum_i \sum_j k_{tdij} x_i x_j \tag{34c}$$

$$k_t^0 = k_{tc}^0 + k_{td}^0 \quad (i,j = 1,\ 2 \text{ and } 3) \tag{34d}$$

Here, k_{pji} is the propagation rate constant between radicals M_j* and vinyls M_i, k_{tcij} and k_{tdij} are the termination rate constants between radicals of types M_i* and M_j* by coupling (c) and by disproportionation (d), respectively, x_j is the instantaneous mole fraction of the radical M_j*, i.e. $x_j = [M_j*]/[R^*]$, where $[R^*]$ is the total radical concentration defined by $[R^*] \equiv \sum_j [M_j*]$. The instantaneous mole fraction of the radical species x_j can easily be evaluated as in a terpolymerization. Invoking the steady-state approximation for each of the radical species separately, and assuming that the propagation rates are much larger than both the initiation and termination rates, one obtains:

$$x_1 : x_2 : x_3 = 1 : a : b \tag{35a}$$

where

$$a = \frac{k_{p12}[M_2]\{k_{p31}[M_1] + k_{p32}[M_2] + (k_{p13}k_{p32}/k_{p12})[M_3]\}}{k_{p21}[M_1]\{k_{p31}[M_1] + k_{p32}[M_2] + (k_{p31}k_{p23}/k_{p21})[M_3]\}} \tag{35b}$$

$$b = \frac{(k_{p13} + ak_{p23})[M_3]}{k_{p31}[M_1] + k_{p32}[M_2]} \tag{35c}$$

Note that for the crosslinking copolymerization of styrene (S) with technical divinylbenzene (DVB), which is a mixture of meta (m) and para (p) isomers of DVB as well as of ethyl styrene (ES), six types of vinyl groups exist: those on S, m-ES, p-ES, m-DVB, p-DVB, and on the polymer chains (pendant vinyls). Eq. (1) can also be applied to this reaction system with $i, j = 1$–6.

In FCC, the propagation rate constants of the elementary reactions for monomeric vinyls are reaction controlled up to about 80% of the monomer conversion. Therefore, it is reasonable to assume constant propagation rate constants during the reactions. However, termination rates of polymer radicals are diffusion controlled. Many models have been proposed to calculate the diffusion controlled termination rate constant k_t during the linear and crosslinking polymerizations. The resulting expressions involve, however, parameters that are not available for real systems. Tobita and Hamielec suggested the following empirical equations for the diffusion controlled termination in FCC [261]:

$$k_t = k_t^0 \text{ for } x < Z_2 \tag{34e}$$

$$k_t = k_t^0 \exp\{-Z_1(x - Z_2)\} \text{ for } x > Z_2 \tag{34f}$$

where x is the monomer conversion, Z_1 and Z_2 are adjustable parameters. In S–DVB copolymerization, the termination reactions are chemically controlled prior to gelation but become diffusion controlled beyond gelation [267]. Thus, the parameter Z_2 equals to the monomer conversion at the gel point x_c. The parameter Z_1 describing the variation of k_t with the monomer conversion x was evaluated from the experimental time-conversion data of S–DVB copolymerization [268]. Calculation results give $Z_1 = 15 \pm 1$, independent on the level of DVB (4–8%) and on the polymerization temperature (70–90°C) [268]. Applying Eqs (34a)–(34f), one may derive the rate equations for the concentration of the initiator I and vinyl groups M_i as follows

$$r_I = -k_d[I] \tag{36}$$

$$r_{M_1} = -k_{p1}[R^*][M_1] \tag{37}$$

$$r_{M_2} = -2k_{p2}[R^*][M_2] \tag{38}$$

$$r_{M_3} = (1 - k_{cyc})k_{p2}[M_2][R^*] - (1 + k_{mc})k_{p3}[R^*][M_3] \tag{39}$$

where

$$[R^*] = (2f \, k_d[I]/k_t)^{0.5} \tag{40}$$

f is the initiator efficiency, k_d the decomposition rate constant of the initiator, k_{cyc} the fraction of DVB units consumed by cyclization reactions and k_{mc} is the average number of multiple crosslinks formed per intermolecular link.

In the characterization of gel forming systems, an important property is the distribution of molecular weights of polymer molecules. Let $[P_r]$ be the concentration of polymer molecules composed of r structural units, normalization gives

$$Q_n = \sum_{r=1}^{\infty} r^n[P_r] \tag{41}$$

where Q_n is the nth moment of the polymer distribution ($n = 0, 1, 2, \ldots$). The ith average chain length of molecules ($i = 1, 2, 3, \ldots$) is defined as

$$\bar{X}_i = \frac{Q_i}{Q_{i-1}} \tag{42}$$

For example, the second average of the chain length distribution called weight-average chain length is given by $\bar{X}_2 = Q_2/Q_1$. Up to the onset of gelation, all molecules present in FCC system are finite. At the incipient formation of an infinite structure, which is called the gel point, the second moment of the polymer distribution, i.e. the weight-average chain length of polymers diverges:

$$\lim_{t \to t_c} Q_2 = \infty \tag{43}$$

where t_c is the time required for the onset of gelation. Beyond the gel point, both an infinite network (gel) and finite molecules (sol) coexist in the polymerization system. The kinetic treatment of the post-gelation period assumes a steady state concentration for the radical concentration in the sol and in the whole reaction system. Using this approach, the moment equations of the polymer distribution in vinyl/divinyl monomer copolymerization both before and after the gel point were derived previously [263–265].

In a batch isothermal crosslinking copolymerization, the reaction volume V will also change during the reactions due to the differences in the densities of the monomer d_M (monomer densities are assumed to be equal) and the polymer d_P. If S represents the concentration of species I, M_i and the moments of the polymer distribution Q_n, a mass balance requires:

$$r_S = \frac{d(VS)}{V \, dt} = \frac{dS}{dt} + \frac{S}{V}\frac{dV}{dt} \tag{44}$$

Table 4

Kinetic constants and parameters for S-commercial DVB copolymerization using dibenzoyl peroxide as an initiator. [255] k_{p2}' and k_{p2}'' represent the propagation rate constants between radicals and m-DVB or p-DVB, respectively, and $\bar{r}_{32}$ is the average reactivity ratio of pendant vinyls to monomeric vinyls on DVB isomers

Constant:	Reference
$f = 0.5$	
$k_d = 6.38 \times 10^{13} \; s^{-1} \; \exp\left[-124.3 \; \text{kJ mol}^{-1}/(RT)\right]$	[269]
$k_{p1} = 2.4 \times 10^8 \; \text{l mol}^{-1}.s^{-1} \; \exp\left[-37.5 \; \text{kJ mol}^{-1}/(RT)\right]$	[270]
$k_{p2'} = k_{p1}/0.88$	[271]
$k_{p2''} = k_{p1}/1.18$	[271]
$\bar{r}_{32} = 1/10$	[266]
$k_{cyc} = 0.3$	[222]
$k_{mc} = 0$	
$k_{tc}^0 = 1.26 \times 10^9 \; \text{l mol}^{-1} \; s^{-1} \; \exp\left[-7.03 \; \text{kJ mol}^{-1}/(RT)\right]$	[269]
$k_{td}^0 = 0$	[269]
$d_M = 924 - 0.918\,(T - 273) \; \text{g l}^{-1}$	[272]
$d_P = 1084.8 - 0.605(T - 273) \; \text{g l}^{-1}$	[272]

where dV/dt is the rate of volume change, which, assuming ideal solutions, is given by:

$$\frac{dV}{dt} = -\epsilon V \sum_i r_{M_i} \bar{V}_i \quad (i = 1, \, 2' \text{ and } 2'') \tag{45}$$

where $\bar{V}_i$ is the molar volume of the monomer with vinyl group of type i and ϵ is the contraction factor ($\epsilon = 1 - d_M/d_P$).

Thus, if the rate constants and the parameters are known, the mass balance equations of the kinetic model represented by Eq (44) can be solved numerically to predict the vinyl group conversions, gel points, chain length averages and gel crosslink density as a function of the reaction time. The independent variable reaction time t can be replaced with the mole conversion x or the volume conversion α of the monomers using the equations:

$$x = \frac{Q_1 V}{M_0 V_0} \tag{46}$$

$$\alpha = 1 - \left(\frac{1 + f_2 \Delta \bar{V}/\bar{V}_1}{1 + f_{20} \Delta \bar{V}/\bar{V}_1} \right)(1 - x) \tag{47}$$

where V_0 is the initial volume, M_0 is the initial monomer concentration, $\Delta \bar{V} = \bar{V}_2 - \bar{V}_1$, f_2 and f_{20} are the mole fractions of DVM at conversion x and at zero conversion, respectively.

7.4. Theoretical predictions

The model was solved recently for a batch isothermal S-commercial DVB copolymerization in the presence of dibenzoyl peroxide as the initiator [255]. For the solution of the kinetic model, the following reasonable approximations were also made: (i) the propagation, crosslinking and termination rate
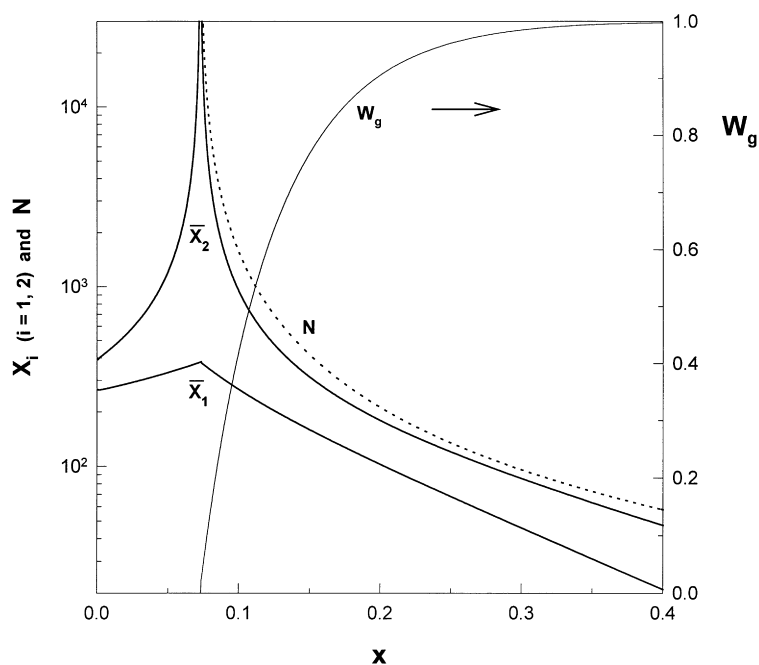
Fig. 34. The weight fraction of gel W_g, the number- and weight-average degrees of polymerization of branched molecules ($\bar{X}_1$ and $\bar{X}_2$), and the number of segments in the network chains N shown as a function of the monomer conversion x in S–DVB copolymerization. DVB = 70 mol%. $\nu_2^{00} = 0.20$. Temperature = 70°C. [I] = 0.1 M.

constants are independent of the type of the radical end, i.e. $k_{p11} = k_{p21} = k_{p31} = k_{p1}$, etc. (ii) The initiator efficiency is 0.5. (iv) The reactivity ratio of S with the first double bond of *m*- and *p*-DVB ($r_{12'}$ and $r_{12''}$, respectively) are temperature-independent in the temperature range from 50 to 100°C. (v) Previous experimental studies indicate that, in a wide range of the crosslinker concentration, the pendant vinyl group reactivity is ten to hundred fold smaller than the reactivity of the vinyl groups on divinyl monomers [266,267]. For the simulation we assume that $\bar{r}_{32} = 1/10$ in S–DVB copolymerization system in the presence of inert diluents.

The values of the kinetic constants and the parameters used in the calculations are collected in Table 4. For the solution of the thermodynamic-kinetic model, the gel point conversion x_c and the values of W_g, $y(\bar{X}_1)$, and N were first calculated using the kinetic rate equations as a function of the monomer conversion *x*. Then, these data were used for the solution of the thermodynamic equations of the model to predict the critical conversion for the onset of a phase separation in FCC as well as the volume fraction of the separated phase ($1 - \nu_g$), which corresponds to, assuming isochoric conditions, the total porosity P of the final copolymer network. Solution of the thermodynamic equations require the values of the interaction parameters χ_{12}, χ_{13}, and χ_{23}. Since the sol molecules and the gel have the same chemical composition, it was assumed that $\chi_{23} = 0$. The diluent in S–DVB copolymerization (component 1) consists of the unreacted monomers and of the (non)solvent (pore forming agent), which changes its composition depending on the monomer conversion. As a result, the overall solvating power of the component 1 for the polymer changes as the monomers are consumed in the polymerization. Thus, χ_{12} can be calculated from the monomer–polymer (χ_{12}^{mon}) and solvent–polymer (χ_{12}^{sol}) interaction parameters
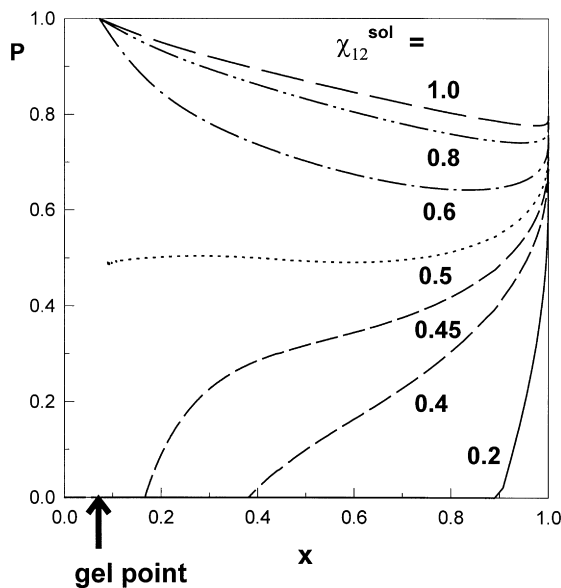
Fig. 35. Variation of the total porosity P of S–DVB networks with the monomer conversion x in the presence of various diluents. The diluent–polymer interaction parameter values χ_{12}^{sol} used in the calculations are indicated in the figure. See legend to Fig. 34 for the reaction conditions.

as:

$$\chi_{12} = \chi_{12}^{mon} + (\chi_{12}^{sol} - \chi_{12}^{mon})\Phi_s \tag{48a}$$

where Φ_s is the volume fraction of the (non)solvent in the diluent mixture, i.e.

$$\Phi_s = \frac{1 - \nu_2^{00}}{1 - \alpha\,\nu_2^{00}} \tag{48b}$$

χ_{12}^{mon} is reported to be 0.42 and χ_{12}^{sol} represents the thermodynamic quality of the pore forming agent, which is one of the independent variables of the model.

Fig. 34 shows the sol and gel properties as a function of the monomer conversion x in S–DVB copolymerization at 70°C in the presence of 0.1 M dibenzoyl peroxide as the initiator. Initial monomer mixture contains 70 mol% DVB isomers and the total monomer concentration is 20 vol% ($\nu_2^{00} = 0.20$). The weight-average polymerization degree of branched polymers, $\bar{X}_2$, goes to infinity at $x = 0.073$, which corresponds to the critical conversion x_c for the onset of gelation. Beyond the gel point, the amount of polystyrene chains incorporated into the network, W_g, increases and the number of segments between successive crosslinks, N, decreases abruptly. At the same time, the size of the soluble polymers rapidly decreases due to the predominant crosslinking reactions between the sol molecules of larger sizes and the gel. At $x > 0.3$, the gel fraction approaches to unity and the size of soluble polymers ($\bar{X}_1$ and $\bar{X}_2$) decreases to the size of the primary molecules. These are the well known features of S–DVB copolymerization carried out in the presence of a high amount of DVB.

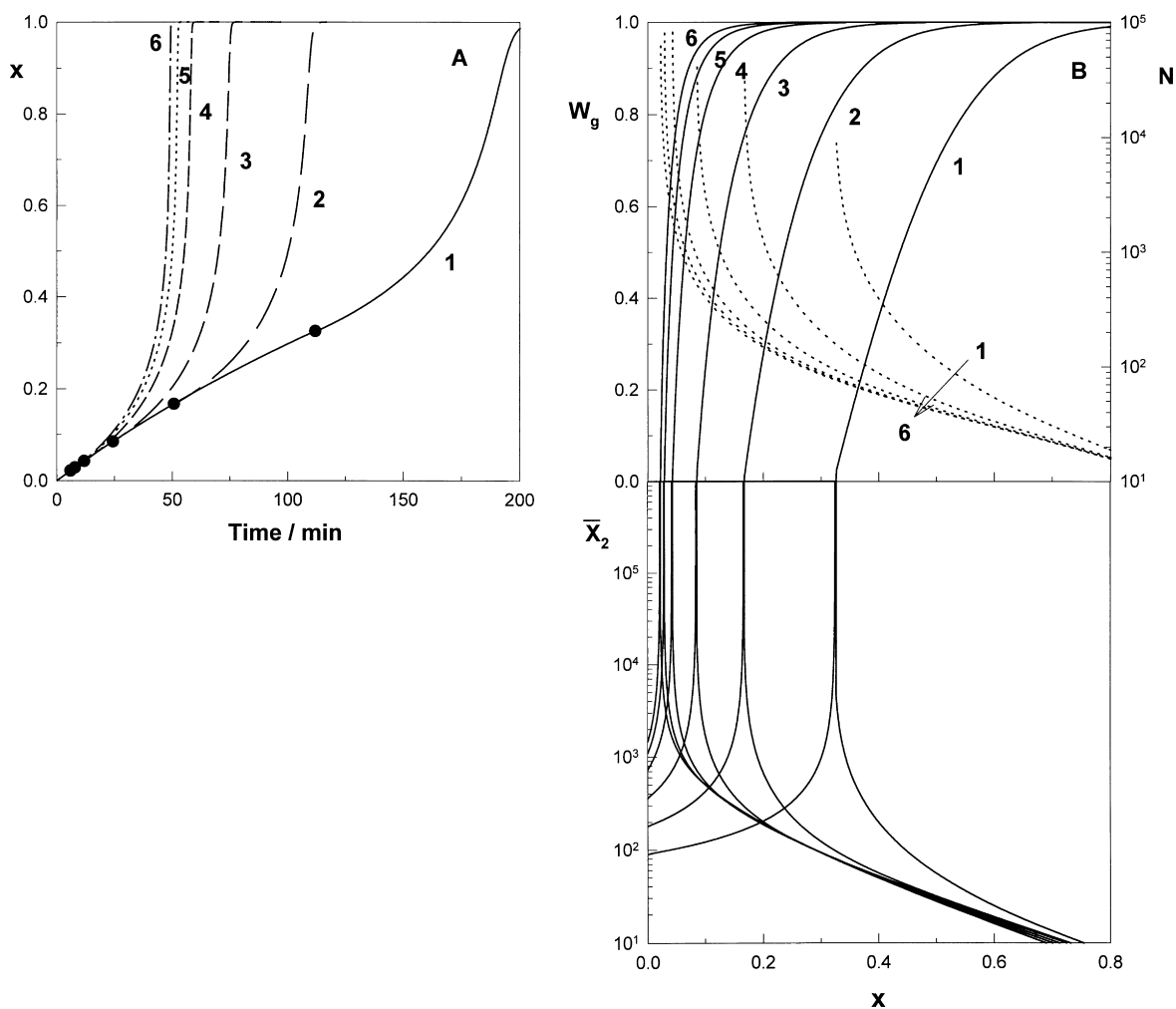For the same reaction conditions, the effect of the thermodynamic quality of the diluent represented by

Fig. 36. (A) Variation of monomer conversion x with the reaction time in S–DVB copolymerization at various initial monomer concentrations. The gel points are shown as filled circles. DVB = 50 mol%. $[I]_0 = 0.1$ M. Temperature = 70°C. Volume fraction of the monomers in the initial monomer mixture $\nu_2^{00} = 0.05$ (1), 0.10 (2), 0.20 (3), 0.40 (4), 0.60 (5), and 0.80 (6). (B) The weight fraction of gel W_g, the number of segments in the network chains N (dotted curves), and the weight-average degree of polymerization of branched molecules $\bar{X}_2$ shown as a function of the monomer conversion x at various initial monomer concentrations [255].

χ_{12}^{sol} on the porosity development in S–DVB copolymers is shown in Fig. 35. For $\chi_{12}^{sol} < 0.5$, i.e. in the presence of good solvating diluents, the reaction system phase separates beyond the gel point due to the crosslink density (ν)-induced syneresis. Thus, in accord with the experimental observations, porous S–DVB networks can be prepared even in the presence of good solvents as a diluent. As the monomer conversion increases, the porosity also increases due to the simultaneous increase of the crosslink density of the network N^{-1}. For $\chi_{12}^{sol} \geq 0.5$, i.e. in the presence of precipitating diluents, the polymerization system is discontinuous at the gel point because of the repulsive interactions between the polymer segments and solvent molecules (χ-induced syneresis) which induce phase separation prior
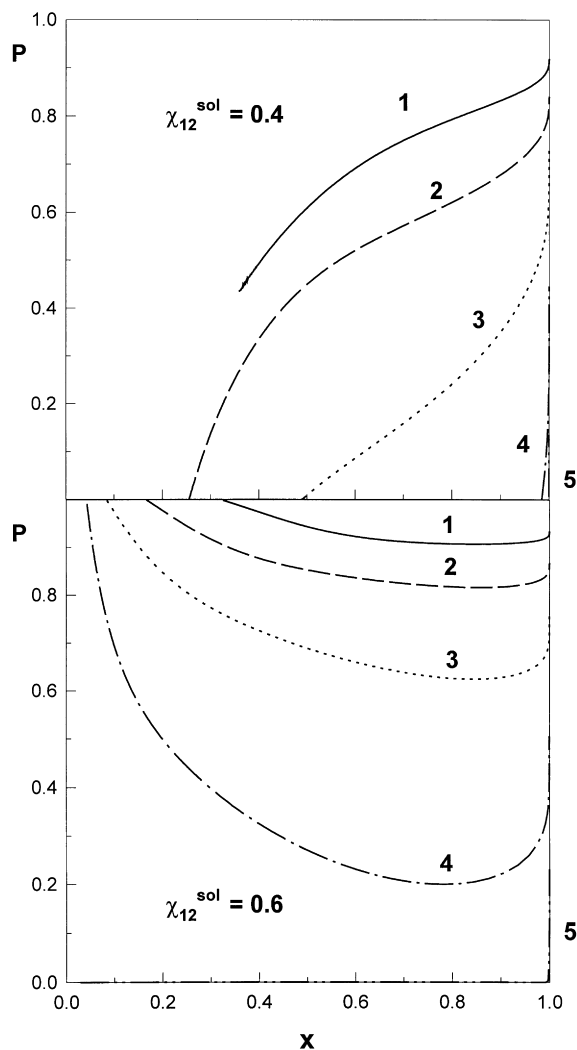
Fig. 37. Variation of the total porosity P of S–DVB networks formed in S–DVB copolymerization with the monomer conversion x for various initial monomer concentrations ν_2^{00}. [255] DVB = 50 mol%, $[I]_0 = 0.1$ M. Temperature = 70°C. χ_{12}^{sol} values used in the calculations are indicated in the figure. Volume fraction of the monomers in the initial monomer mixture $\nu_2^{00} = 0.05$ (1), 0.10 (2), 0.20 (3), 0.40 (4), and 0.60 (5).

to gelation. Thus, the kinetic gel point x_c, at which the second moment of the polymer distribution diverges, does not correspond to a macrogelation point; it rather corresponds to a critical point, at which microgel or macrogel particles start to appear in the reaction system containing unreacted monomers, precipitating diluent and soluble polymers. Beyond this point, the porosity decreases on increasing the monomer conversion. This is due to the fact that as the gel grows, that is, as the weight fraction of the gel W_g increases, the volume of the separated phase necessarily decreases. The porosity starts to increase at high monomer conversions due to the predominant crosslinking reactions, which reduces the volume of
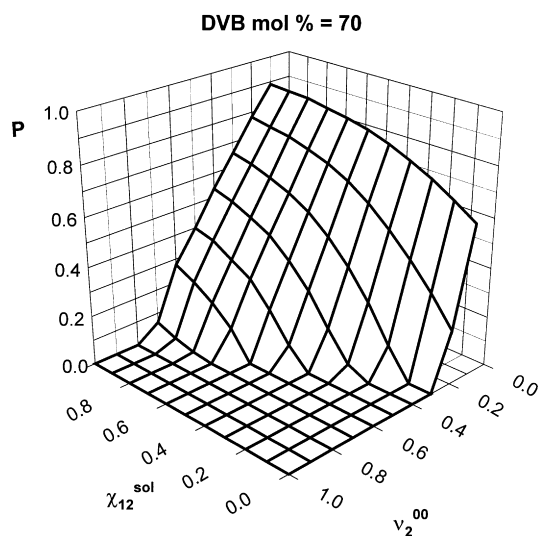
DVB mol % = 70

Fig. 38. The total porosity P of S–DVB networks formed at $x = 0.99$ plotted as a function of the quality χ_{12}^{sol} and the amount ν_2^{00} of the diluent present during the polymerization. [255]DVB = 70 mol%, $[I]_0 = 0.1$ M. Temperature = 70°C.

the gel phase. These predictions of the model were also confirmed by experiments, as seen in Figs. 9 and 10.

Effect of the initial monomer concentration (ν_2^{00}) on the kinetics of S–DVB copolymerization is shown in Fig. 36. The gel point conversions x_c calculated from $\bar{X}_2$ versus x curves (Fig. 36B) are illustrated in Fig. 36A as filled circles. Under the selected reaction conditions (50 mol% DVB, 70°C, $[I]_0 = 0.1$ M), as the initial monomer concentration increases from 5 to 80 v/v%, the gel point conversion x_c at which $\bar{X}_2$ goes to infinity decreases from 0.326 to 0.022. The acceleration of the polymerization and crosslinking reactions becomes significant on increasing the monomer concentration due to the earlier gelation. Also, the growth rate of the gel in terms of its mass (W_g) and its crosslink density (N^{-1}) increases significantly on increasing the monomer concentration in the initial reaction mixture.

Fig. 37 illustrates the variation of porosity P of S–DVB networks with conversion x for various initial monomer concentrations. The monomer concentration affects significantly the porosity of the copolymer networks. In the presence of a good solvent ($\chi_{12}^{sol} = 0.4$), the reaction system phase separates at or beyond gelation; the higher the initial degree of dilution of the reaction system, the higher the porosity of the resulting copolymer network. The porosity increases on increasing the monomer conversion due to the simultaneous increase of the crosslink density. However, in the presence of a poor solvent ($\chi_{12}^{sol} = 0.6$), the porosity first decreases with monomer conversion due to increased volume of the gel phase but then, it increases again due to the crosslinking reactions.

The results demonstrate that the networks prepared in nonsolvating diluents or in more diluted solutions exhibit larger porosity values. These dependencies are collected in Fig. 38 for a wide range of parameter values, which shows the variation of porosity P as a function of the quality and the amount of the diluent present during the polymerization. Calculations were for 70 mol% DVB in the initial
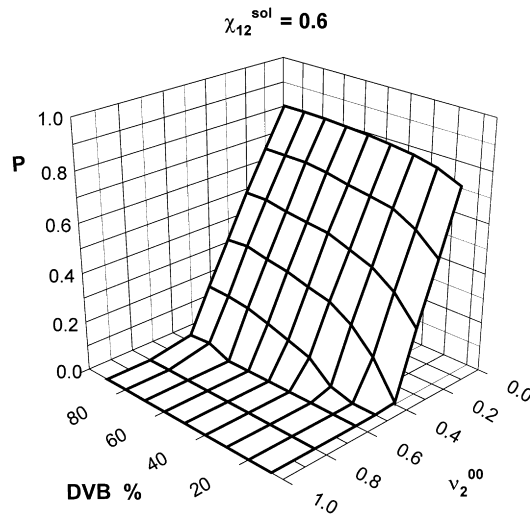
Fig. 39. The total porosity P of S–DVB networks formed at $x = 0.99$ plotted as a function of the initial concentrations of the DVB and the total monomers. [255] $\chi_{12}^{\text{sol}} = 0.60$. $[I]_0 = 0.1$ M. Temperature $= 70°$C.

monomer mixture and for a monomer conversion of $x = 0.99$. It is seen that the final porosity of S–DVB networks strongly depends both on the degree of dilution ν_2^{00} and on the extent of the thermodynamic interactions between the diluent and network segments χ_{12}^{sol}. Comparison of the model predictions with the experimental data (Figs. 12–14) indicates that the theory predicts all the trends observed by experiment.

In Fig. 39, the calculated porosities of S–DVB networks formed at a monomer conversion $x = 0.99$ are shown as a function of the DVB and the initial monomer concentration. It is seen that the porosity of S–DVB networks increases with increasing DVB content of the monomer mixture. In the presence of sufficient amount of DVB, the porosity does not change with a further increase in the DVB concentration. The maximum value of porosity obtained at high DVB contents is close to the amount of the diluent present during the reactions. Moreover, Fig. 39 also indicates that, to obtain porous copolymers, a critical amount of DVB, or, a critical degree of initial monomer dilution is required. The critical DVB concentration decreases with increasing degree of dilution of the monomers. A comparison of Fig. 39 with the experimental data in Fig. 15 shows that the predictions of the model are in excellent agreement with the experimental data.

The effects of the polymerization temperature and the initiator concentration on the porosity of S–DVB networks were also studied using the model [255]. The porosity of partially formed networks ($x < 0.5$) increases with increasing temperature or with increasing initiator concentration. Thus, the partially formed networks obtained at higher temperatures or at higher initiator concentrations should exhibit higher porosities due to the delayed gelation and lower gel fractions. Calculations also indicate that the final porosity of the networks slightly increases on decreasing the polymerization temperature or the initiator concentration. However, this effect is, compared to the other effects insignificant [255].

8. Concluding remarks

Macroporous copolymer networks form as a result of a phase separation during the free-radical crosslinking copolymerization of vinyl and divinyl monomers in the presence of an inert diluent. In this article, we have outlined the experimental techniques developed in recent years for the synthesis of macroporous copolymer networks. It has been demonstrated that a variety of porous structures can be obtained during the crosslinking process by changing the independent variables of the network synthesis, i.e. the extent of the polymer–(diluent + monomer) interactions, the amounts of the crosslinker and the diluent as well as the initiator concentration or the polymerization temperature.

The reaction system leading to macroporous networks is a (quasi)ternary system composed of a polymer network, soluble polymers, and low molecular compounds (monomers and diluent). All concentrations and properties of the components of the system change continuously during the crosslinking process. This article also demonstrates that the theoretical models recently developed correctly predict the phase separation condition during the crosslinking process as well as the total porosity of the resulting macroporous networks.

It is hoped that the present paper will stimulate additional experimental efforts on the synthesis of macroporous networks with uniform pores of desired sizes. Open problems for future study in connection with the theoretical modeling of macroporous network formation include the prediction of the pore size distribution of the material from the synthesis parameters.

Acknowledgements

References

[1] Topp NE, Pepper KW. J Chem Soc 1949:3299.
[2] D'Alelio GF. US Patent 2,366,007, 1945.
[3] Pepper KW. J Appl Chem 1951:124.
[4] Staudinger H, Huseman E. Berichte 1935;68:1618.
[5] Dusek K. Chem Prumysl 1961;11:439.
[6] Dusek K. Collection Czech Chem Commun 1963;27:2841.
[7] Seidl J, Malinsky J. Chem Prumysl 1963;13:100.
[8] Dusek K. Collection Czech Chem Commun 1963;28:2512.
[9] Malinsky J, Rahm J, Krska F, Seidl J. Chem Prumysl 1963;13:386.
[10] Dusek K. J Polym Sci B 1965;3:209.
[11] Abrams IM. Ind Engng Chem 1956;48:1469.
[12] Meitzner EF, Oline JA. US Patent, 749,526, 1958.
[13] Abrams IM. US Patent, 763,511, 1958.
[14] Lloyd WG, Alfrey T. J Polym Sci 1962;62:301.
[15] Kunin R, Meitzner EF, Bortnick N. J Am Chem Soc 1962;84:305.
[16] Kunin R, Meitzner EF, Oline JA, Fisher S, Frish N. Ind Engng Chem Prod Res Develop 1962;1:140.

[17] Kun KA, Kunin R. J Polym Sci 1964;B2:587.
[18] Kun KA. J Polym Sci A 1965;3:1833.
[19] Millar JR, Smith DG, Marr WE, Kressman TRE. J Chem Soc 1963:218.
[20] Millar JR, Smith DG, Marr WE, Kressman TRE. J Chem Soc 1963:2779.
[21] Millar JR, Smith DG, Marr WE, Kressman TRE. J Chem Soc 1964:2740.
[22] Millar JR, Smith DG, Kressman TRE. J Chem Soc 1965:304.
[23] Seidl J, Malinsky J, Dusek K, Heitz W. Adv Polym Sci 1967;5:113.
[24] Dusek K. In: Haward EN, editor. Developments in polymerization, vol. 3. London: Applied Science, 1982. p. 143.
[25] Guyot A, Bartholin M. Prog Polym Sci 1982;8:277.
[26] Kun KA, Kunin R. J Polym Sci 1967;C16:1457.
[27] Sing KSW, Everett DH, Haul RAW, Moscou L, Pierotti RA, Rouquerol J, Siemieniewska T. Pure Appl Chem 1985;57:603.
[28] Flodin P. Makromol Chem Macromol Symp 1988;22:253.
[29] Haupke K, Hoffmann H. Z Chem 1968;8:463.
[30] Haupke K, Pientka V. J Chromatogr 1974;102:117.
[31] Jacobelli H, Bartholin M, Guyot A. Angew Makromol Chem 1979;80:31.
[32] Guyot A. Makromol Chem Macromol Symp 1987;10/11:461.
[33] Guyot A. In: Sherrington DC, Hodge P, editors. Syntheses and separations using functional polymers, Chichester: Wiley, 1988. p. 1.
[34] Guyot A. Pure Appl Chem 1988;60:365.
[35] Sederel WL, De Jong GJ. J Appl Polym Sci 1973;17:2835.
[36] Rabelo D, Coutinho FMB. Macromol Symp 1994;84:341.
[37] Haupke K, Schwachula G. Plaste und Kautschuck 1985;2:48.
[38] Xie S, Svec F, Frechet JMJ. J Polym Sci A, Polym Chem 1997;35:1013.
[39] Tuncel A, Ecevit K, Kesenci K, Piskin E. J Polym Sci, Polym Chem Ed 1996;34:45.
[40] Wojaczynska M, Kolarz BN. J Chromatogr 1986;358:129.
[41] Kolarz BN, Lucynski J, Trochimczuk A, Wojaczynska M. J Chromatogr 1987;408:308.
[42] Wojaczynska M, Kolarz BN, Hlavata D, Liesiene J, Gorbunov A. Makromol Chem 1992;193:2259.
[43] Dragan S, Grigoriu G. Angew Makromol Chem 1992;200:27.
[44] Kolarz BN, Trochimczuk A, Bryjak J, Wojaczynska M, Dziegielewski K, Noworyta A. Angew Makromol Chem 1990;179:173.
[45] Kolarz BN, Wojaczynska M, Trochimczuk A, Lucynski J. Polymer 1988;29:1137.
[46] Trochimczuk A, Kolarz BN. Polymer 1989;30:369.
[47] Trochimczuk A, Pielichowski J, Kolarz BN. Eur Polym J 1990;26:959.
[48] Kolarz BN, Trochimczuk A, Wojaczynska M. Angew Makromol Chem 1991;193:21.
[49] Vlad C, Poinescu IC, Costea E. Eur Polym J 1996;32:1067.
[50] Vlad C, Poinescu IC, Barbu M. Eur Polym J 1994;30:863.
[51] Poinescu IC, Vlad C, Ioanid G. J Appl Polym Sci 1996;59:991.
[52] Matynia T, Gawdzik B. Angew Makromol Chem 1987;147:123.
[53] Gawdzik B, Matynia T. Angew Makromol Chem 1987;152:33.
[54] Wojaczynska M, Marousek V, Kolarz BN. React Polym 1989;11:141.
[55] Svec F, Hradil J, Coupek J, Kalal J. Angew Makromol Chem 1975;48:135.
[56] Smigol V, Svec F. J Appl Polym Sci 1992;46:1439.
[57] Smigol V, Svec F, Frechet JMJ. Macromolecules 1993;26:5615.
[58] Kuroda H, Osawa Z. Eur Polym J 1995;31:57.
[59] Koilpillai L, Gadre RA, Bhatnagar S, Rajan CR, Ponrathnam S, Kumar KK, Ambekar GR, Shewale JG. J Chem Technol Biotechnol 1990;49:173.
[60] Horak D, Labsky J, Pilar J, Bleha M, Pelzbauer Z, Svec F. Polymer 1993;34:3481.
[61] Svec F, Labsky J, Lanyova L, Hradil J, Pokorny S, Kalal J. Angew Makromol Chem 1980;90:47.
[62] Bennett DJ, Burford RP, Davis TP, Tilley HJ. Polym Int 1995;36:219.
[63] Coupek J, Krivakova M, Pokorny S. J Polym Sci C 1973;42:185.
[64] Okay O, Gurun C. J Appl Polym Sci 1992;46:401.

[65] Horak D, Lednicky F, Bleha M. Polymer 1996;37:4243.

[66] Chirila TV, Chen Y-C, Griffin BJ, Constable IJ. Polym Int 1993;32:221.

[67] Murphy SM, Skelly PJ, Tighe BJ. J Mater Chem 1992;2:1007.

[68] Wu XS, Hoffman AS, Yager P. Polym Sci Part A, J Polym Chem 1992;30:2121.

[69] Okay O. J Appl Polym Sci 1987;34:307.

[70] Ogawa N, Honmyo K, Harada K, Sugii A. J Appl Polym Sci 1984;29:2851.

[71] Galina H, Kolarz BN. J Appl Polym Sci 1979;23:3017.

[72] Galina H, Kolarz BN. J Appl Polym Sci 1979;24:891.

[73] Galina H, Kolarz BN. J Appl Polym Sci 1979;24:901.

[74] Skovby MHB, Kops J. J Appl Polym Sci 1990;39:169.

[75] Moustafa AB, Faizalla A. J Appl Polym Sci 1999;73:149.

[76] Kolarz BN, Wojaczynska M, Bryjak J, Pawlow B. React Polym 1994;23:123.

[77] Kolarz BN, Trochimczuk A, Wojaczynska M, Drewniak M. Angew Makromol Chem 1994;217:19.

[78] Shea KJ, Stoddard GJ, Shavelle DM, Wakui F, Choate RM. Macromolecules 1990;23:4497.

[79] Anand PS, Pall G, Reddy KA, Dasare BD. J Polym Mater 1985;2:227.

[80] Kucuk I, Kuyulu A, Okay O. Polym Bull 1995;35:511.

[81] Wojcik AB. J Appl Polym Sci 1985;30:781.

[82] Wojcik AB. Angew Makromol Chem 1984;121:89.

[83] Narasimhaswamy T, Reddy BSR. J Appl Polym Sci 1991;43:1645.

[84] Rosenberg JE, Flodin P. Macromolecules 1986;19:1543.

[85] Rosenberg JE, Flodin P. Macromolecules 1987;20:1518.

[86] Schmid A, Kulin LI, Flodin P. Makromol Chem 1991;192:1223.

[87] Reinholdsson P, Hargitai T, Isaksson R, Törnell B. Angew Makromol Chem 1991;192:113.

[88] Walenius M, Flodin P. Br Polym J 1990;23:67.

[89] Schmid AB, Flodin P. Eur Polym J 1993;29:469.

[90] Schmid A, Flodin P. Makromol Chem 1992;193:1579.

[91] Kolarz BN, Wojaczynska M, Pielichowski J. Angew Makromol Chem 1991;192:27.

[92] Janssen JC, Klein J, Widdecke H. Makromol Chem 1987;188:1447.

[93] Coutinho FMB, Siqueira MIN, Barbosa CR. Eur Polym J 1990;26:1189.

[94] Coutinho FMB, Luz CTL. Eur Polym J 1993;29:1119.

[95] Luca C, Neagu V, Poinescu I, Simionescu BC. Angew Makromol Chem 1994;222:1.

[96] Li W-H, Stöver HDH. J Polym Sci A, Polym Chem 1998;36:1543.

[97] Chung D-YD, Bartholin M, Guyot A. Angew Makromol Chem 1982;103:109.

[98] Rabelo D, Coutinho FMB. Polym Bull 1994;33:493.

[99] Poinescu IC, Beldie C, Vlad C. J Appl Polym Sci 1984;29:23.

[100] Poinescu IC, Carpov A. Rev Rom Chim 1989;34:1061.

[101] Okay O. J Appl Polym Sci 1986;32:5533.

[102] Okay O. Angew Makromol Chem 1988;157:1.

[103] Okay O. Angew Makromol Chem 1988;157:15.

[104] Howard GJ, Midgley CA. J Appl Polym Sci 1981;26:3845.

[105] Wojaczynska M, Kolarz BN. J Appl Polym Sci 1995;56:433.

[106] Poinescu I, Popescu V, Carpov A. Angew Makromol Chem 1985;135:21.

[107] Okay O, Soner E, Gungor A, Balkas TI. J Appl Polym Sci 1985;30:2065.

[108] Jacobelli H, Bartholin M, Guyot A. J Appl Polym Sci 1979;23:927.

[109] Dragan S, Csergö D, Manolescu I, Carpov A. React Polym 1987;5:123.

[110] Iayadene F, Guettaf H, Bencheikh Z, Saggou A, Rabia I. Eur Polym J 1996;32:1091.

[111] Poinescu IC, Beldie C. Angew Makromol Chem 1988;164:45.

[112] Poinescu I, Vlad C, Carpov A, Ioanid A. Angew Makromol Chem 1988;156:105.

[113] Coutinho FMB, Cid RCA. Eur Polym J 1990;26:1185.

[114] Coutinho FMB, Rabelo D. Eur Polym J 1992;28:1553.

[115] Wieczorek PP, Ilavsky M, Kolarz BN, Dusek K. J Appl Polym Sci 1982;27:277.

[116] Rabelo D, Coutinho FMB. Polym Bull 1994;33:487.

[117] Wang QC, Svec F, Frechet JMJ. J Polym Sci, Polym Chem Ed 1994;32:2577.
[118] Poinescu I, Vlad CD, Carpov A. React Polym 1984;2:261.
[119] Cheng CM, Micale FJ, Vanderhoff JW, El-Aasser MS. J Colloid Interface Sci 1992;150:549.
[120] Takeda K, Akiyama M, Yamamizu T. Angew Makromol Chem 1988;157:123.
[121] Djahieche A, Rabia I, Revillon A. Angew Makromol Chem 1994;222:89.
[122] Menger FM, Tsuno T, Hammond GS. J Am Chem Soc 1990;112:1263.
[123] Stoffer JO, Bone T. J Dispersion Sci Technol 1980;1:393.
[124] Sasthav M, Raj WRP, Cheung HM. J Colloid Interface Sci 1992;152:376.
[125] Haque E, Qutubuddin S. J Polym Sci, Polym Lett Ed 1988;26:429.
[126] Sasthar M, Cheung HM. Langmuir 1991;7:1378.
[127] Guo JS, El-Aasser MS, Vanderhoff JW. J Polym Sci, Polym Chem Ed 1989;27:691.
[128] Jayakrishna A, Shah DO. J Polym Sc, Polym Lett Ed 1984;22:31.
[129] Candau F. In: Mark HF, Bikales NM, Overberger CG, Menges G, editors. Encyclopedia of polymer science and engineering, vol. 9. New York: Wiley, 1987 (718pp.).
[130] Morse LD, Grundner WT, Calmon C. German Offen 1,939,405, 1970.
[131] Zhu XX, Banana K, Yen R. Macromolecules 1997;30:3031.
[132] Zhu XX, Banana K, Liu HY, Krause M, Yang M. Macromolecules 1999;32:277.
[133] Menger FM, Tsuno T. J Am Chem Soc 1990;112:6723.
[134] Smith DH. J Colloid Interface Sci 1985;108:471.
[135] Barby D, Haq Z. European Patent 0,060,138, 1982.
[136] Sherrington DC. Makromol Chem Macromol Symp 1993;70/71:303.
[137] Hainey P, Huxham IM, Rowatt B, Sherrington DC, Tetley L. Macromolecules 1991;24:117.
[138] Davankov VA, Tsyurupa MP. React Polym 1990;13:27.
[139] Davankov VA, Tsyurupa MP. Pure Appl Chem 1989;61:1881.
[140] Davankov VA, Rogozhin SV, Tsjurupa MP. Angew Makromol Chem 1973;32:145.
[141] Davankov VA, Tsyurupa MP, Rogozhin SV. Angew Makromol Chem 1976;53:19.
[142] Tsyurupa MP, Andreeva AI, Davankov VA. Angew Makromol Chem 1978;70:179.
[143] Davankov VA, Tsyurupa MP. Angew Makromol Chem 1980;91:127.
[144] Negre M, Bartholin M, Guyot A. Angew Makromol Chem 1979;80:19.
[145] Tsyurupa MP, Mrachkovskaya TA, Maslova LA, Timofeeva GI, Dubrovina LV, Titova EF, Davankov VA, Menshov VM. React Polym 1993;19:55.
[146] Bradford EB, Vanderhoff JW. J Appl Phys 1955;26:684.
[147] Ugelstad J, Kaggerud KH, Hansen FK, Berge A. Makromol Chem 1979;180:737.
[148] Ugelstad J, Mork PC, Kaggerud KH, Ellingsen T, Berge A. Adv Colloids Interface Sci 1980;13:101.
[149] Ugelstad J. US Patent 4,459,378, 1984.
[150] Ellingsen T, Aune O, Berge A, Kilaas L, Schmid R, Stenstad P, Ugelstad J, Hagen S, Weng E, Johansen L. Makromol Chem Macromol Symp 1993;70/71:315.
[151] Cheng CM, Micale FJ, Vanderhoff JW, Aasser MS. J Polym Sci, Polym Chem Ed 1992;30:235.
[152] Cheng CM, Vanderhoff JW, El-Aasser MS. J Polym Sci, Polym Chem Ed 1992;30:245.
[153] Frechet JMJ. Makromol Chem Macromol Symp 1993;70/71:289.
[154] Wang QC, Hosoya K, Svec F, Frechet JMJ. Anal Chem 1992;64:1232.
[155] Wang QC, Svec F, Frechet JMJ. Polym Bull 1992;28:569.
[156] Galia M, Svec F, Frechet JMJ. J Polym Sci, Polym Chem Ed 1994;32:2169.
[157] Ugelstad J, Mork PC, Schmid R, Ellingsen T, Berge A. Polym Int 1993;30:157.
[158] Kolarz BN, Trochimczuk A, Wojczynska M. Angew Makromol Chem 1988;162:193.
[159] Kolarz BN, Lobarzewski J, Trochimczuk A, Wojczynska M. Angew Makromol Chem 1989;171:201.
[160] Kolarz BN, Wojczynska M, Herman B. React Polym Ion Exch Sorbents 1989;11:29.
[161] Trochimczuk A, Kolarz BN. React Polym Ion Exch Sorbents 1989;11:135.
[162] Jelinkova M, Shataeva LK, Tischenko GA, Svec F. React Polym Ion Exch Sorbents 1989;11:253.
[163] Horak D, Svec F, Kalal J, Gumargalieva K, Adamyan A, Skuba N, Titova M, Trostenyuk N. Biomaterials 1986;7:188.
[164] Mueller KF, Heiber SJ, Plankl WL. US Patent 4,224,427, 1977.
[165] Robert CCR, Buri PA, Peppas NA. J Appl Polym Sci 1985;30:301.

[166] Barr-Howell BD, Peppas NA. Eur Polym J 1987;23:591.

[167] Scranton AB, Mikos AG, Scranton LC, Peppas NA. J Appl Polym Sci 1990;40:997.

[168] Jayakrishnan A, Sunny MC, Thanoo BC. Polymer 1990;31:1339.

[169] Kraemer DM, Lehman K, Pennewiss H, Plainer H, Schweder R. US Patent, 4,070,348, 1978.

[170] Kraemer DM, Pennewiss H, Plainer H, Schnee R. European Patent 58,767, 1982.

[171] Skelly PJ, Tighe BJ. Polym Commun 1979;20:1051.

[172] Denizli A, Kiremitci M, Piskin E. Biomaterials 1986;7:363.

[173] Patel SK, Rodriguez F, Cohen C. Polymer 1989;30:2198.

[174] Dawkins JV, Gabbott NP. Polymer 1981;22:291.

[175] Dawkins JV, Gabbott NP, Montenegro ANC, Lloyd LL, Warner FP. J Chromatogr 1986;371:283.

[176] Meehan E, Lloyd LL, McConville JA, Warner FP, Dawkins JV, Gabbott NP. J Appl Polym Sci, Appl Polym Symp 1991;48:3.

[177] Ogino K, Sato H. Kobunshi Ronbunshu 1989;46:667.

[178] Park TG, Hoffman AS. Biotechnol Prog 1994;10:82.

[179] Kayaman N, Kazan D, Erarslan A, Okay O, Baysal BM. J Appl Polym Sci 1998;67:805.

[180] Antonietti M, Caruso RA, Göltner CG, Weissenberger MC. Macromolecules 1999;32:1383.

[181] Wichterle O, Lim D. Nature (London) 1960;185:117.

[182] Ilavsky M, Prins W. Macromolecules 1970;3:425.

[183] Peppas NA, Moynihan HJ. In: Peppas NA, editor. Hydrogels in medicine and pharmacy, vol. 2. Boca Raton, FL: CRC Press, 1987. p. 49–64.

[184] Mathur AM, Moorjani SK, Scranton AB. J Macromol Sci, Rev Macromol Chem Phys 1996;C36:405.

[185] Wichterle O. In: Mark HF, Gaylard NG, Bikales NM, editors. Encyclopedia of polymer science and technology, vol. 15. New York: Wiley–Interscience, 1971. p. 273–91.

[186] Yasuda H, Gochin M, Stone W. J Polym Sci 1966;A-1(4):2913.

[187] Hasa J, Janacek J. J Polym Sci C 1967;16:317.

[188] Wichterle O, Chromecek R. J Polym Sci C 1969;16:4677.

[189] Kopecek J, Lim D. J Polym Sci 1971;A-1(9):147.

[190] Warren T, Prins W. Macromolecules 1972;5:506.

[191] Peppas NA, Moynihan HJ, Lucht LM. J Biomed Mater Res 1985;19:397.

[192] Huglin MB, Yip DCF. Macromolecules 1992;25:1333.

[193] Chen Y-C, Chirila TV, Russo AV. Mater Forum 1993;17:57.

[194] Oxley HR, Corkhill PH, Fitton JH, Tighe BJ. Biomaterials 1993;14:1064.

[195] Hirokawa Y, Tanaka T. J Chem Phys 1984;81:6379.

[196] Gehrke SH. Adv Polym Sci 1993;110:67.

[197] Kabra BG, Gehrke SH. Polymer Commun 1991;32:322.

[198] Rathjen CM, Park C-H, Goodrich PR, Walgenbach DD. Polym Gels Networks 1995;3:101.

[199] Gotoh T, Nakatani Y, Sakohara S. J Appl Polym Sci 1998;69:895.

[200] Svec F. Angew Makromol Chem 1986;144:39.

[201] Gardon JL. In: Mark HF, Gaylord NG, Bikales NM, editors. Encyclopedia of polymer science and technology, vol. 3. New York: Interscience, 1965. p. 833.

[202] Rabelo D, Coutinho FMB. Polym Bull 1994;33:479.

[203] Richter H-P, Ködderitzsch H, Schwachula G, Haupke K. Plaste und Kautschuck 1981;3:133.

[204] Rabelo D, Coutinho FMB. Polym Bull 1993;30:725.

[205] Wall J. In: Hren JJ, Goldstein JI, Joy DC, editors. Introduction to analytical electron microscopy, New York: Plenum Press, 1979. p. 333–42.

[206] Huxham IM, Rowatt B, Sherrington DC, Tetley L. Polymer 1992;13:2769.

[207] Gregg SJ, Sing KSW. Adsorption, surface area and porosity. 2nd ed. New York: Academic Press, 1982 p. 116–68.

[208] Halasz I, Martin K. Angew Chem, Int Ed Engl 1978;17:901.

[209] Halasz I, Vogtel P. Angew Chem, Int Ed Engl 1980;19:24.

[210] Crispin T, Halasz I. J Chromatogr 1982;239:351.

[211] Gregg SJ, Sing KSW. Adsorption, surface area and porosity, 2nd ed. New York: Academic Press, 1982. p. 173–90.

[212] Washburn EW. Proc Nat Acad Sci US 1921;7:115.

[213] Albright RL. React Polym 1986;4:155.

[214] Brunauer S, Emmett PH, Teller E. J Am Chem Soc 1938;60:309.

[215] Huglin MB, Yip DCF. Makromol Chem Rapid Commun 1987;8:237.

[216] Flory PJ. J Am Chem Soc 1941;63:3083.

[217] Funke W, Okay O, Muller B-J. Adv Polym Sci 1998;136:139.

[218] Dusek K. In: Chompff AJ, Newman S, editors. Polymer networks: structure and mechanical properties. New York: Plenum Press, 1971. p. 245–60.

[219] Okay O, Akkan U. Polym Bull 1998;41:363.

[220] Sherrington DC, Hodge P. Syntheses and separations using functional polymers. New York: Wiley, 1989.

[221] Kun KA, Kunin R. J Polym Sci A1 1968;6:2689.

[222] Okay O, Kurz M, Lutz K, Funke W. Macromolecules 1995;28:2728.

[223] Erbay E, Okay O. Polym Bull 1998;41:379.

[224] Okay O. Unpublished.

[225] Erbay E, Okay O. J Appl Polym Sci 1999;71:1055.

[226] Wieczorek PP, Kolarz BN, Galina H. Angew Makromol Chem 1984;126:39.

[227] Jun Y, Rongnan X, Juntan Y. J Appl Polym Sci 1989;38:45.

[228] Sanetra R, Kolarz BN, Wlochowicz A. Angew Makromol Chem 1986;140:41.

[229] Shea KJ, Sasaki DY, Stoddard GJ. Macromolecules 1989;22:1722.

[230] Shea KJ, Stoddard GJ. Macromolecules 1991;24:1207.

[231] Beldie C, Poinescu IC, Cotan V. J Appl Polym Sci 1984;29:13.

[232] Svec F, Frechet JMJ. Macromolecules 1995;28:7580.

[233] Flory PJ. Principles of polymer chemistry. Ithaca, New York: Cornell University Press, 1953.

[234] Okay O, Gurun C. J Appl Polym Sci 1992;46:421.

[235] Beranova H, Dusek K. Collection Czech Chem Commun 1969;34:2932.

[236] Galina H, Kolarz BN. Polym Bull 1980;2:235.

[237] Okay O. Angew Makromol Chem 1987;153:125.

[238] Krska F, Stamberg J, Pelzbauer Z. Angew Makromol Chem 1968;3:149.

[239] Hilgen H, De Jong GJ, Sederel WL. J Appl Polym Sci 1975;10:2647.

[240] Kolarz BN, Wieczorek PP, Wojaczynska M. Angew Makromol Chem 1981;96:193.

[241] Baldrian J, Kolarz BN, Galina H. Collection Czech Chem Commun 1981;46:1675.

[242] Kolarz BN, Wieczorek PP. Angew Makromol Chem 1981;96:201.

[243] Hradil J, Svec F. Angew Makromol Chem 1985;130:81.

[244] Luca C, Poinescu IG, Avram E, Ioanid A, Petrariu I, Carpov A. J Appl Polym Sci 1983;28:3701.

[245] Ellis TS, Karasz FE, Ten Brinke G. J Appl Polym Sci 1983;28:23.

[246] Okay O, Balkas TI. J Appl Polym Sci 1986;31:1785.

[247] Galina H, Kolarz BN, Wieczorek PP, Wojcynska M. Br Polym J 1985;17:215.

[248] Okay O. Angew Makromol Chem 1986;143:209.

[249] Wlochowicz A, Sanetra R, Kolarz BN. Angew Makromol Chem 1988;161:23.

[250] Dusek K. J Polym Sci, Polym Lett 1965;3:209.

[251] Dusek K. J Polym Sci 1967;C16:1289.

[252] Dusek K, Prins W. Adv Polym Sci 1969;6:1.

[253] Boots HMJ, Kloosterboer JG, Serbutoviez C, Touwslager FJ. Macromolecules 1996;29:7683.

[254] Okay O. Polymer 1999;40:4117.

[255] Okay O. J Appl Polym Sci 1999;74:2181.

[256] Flory PJ, Rehner J. J Chem Phys 1943;11:521.

[257] Frenkel J. Rubber Chem Technol 1940;13:264.

[258] Mikos AG, Takoudis CG, Peppas NA. Macromolecules 1986;19:2174.

[259] Aso C. J Polym Sci 1959;39:475.

[260] Tobita H, Hamielec AE. Makromol Chem, Macromol Symp 1988;20/21:501.

[261] Tobita H, Hamielec AE. Macromolecules 1989;22:3098.

[262] Fukuda T, Ma Y-D, Inagaki H. Macromolecules 1985;18:17.

[263] Okay O. Polymer 1994;35:796.

[264] Okay O. Polymer 1994;35:2613.

[265] Okay O. Macromol Theory Simul 1994;3:417.

[266] Okay O, Naghash HJ, Pekcan O. Macromol Theory Simul 1995;4:967.

[267] Okay O, Kaya D, Pekcan O. Polymer 1999;40:6179.

[268] Sajjadi S, Keshavarz SAM, Nekoomanesh M. Polymer 1996;37:4141.

[269] Biesenberger A, Sebastian DH. Principles of polymerization engineering. New York: Wiley, 1983.

[270] Brandrup J, Immergut EH. Polymer handbook, II-45. New York: Wiley, 1975.

[271] Hild G, Okasha R. Makromol Chem 1985;186:93.

[272] Hui AWT, Hamielec AE. Polymer 1972;16:749.